Non-equilibrium molecular dynamics simulations

applications to oscillating chemical reactions and inelastic colliding particles

Geisshirt, Kenneth

Publication date:
1997

Non-Equilibrium Molecular Dynamics Simulations: Application to Oscillating Chemical Reactions and Inelastic Colliding Particles

A Ph.D. thesis in Chemistry/Soft Material Science, December 1997

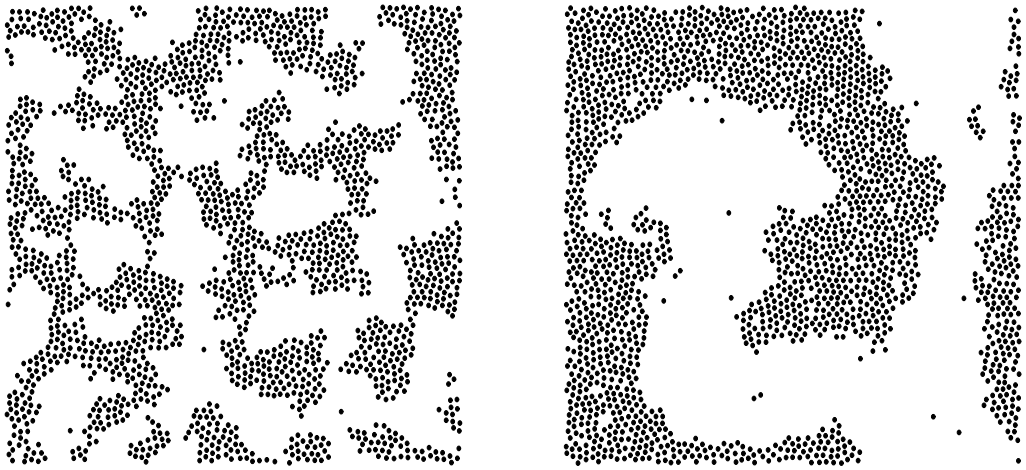

Kenneth Geisshirt
Department of Life Sciences and Chemistry
Roskilde University
E-mail: kneth@chem.ruc.dk

The pictures on the front page are snapshots from simulations of a two-component Lennard-Jones system above and below the critical temperature.

The thesis was produced using freeware only. The text was typeset using LaTeX, the graphs were produced by `GNUplot` and `ACEgr`, and the drawings were drawn in `xfig`. The final PostScript file was processed on a pc running Linux.

Abstract

The thesis is an investigation of non-equilibrium phenonema. The method imployed is Molecular Dynamics which in its simple form is a numerical solution of the classical equations of motion. Two systems are studied by this simulational method.

The first system is an oscillating chemical reaction competing with a phase separation process. The oscillating chemical reaction is kept far from equilibrium by driving it energetically. It is shown that the Molecular Dynamics method is able to reproduce the macroscopic phenomena. Moreover, it is shown that the phase separation process can modify the underlying chemical kinetics of the reaction.

The second system is a dissipative gas coupled to a number of thermostating devices. The dissipative gas is a model of a granular medium, and work presented in the thesis cast light on the pattern formation in dissipative gases.

Resumé

Afhandlingen er en undersøgelse af ikke-ligevægtsfænomener. Den brugte metode er Molecular Dynamics som i den simpleste formulering er en numerisk løsning af de klassiske bevægelsesligninger. To systemer er blevet undersøgt ved hjælp af denne simuleringsmetode.

Det første system er en oscillerende reaktion i konkurrence med en faseadskillelsesproces. Den oscillerende reaktion er holdt langt fra ligevægt ved at drive den energetisk. Det vises at Molecular Dynamics er i stand til at reproducere de makroskopiske fænomener. Endvidere vises det, at faseadskillelsesprocessen kan ændre reaktionens underliggende kinetik.

Det andet system er en dissipativ gas koblet til en række termostaterende anordninger. Den dissipative gas er en model af et granulært medium, og arbejdet præsenteret i afhandlingen kaster lys på mønsterdannelsesprocessen i dissipative gasser.

Preface

This thesis is the result of my graduate work carried out at Department of Life Sciences and Chemistry, Roskilde University during the period December 1994–November 1997. The thesis is submitted as a partial fulfilment of a Danish Ph.D.-degree.

The topic of the thesis is computational studies of non-equilibrium states using Molecular Dynamics. More precisely I have been engaged in two projects:

- The influence of phase separation on an oscillating chemical reaction.
- Temperature-control of granular media - in this thesis modelled as particles undergoing inelastic collisions

The two projects are very different in nature but the numerical technique is the same.

The intended reader is in principle me *i.e.*, I have written a thesis that I would have found valuable three years ago when I began my Ph.D. studies. A number of papers is enclosed as appendices. An outline of the chapters in the thesis is:

Chapter 1 is meant as a justification of the use of computer simulations in the physical sciences.

Chapter 2 introduces both classical and statistical mechanics.

Chapter 3 discusses phase transitions and the emphasis is on phase separation.

Chapter 4 is about chemical kinetics. The chapter introduces the topics which are applied to the simulational results presented in chapter 7.

Chapter 5 deals with the granular state of matter which is typically modelled as particles undergoing inelastic collisions. The basic phenomenology of granular media is introduced.

Chapter 6 discusses the numerical techniques which have been applied in order to obtain the results presented in chapter 7 and chapter 8.

Chapter 7 presents the results from simulations of a simple oscillating chemical reaction.

Chapter 8 discusses how to control the temperature of many-particle systems and the phenomenology associated with particles undergoing inelastic collisions coupled to various thermostats.

Appendix A is a paper about the role of computer in modern chemistry [24].

Appendix B is a contribution to the 9th annual workshop of simulational physics at University of Georgia [27].

Appendix C is a paper on phase separation and chemical reactions [26].

Appendix D is a paper on the thermostating of dissipative gases [25].

Acknowledgements

There are so many to thank. Let me first of all thank my two supervisors, Eigil L. Præstgaard and Søren Toxværd. I also wish to thank Paz Padilla for the good team work on the granular medium.

The students, the staff, and the faculty at the Department of Life Sciences and Chemistry have made the work at the department very pleasant. Especially I wish the thank the “snitte team” for many good discussions and small talks and my two proof readers, Morten Christoffersen and Thure Skovsgaard

Finally, I wish to thank my family and especially my parents. Their faith in me have made all it possible.

Kenneth Geisshirt
Roskilde, December 1997
Corrections: January 1998

CONTENTS

LIST OF FIGURES

Symbols, abbreviations, and units

Symbol	Meaning
l	litre
m	meter
GB	gigabyte (1073741824 bytes)
mol	mole
M	mole per litre
K	Kelvin
J	Joule
N_{Av}	Avogadro's constant, $6.02214 \cdot 10^{23} \mathrm{mol}^{-1}$
k_B	Boltzmann's constant, $1.38066 \cdot 10^{-23}$ J K^{-1}
R	gas constant, 8.31451 J K^{-1} mol^{-1}
$\log$	natural logarithm (base e)
$x \mod y$	x modulus y
$\mathbf{x}$	vector x
$\mathbf{A}$	matrix A
$\imath$	imaginary unit, $\sqrt{-1}$
∇	gradient, $\frac{\partial}{\partial x} + \frac{\partial}{\partial y} + \ldots$
$p \wedge q$	p logical-and q
$\mathbf{x} \cdot \mathbf{y}$	dot product, $\sum_i x_i y_i$
E_{tot}	total energy
E_{kin}	kinetic energy
E_{pot}	potential energy
$\mathcal{H}$	Hamiltonian
Q_N	canonical partition function
$\mathbf{r}$	position

$\mathbf{v}$	velocity
$\mathbf{p}$	momentum
$\mathbf{a}$	acceleration
$\mathbf{F}$	force
m	mass
$\langle \cdot \rangle$	(ensemble) average
$\bar{\cdot}$ (time) average	
$[X]$	(molar) concentration of X
T	temperature
β	inverse temperature, $1/k_B T$
$\mathcal{T}$	granular temperature
V	volume
A	(Helmholtz) free energy
U	internal energy
C_V	heat capacity at constant volume
ρ	density
P	pressure
Γ	collision rate
P_r	reaction probability
R_{reac}	diameter of encounter complex
r_{coll}	collision distance
LJ	Lennard-Jones
MC	Monte Carlo
MD	Molecular Dynamics

CHAPTER 1

Computational Science

The present thesis is about computer simulations of statistical-mechanical systems. In this chapter we will take a closer look at the branch of science called *computational science*. The chapter is not restricted to chemistry, and we have tried to write it in general terms but most of the examples will come from chemistry since the author is most familiar with chemistry.

1.1 The new branch

Science - here understood as the physical sciences including physics and chemistry - has traditionally been divided into two branches or legs: theory and experiment. The experiment is nowadays seen as the notion that makes *e.g.*, chemistry, scientific. The experiment was introduced in science during the scientific revolution 3–4 centuries ago [84]. Before then, science was mainly theoretical.

The introduction of the computer into science has started a new revolution: a new branch of science is emerging, namely computational science. No precise definition of computational science exists, and the question can easily trigger a passionate debate among computational scientists - recently Hocquet asked[1] whether computational chemistry was restricted to molecular modelling, and his question started a long and interesting debate. According to our personal taste, we will adopt the definition by Golub *et al.* [33]:

[1]The debate was running on the Internet through the "Computational Chemistry List" (a mailing list), and an archive of the contributions can be found at `http://ccl.osc.edu/ccl/archived_messages.html` .

> Computational science is the set of tools, techniques, and theories used to solve problems in science and engineering by a computer.

One of the first clear examples of computational investigation of physical properties is the study by Metropolis *et al.* [56]. In 1953 Metropolis *et al.* published a paper which introduced the Monte Carlo (MC) method. Shortly thereafter Alder *et al.* [1] introduced the Molecular Dynamics (MD) method. Adler *et al.* and Metropolis *et al.* were interested in the equation of state and phase transitions of simple liquids.

1.2 Theoretical or experimental?

Science has traditionally been divided into two branches; theoretical and experimental. One can put forward the question, whether computational science is experimental or theoretical.

We can easily answer the question: Computational science is neither experimental nor theoretical, but it does have notion in common with both. Computational science requires software which is produced by programming. Programming is the process where ideas are formalised and written as a computer program. The notation used in programming is not formulœ as in the theoretical approach but a programming language. Still, the notation is unambiguous as the mathematical notation, and this aspect of computational science is close to theoretical science. However, the computer can be regarded as an instrument, and then computational science suddenly has an experimental orientation [60]. Rapaport [71] has pro-arguments for the term "numerical experiment". Moreover, Rapaport argues, the distinction between computational methods and theoretical approaches is the cost; theory can be done with a piece of paper and a pencil, while computations require an investment in hardware.

Traditionally, science has tried to construct theories that explain experiments to some extend or to conduct experiments that can verify a given theory. Figure 1.1 shows the role of computational science. Theories are used to obtain approximations and general explanations of the experimental data. The computer simulations are instead used to investigate the model of the experiment in a more naive fashion than it is analytically possible.

Let us - through an example - explain the ideas formulated above. Consider a simple liquid; it could be methane, CH_4. We can, by experimental means, measure a given physical quantity; for instance the pressure at a given temperature and density. Methane is a simple liquid, and we will expect that it behaves as a classical-mechanical system *i.e.,* we will expect that the Hamiltonian equations

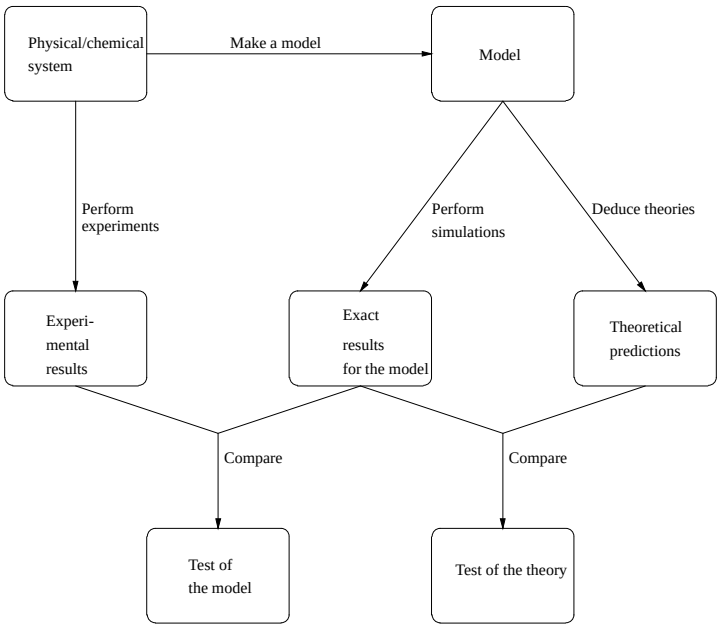

Figure 1.1: The relationship between experiment, computer simulation and theory in modern physical science. From [24] and inspired by [2].

of motion are applicable, and the interaction potential is the Lennard-Jones potential, see *e.g.*, Hansen *et al.* [38]. It is possible from the interaction potential to evaluate the next few virial coefficients, and use these to obtain approximative values of the pressure as function of temperature and density. This is the theoretical or analytical approach. The brute-force method (or the naive method) is to numerically solve the equations of motion and calculate the pressure at a given density and temperature. This approach is exact in the sense that the only two approximations used are the application of classical mechanics and the numerical scheme/the computer program. All three approaches provide us with a set of data, which can now be compared and the model and the approximation in the theoretical derivation can be verified or falsified by comparing with the experimental data.

1.3 Validation

In science in general, the concept of validation covers the process of comparing the real-world facts and the predictions of the model, and then conclude whether the model is reliable or not. The use of computers to make the predictions, makes the validation process a bit more complicated.

The complication of the validation process comes from the nature of the solution strategy: the predictions by the model are obtained by the use of a computer program. Typically, the computer program is written by the scientist himself. The first step in making reliable predictions is to justify that the computer program works correctly.

The verification of computer programs is not a trivial matter, and scientific programs might be even harder to verify. A typical verification of a computer program is to test the program. The test procedure is based on the idea that the program maps an input space on an output space. For example, a user working with a database at the library, the queries he types (the name of the author, *etc*.) is the input space, and the records that the database program prints are the output. Most computer programs are deterministic *i.e.,* the mapping between the input and the output is a deterministic mapping (the mapping is mathematically speaking surjective and not invertible). The testing procedure used is the following: the programmer constructs by hand the output associated with a given input (this is called a test example). If the program returns the same output as the programmer deduced, the program is less likely to contain errors. The art of testing is then to construct test examples which are as orthogonal as possible, so the testing period will be as short as possible. This test procedure is discussed at length by Myers [61].

Now the construction of test examples is not as simple as outlined above. The reason why we write computer programs for scientific purposes is that we cannot solve the problem by hand *i.e.,* map the input space onto the output space. Three procedures can then be persuited:

- The reproduction of data obtained from other sources. In some fields, a set of test examples might exist.
- Often in some limiting cases, the solution can be found analytically. This can be used to construct test examples. For example, we can easily solve 2 linear equations with 2 unknown variables, and this can be used to test a general linear equation solver.
- One can monitor some quantity which value is known from some exact analysis of the problem.

The last point is useful when it comes to statistical-mechanical simulations. As an example consider a system of N particles in a microcanonical ensemble. We know that the total energy E_{tot}, is a conserved quantity *i.e.,* E_{tot} must be constant. One can print E_{tot} as function of time, and if it is constant (within the precision of the computer) we have increased the degree of reliability of the program.

1.4 Simulational or computational scientists

So far we have discussed computational science, but one sees a division of the scientific community in the way, its members use computing equipment. Scientists doing simulations or calculations can be divided into two types. This classification is discussed by Mouritsen [60]. The types are:

- The type that happily spend hours (or even weeks or months) on writing computer programs. Designing and implementing the computer program is more satisfactory for them than the actual scientific problem. We will call them *computational scientists*.
- The second type is the scientist who is a user of a simulation program. He has never written a simulation program but the computing system (hardware and software) is his major scientific equipment. This type is called the *simulational scientist*.

The classification above is of course extreme, and most scientists who use computers, are somewhere in between. The two types have advantages and disadvantages. The computational scientist knows everything about the computational method - its strong and weak points. But he works slowly, in the sense that he does not solve many problems but develops new computational methods. The simulational scientist, on the other hand, solves many scientific problems, but has to rely on computer programs written by others. He tends to regard the computer (hardware and software) as a black box. Neither of two types are the best, but it seems to us that the population of simulational scientists is growing faster than the population of computational scientists. The desktop computers have become fast enough to solve large problems, and many problems can be solved by using commercial software packages *e.g.*, quantum chemical problems.

Even though commercial software packages can solve many of the (standard) problems in science, we strongly believe that the best scientific programs are written by computational scientists. A person trained in science will, in general, be better to solve computational problems related to science than the average programmer.

1.5 Concluding remarks

The application of computers to scientific problems creates new problems. But it also introduces new solution methods. Problems which were regarded as impossible to solve, can now be examined numerically. We regard this development as very exciting.

Moreover, computer simulations may also save us from many problems, and be able to create short-cuts. In the pharmaceutical industry, computer simulation techniques can be used to "test" compounds; it is often referred to as *rational drug design*. The excellent book by Grant *et al.* [35] shows many of the modern application of computer in chemistry, and we strongly believe that computers will help both life sciences and physical sciences in solving complex problems in the future.

CHAPTER 2

Mechanics

In this chapter we will outline classical mechanics. It is not a tutorial and the purpose is to enable the reader to understand later chapters. Classical mechanics can without problems be applied to many systems. In this thesis classical mechanics is used to describe microscopic details of simple liquids. This approximation is valid at high temperatures. High temperatures are not high in the everyday meaning of the word *e.g.*, classical mechanics is suitable to describe methane (CH_4) at 90 K.

Moreover, we will discuss statistical mechanics which is the underlying basis of the thesis. Briefly stated, statistical mechanics links the microscopic world (a many-body problem) with the macroscopic world (thermodynamics).

2.1 Classical mechanics

Classical mechanics is one of the major physical theories. The most well-known textbook is probably the textbook by Goldstein [32], and we will only cite this textbook.

The most important physical law in mechanics is Newton's second law. It relates the acceleration of a body to the force acting on the body. More precisely it is

$$\mathbf{F} = m\mathbf{a} \tag{2.1}$$

where $\mathbf{F}$ is the force, $\mathbf{a}$ the acceleration, and m is the mass of the body. Since the

acceleration is the second derivative of the position $\mathbf{r}$, we can easily write down the equations of motion. For an N-body system, the equations of motion are

$$\frac{\mathrm{d}\mathbf{r}_i}{\mathrm{d}t} = \mathbf{v}_i \tag{2.2a}$$

$$\frac{\mathrm{d}\mathbf{v}_i}{\mathrm{d}t} = \frac{\mathbf{F}_i}{m_i} \tag{2.2b}$$

where $\mathbf{v}_i$ is the velocity of the ith body.

The equations of motion can be written in many different ways. The Hamiltonian formulation is very useful, and which is equivalent to the formulation above. We begin by writing down a function called the Hamiltonian, $\mathcal{H}$. The equations of motion is then given by

$$\frac{\mathrm{d}\mathbf{r}_i}{\mathrm{d}t} = \frac{\partial \mathcal{H}}{\partial \mathbf{p}_i} \tag{2.3a}$$

$$\frac{\mathrm{d}\mathbf{p}_i}{\mathrm{d}t} = -\frac{\partial \mathcal{H}}{\partial \mathbf{r}_i} \tag{2.3b}$$

where $\mathbf{p}_i$ is the momentum of the ith body. The partial differentiation on the right hand side should be interpreted as a compact notation of partial differentiation with respect to the component in each direction.

2.1.1 Basic properties

The Hamiltonian $\mathcal{H}$, is composed of two terms which dependent on either the positions or the momenta *i.e.*,

$$\mathcal{H}(\mathbf{r}_i, \mathbf{p}_i) = K(\mathbf{p}_i) + V(\mathbf{r}_i) \tag{2.4}$$

The first term K, can be shown to be the kinetic energy E_{kin} *i.e.*,

$$E_{\text{kin}} = K = \frac{1}{2}\sum_{i=1}^{N} \frac{1}{m_i}|\mathbf{p}_i|^2 \tag{2.5}$$

The second term is the potential energy, *i.e.*, $V = E_{\text{pot}}$. The Hamiltonian is, in other words, the total energy, and Liouville's theorem states that for an isolated system the Hamiltonian is constant which implies that the total energy is constant.

The equations of motion are time reversible. This means that there is no arrow of time; the future and the past are equal in the sense that a change of sign transforms the future into the past and *vice versa*.

2.1.2 The force term

The force, $\mathbf{F}_i$, in equation (2.2) represents the interaction between the N bodies. For the ith body, we will assume that the force can be written as

$$\mathbf{F}_i = \sum_{i \neq j} \mathbf{f}_{ij} \tag{2.6}$$

where $\mathbf{f}_{ij}$ is the force between body i and j. For the systems studied in the present thesis, the force term $\mathbf{f}_{ij}$ will only depend on the separation of the bodies *i.e.*, on $\mathbf{r}_i - \mathbf{r}_j$ only. The force is antisymmetric when indexes are interchanged *i.e.*, $\mathbf{f}_{ij} = -\mathbf{f}_{ji}$.
The force $\mathbf{f}_{ij}$, is related to the potential u, as

$$\mathbf{f}_{ij} = -\nabla u(r_{ij}) \tag{2.7}$$

The potential is the model of the system; it covers the details on how the bodies or particles interact. A celebrated potential is the Lennard-Jones potential which is

$$u_{\mathrm{LJ}} = 4\epsilon \left[\left(\frac{\sigma}{r} \right)^{12} - \left(\frac{\sigma}{r} \right)^{6} \right] \tag{2.8}$$

where the parameter σ is the characteristic length scale and ϵ is the energy scale. The Lennard-Jones potential is often used when simple liquids (*e.g.*, argon and methane) are simulated. The parameters are determined by the substance under investigation.

2.2 Statistical mechanics

Statistical mechanics is a formal (mathematically rigorous) procedure which connects the microscopic world (atoms, molecules) with the macroscopic world. The procedure is statistical in nature *i.e.*, it can be used for computing averages instead of detailed dynamics.

For example, a glass of water (0.2 litre) contains $11.1\mathrm{mol}$ or $6.7 \cdot 10^{24}$ molecules. Each water molecule has 18 degrees of freedom, saying a glass of water has 2×10^{26} degrees of freedom. Just storing a snapshot (all degrees of freedom at one point in time) would require $3.6 \cdot 10^{17}\mathrm{GB}$ assuming only single precision. If a harddisk is $10^{-3}\mathrm{m}$ thick, and we use $3.6\mathrm{GB}$ disks, the stack of harddisks would be $10^{14}\mathrm{m}$ tall. This should be compared to the distance between the earth and the sun which is $1.5 \cdot 10^{11}\mathrm{m}$. This example clearly shows that knowledge of the detailed dynamics of the water molecules in a glass is impossible, and it serves as the motivation for introducing statistical mechanics in order to obtain knowledge of many-body systems.

Since this chapter is **not** intended to be a complete tutorial of statistical mechanics, let me therefore mention two textbooks, I have enjoyed reading:

- Huang [43] gives an easy introduction. The text is not rigorous and it serves as a gentle introduction of the key ideas. The book must be considered as a "classical" text in the sense that it has a physical origin.

- Andersen [3] is a "modern" text. "Modern" refers to the way the topic is approached - Andersen uses probability theory and information theory and deduces first a general statistical mechanics which he later applies to physical systems.

2.2.1 Ensembles

An ensemble can defined in many different ways, and we will use a pragmatic definition.

We define an ensemble as a many-body system where a number of thermodynamical variables are fixed. Two ensembles are of interest in this thesis; the microcanonical and the canonical ensemble. An ensemble defines the macroscopic state of the system, and the dynamics is defined by a Hamiltonian.

The microcanonical ensemble is an NVE ensemble *i.e.*, it is a system where the number of particles N, the volume V and the total energy E are constant. The Hamiltonian which describes the microcanonical ensemble is the Hamiltonian in equation (2.4).

The canonical ensemble is in many aspects more interesting. The three variables which are constant, are the number of particles, the volume, and the temperature. In section 2.4 we will discuss the Hamiltonian for this ensemble.

2.2.2 The partition function

One of the key concept in statistical mechanics is the partition function. Let us assume that $\mathcal{H}$ is the Hamiltonian of a many-body system. The canonical partition function Q_N, for an N-particle system is then given as

$$Q_N(T,V) = \frac{1}{h^{3N}N!}\int \exp(-\beta\mathcal{H})\mathrm{d}\mathbf{r}^N\mathrm{d}\mathbf{p}^N \tag{2.9}$$

where T is the temperature, V the volume, h is a normalisation constant, and β is $1/k_BT$. The integration is over the positions and momenta of all particles. We have $6N$ integrals which in most cases is impossible to solve analytically. In section 2.3 we will consider a system which can be treated analytically.

2.2.3 Thermodynamics and fluctuations

The aim of statistical mechanics is to calculate thermodynamic properties from the knowledge of the microscopic details of a many-body system. One simple relation connects the macroscopic world with its microscopic details. The connection relates the (Helmholtz) free energy A, and the (canonical) partition function Q_N as

$$A = -k_BT\log Q_N(T,V) \tag{2.10}$$

In principle all thermodynamical quantities can trivially be derived from this point. In reality, the partition function is only possible to compute exactly for a few examples, and computer simulations are the only possible way of examining the problem of interest. In the remaining part of the section we will look at a few consequences of equation (2.10).

Consider the internal energy, U. From a thermodynamical point of view it is given by [5]

$$U = \left(\frac{\partial(A/T)}{\partial(1/T)}\right)_V \tag{2.11}$$

The internal energy is equivalent to the total energy for the microscopic system. The total energy, E_{tot}, fluctuates (we are now considering the system with fixed temperature *i.e.,* a closed system, and not an isolated system) around the mean

value. The internal energy is therefore the average of the total energy, and so we have:

$$U = \langle \mathcal{H} \rangle = -\left(\frac{\partial \log Q_N(T,V)}{\partial \beta} \right)_V \tag{2.12}$$

The heat capacity (at constant volume) is in thermodynamics defined as

$$C_V \equiv \left(\frac{\partial U}{\partial T} \right)_V \tag{2.13}$$

Loosely speaking, the heat capacity is a measure of the energy required to heat a system one degree. Using equation (2.10), equation (2.11), and equation (2.12) we obtain an expression for the heat capacity:

$$C_V = \frac{1}{k_B T^2} \left(\langle \mathcal{H}^2 \rangle - \langle \mathcal{H} \rangle^2 \right) \tag{2.14}$$

We see that the heat capacity is a statistical quantity, namely the mean-square deviation of the total energy. The exciting point about equation (2.14) is that heat capacity can be calculated from a system in equilibrium - we do not have to use the experimental procedure *i.e.*, we do not have to add energy and see the temperature raise in order to find the heat capacity. Equation (2.14) is a special case of a more general theorem called the fluctuation-dissipation theorem [43].

2.3 An example

In this section we will consider a simple system. We examine N identical particles with mass m. The Hamiltonian of the system is:

$$\mathcal{H} = \frac{1}{2m} \sum_{i=1}^{N} \mathbf{p}_i^2 \tag{2.15}$$

The equations of motion is easy to derive. They are:

$$\frac{\mathrm{d}\mathbf{r}_i}{\mathrm{d}t} = \frac{\mathbf{p}_i}{m} \tag{2.16a}$$

$$\frac{\mathrm{d}\mathbf{p}_i}{\mathrm{d}t} = \mathbf{0} \tag{2.16b}$$

The equations of motion show that the molecules in a system with a Hamiltonian given by equation (2.15) do not interact. The molecules move in straight lines. The canonical partition function can be evaluated. The integration over the positions gives us V^N, while the integration over momenta is an integration of a Gaussian function. The partition function is:

$$Q_N(V,T) = \frac{1}{h^{3N}N!}V^N\left(\sqrt{\frac{2\pi m}{\beta}}\right)^N \tag{2.17}$$

The Helmholtz free energy A, links us to the thermodynamics of our system, and we obtain

$$A = k_BT(N\log V + \frac{N}{2}(\log(2\pi m) - \log(\beta)) - \log(h^{3N}N!) \tag{2.18}$$

The free energy is not interesting on its own. The pressure of the N molecules is more interesting since it can easily be measured. The pressure P is

$$\begin{aligned} P &= -\left(\frac{\partial A}{\partial V}\right)_T \\ &= -k_BT\left(\frac{\partial N\log V}{\partial V}\right)_T \\ &= \frac{Nk_BT}{V} \end{aligned}$$

which is the equation of state of an ideal gas. That is, an ideal gas is a system where gas molecules do not interact. Moreover, the ideal gas is one of the few microscopic system which we can solve analytically.

2.4 Extended dynamics

The Hamiltionian in equation (2.4) describes the dynamics in the microcanonical ensemble. In 1984 Nosé [63] published paper about a Hamiltonian which can describe the dynamics in the canonical ensemble. Since most of our simulations reported in this thesis have been performed in the canonical ensemble using equations of motion derived from Nosé's Hamiltonian, we will discuss his Hamiltonian.

The Hamiltonian $\mathcal{H}$ is

$$\mathcal{H} = \sum_{i=1}^{N} \frac{\mathbf{p}_i^2}{2m_i s^2} + V(\mathbf{r}) + \frac{p_s^2}{2Q} + g k_B T \log s \tag{2.19}$$

where the two variables s and p_s is the extension of the simple Hamiltonian. The idea is that the particles are coupled to a heat bath which is modelled by s and p_s. The relaxation time of the thermostat is Q. The parameter g is the degree of freedom (plus one).

The (microcanonical) partition function associated with $\mathcal{H}$ is

$$Q = \frac{1}{N!} \iiiint \delta(\mathcal{H} - E) \mathrm{d}\mathbf{r} \mathrm{d}\mathbf{p} \mathrm{d}s \mathrm{d}p_s \tag{2.20}$$

where $\delta(\cdot)$ is the Dirac delta function. We now introduce a new variable, $\mathbf{p}_i'$ as $\mathbf{p}_i/s$, and we have $\mathrm{d}\mathbf{p} = \mathrm{d}(\mathbf{p}'s) = s^{g-1}\mathrm{d}\mathbf{p}'$. Moreover, let $\mathcal{H}'$ be

$$\mathcal{H}' = \sum_{i=1}^{N} \frac{(\mathbf{p}_i')^2}{2m_i s} + V(\mathbf{r})$$

The partition function can now be rewritten as

$$Q = \frac{1}{N!} \iiiint s^{g-1} \delta(\mathcal{H}' + \frac{p_s^2}{2Q} + g k_B T \log s - E) \mathrm{d}\mathbf{r} \mathrm{d}\mathbf{p}' \mathrm{d}s \mathrm{d}p_s \tag{2.21}$$

We can apply the following property of the delta function:

$$\delta(h(s)) = \frac{\delta(s - s_0)}{h'(s)}$$

where s_0 is the root of the function h and h' is the derivative of h. If we let h be

$$h(s) = \mathcal{H}' + \frac{p_s^2}{2Q} + g k_b T \log s - E$$

we find s_0 to be

$$s_0 = \exp\left(-\frac{\mathcal{H}' + p_s^2/2Q - E}{g k_B T}\right)$$

and the derivative is $h'(s) = gk_BT/s$. Finally the delta function can be evaluated to be

$$\delta(h(s)) = \delta\left(s - \exp\left(-\frac{\mathcal{H}' + p_s^2/2Q - E}{gk_BT}\right)\right)\frac{s}{gk_BT} \tag{2.22}$$

Using that the integration of p_s is the integration of a Gaussian function, we obtain

$$Q = \frac{1}{g}\sqrt{\frac{2\pi Q}{k_BT}}\exp(E/k_BT)Q_N \tag{2.23}$$

where Q_N is

$$Q_N = \frac{1}{N!}\iint \exp\left(-\frac{\mathcal{H}'}{k_BT}\right)\mathrm{d}\mathbf{p}'\mathrm{d}\mathbf{r} \tag{2.24}$$

The partition function Q_N is the partition function of a canonical ensemble, and since we have $Q \propto Q_N$ we see that the ensemble generated by the Hamiltonian in equation (2.19) is the canonical ensemble.

The equations of motion which generates the dynamics of particles coupled to a heat bath can be reduced further. Hoover [42] has shown that one variable is sufficient in order to describe the motion of the particles.

It is important to stress that the instantaneous temperature is not constant. The instantaneous temperture Θ is given as

$$\frac{g-1}{2}k_B\Theta = \sum_{i=1}^{N}\frac{\mathbf{p}_i^2}{2m_is^2} \tag{2.25}$$

The instantaneous temperature fluctuates, but the mean value $\langle\Theta\rangle$ is the equilibrium temperature *i.e.*, $\langle\Theta\rangle = T$.

This extension of the equations of motion is often referred to as the Nosé-Hoover thermostat, and in chapter 6 we will discuss an algorithm which implements the Nosé-Hoover thermostat.

CHAPTER 3

Phase Separation

Simple liquids have been studied by computer simulations for more than forty years. The first pioneering studies by *e.g.*, Metropolis *et al.* [56] were concerned with the equation of state. But since the early 1960s the focus has been on phase transitions.

In this chapter we will review some of the basic theories about phase transitions with emphasis on phase separation. We will begin the chapter by giving a few general references: Binder [7] has reviewed the kinetics of phase separation very pedagogically. The best and most general textbook is the textbook by Goldenfeld [30].

3.1 Phase transitions

Phase transitions are a well-known phenomenon in everyday life *e.g.,* the melting of an ice cube. The properties of phase transitions have been studied experimentally and theoretically for more than a century. An early observation was that at some phase transitions the heat capacity is singular at the transition temperature. This observation led Erhenfest to a classification of phase transitions. The classification proposed by Erhenfest is nowadays simplified, and we have only two types of phase transitions:

- the discontinuous transition where the heat capacity is singular
- and the continuous transition where the heat capacity is a continuous function of the temperature

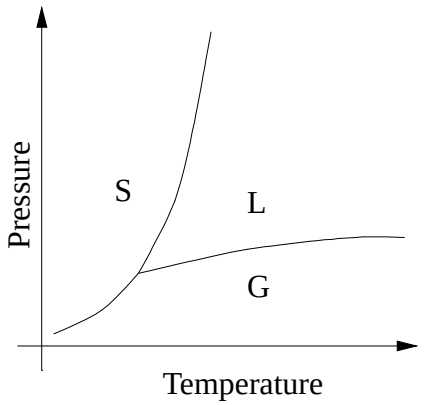

Figure 3.1: A typical phase diagram for a pure substance. The letters S, L, and G denote one phase regions (solid, liquid, and gas).

The melting of ice is an example of a discontinuous phase transition while the structural changes in a lipid is typically a continuous transition.

Let us consider a pure substance *e.g.*, carbon dioxide, CO_2. Given the pressure, the transition temperature from solid to liquid, is uniquely determined. The information *i.e.*, the set of transition pressures and temperature, is called the *phase diagram*. For a pure substance like carbon dioxide a typical phase diagram is sketched in figure 3.1.

The lines in a phase diagram is where the phase transition occurs. These lines are called the coexistence lines because two phases exist *i.e.*, they are in equilibrium.

A coexistence line can be calculated by using the Clapeyron equation *i.e.*,

$$\frac{\mathrm{d}P}{\mathrm{d}T} = \frac{\Delta_{\text{trans}} S_m}{\Delta_{\text{trans}} V_m} \tag{3.1}$$

where P is the transition pressure, T the temperature, $\Delta_{\text{trans}} S_m$ is the change in the molar entropy, and $\Delta_{\text{trans}} V_m$ is the change in the molar volume.

The phase diagram sketched in figure 3.1 is for a pure substance only. If we turn to two-component mixtures, we need one extra variable in order to describe the phase transitions uniquely. Often the mole fraction of one of the species is used, and the phase diagram is three-dimensional.

For a pure substance there exists one point in the phase diagram where the three phases (solid, liquid, gas) coexist. We call this point the *triple point*. It is located where the three coexistence lines meet.

Substance	σ (nm)	ϵ/k_B (K)
He	0.2556	10.2
Ar	3.405	119.8
H_2	2.959	36.7
CH_4	3.817	148.2

Table 3.1: The Lennard-Jones parameters for a number of substances. Data taken from Hansen *et al.* [38].

3.2 Simple liquids

One-component simple liquids have been studied experimentally, computationally and theoretically. We will concentrate on theoretical and computational results on one simple liquid: the Lennard-Jones liquid.

The Lennard-Jones (LJ) liquid can be regarded as a family of liquids *i.e.*, many simple liquids can be approximated well using the Lennard-Jones potential. The LJ potential is a short-range potential which includes two parameters:

$$u(r) = 4\epsilon \left[\left(\frac{\sigma}{r}\right)^{12} - \left(\frac{\sigma}{r}\right)^{6} \right] \tag{3.2}$$

The parameter ϵ is the fundamental energy unit while the parameter σ is the fundamental length unit. Table 3.1 lists values for the parameters for a number of simple liquids.

Hansen *et al.* [39] have performed computer simulations of a three-dimensional Lennard-Jones system, and they have found that the triple point is $\rho \approx 0.85\sigma^3$ and $T \approx 0.68\epsilon/k_B$. Kofke [46] and Panagiotopoulos [65] have numerically studied the liquid-gas transition, and this part of the phase diagram is shown in figure 3.2.

3.3 The scaling hypothesis

In this section we will briefly discuss scaling in the context of phase separation, for a more detailed description see Bray [10]. The physics behind the scaling hypothesis is that only one variable is relevant [10, 30].

If we consider a fluid close to the critical point, we find that the isothermal compressibility κ_T behave as

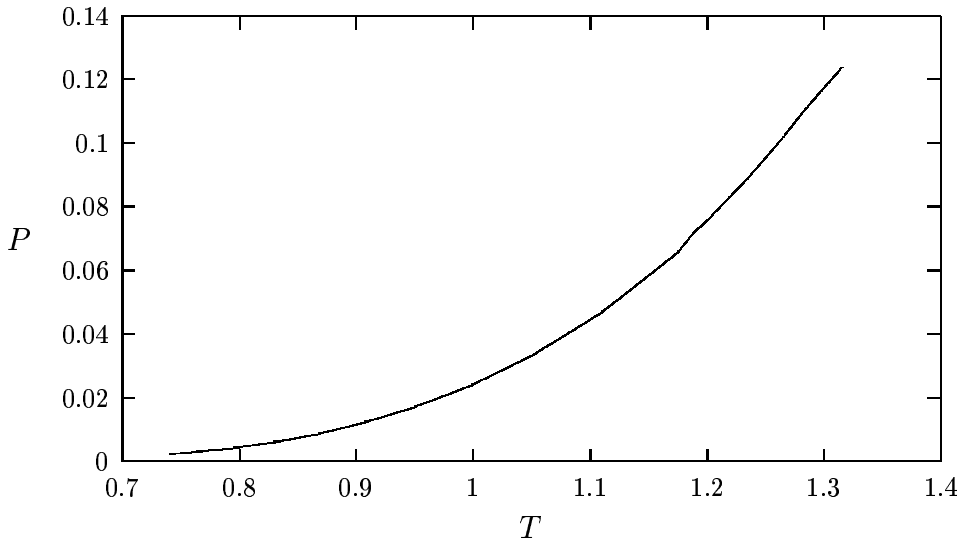

Figure 3.2: The phase diagram of the pure three-dimensional Lennard-Jones system (temperature versus pressure; scaled so $\epsilon = 1$ and $\sigma = 1$). The gas phase is above the curve while the liquid phase exists below the curve. From [46].

$$\kappa_T = -\frac{1}{V}\left(\frac{\partial V}{\partial p}\right)_T \sim |T - T_c|^{-\gamma} \tag{3.3}$$

were T_c is the critical temperature. Moreover, the a similar behaviour is found for the heat capacity, namely

$$C_V \sim |T - T_c|^{-\alpha} \tag{3.4}$$

The scaling described above is the so called static scaling since there is no temporal dependency. A large number of systems has the same value for the exponents even though the system might be of very different nature. This fact has lead the physicists to associate each value with a universality class.

3.4 Phase separation

The basic phenomenology of phase separation is simple [30]. Imagine that we have a mixture of two substances, A and B. At high temperature the two sub-

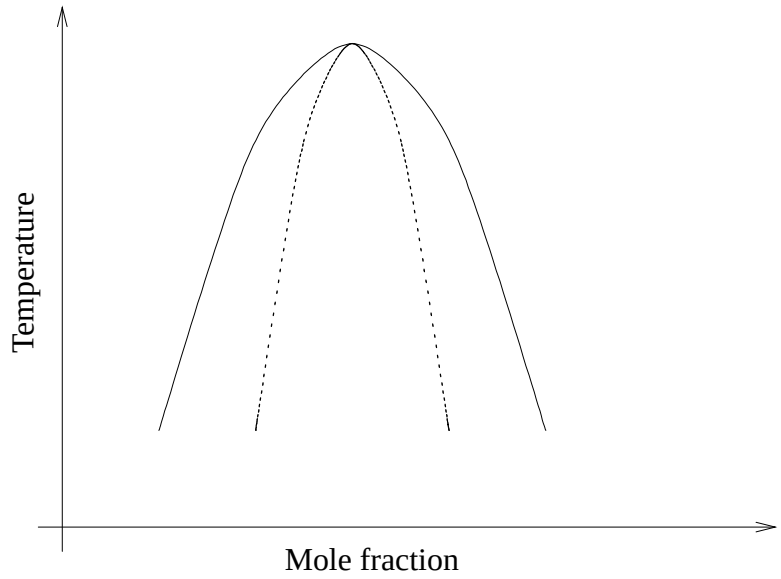

Figure 3.3: A phase diagram for a mixture of two simple liquids. The solid line is the coexistence line while the dashed line is the the spinodal line.

stances will be miscible, and at low temperature they will be immiscible. The transition from miscible to immiscible occurs at a well-defined temperature, T_C.

Consider a mixture of two simple liquids; figure 3.3 outlines the general phase diagram. Outside the solid line the two liquids are miscible, and the line is the coexistence line. Between the solid and the dashed line, the system will phase separate through a nucleation process, and inside the dashed line we will see a spinodal decomposition.

3.4.1 Nucleation

As already mentioned, phase separation through a nucleation occurs between the solid lines and the dashed lines in figure 3.3. Thermal fluctuations form small droplets in a homogeneous phase. The free energy change ΔF, of forming a droplet of radius R is

$$\Delta F = \begin{cases} 4\pi\sigma R^2 - \frac{4}{3}\pi\epsilon R^3 & \text{in three dimensions} \\ 2\pi\sigma R - \pi\epsilon R^2 & \text{in two dimensions} \end{cases} \tag{3.5}$$

where ϵ is the free energy of the bulk and σ is the surface free energy. The critical size, R_c, of a droplet is the maximum in the free energy. When the droplet is larger

than the critical droplet, the droplet will grow. We can find the critical radius by differentiating the free energy and find the root. We find:

$$R_c = \begin{cases} \frac{2\sigma}{\epsilon} & \text{three dimensions} \\ \frac{\sigma}{\epsilon} & \text{two dimensions} \end{cases} \tag{3.6}$$

3.4.2 Spinodal decomposition

Through a spinodal decomposition the system will phase separate by forming a labyrinth structure which coarsen. The kinetics of the spinodal decomposition was first investigated by Cahn *et al.* [13], and the theory now goes under the name *Cahn-Hilliard theory*.

Let us define an order parameter, ψ, as $\psi(\mathbf{r},t) \equiv c(\mathbf{r},t) - c_0$ where $c(\mathbf{r},t)$ is the local concentration, and c_0 is the equilibrium concentration. Moreover, let f denotes the free energy per molecule. The free total energy F in a volume V is

$$F = \int_V f \,\mathrm{d}V \tag{3.7}$$

In order to evaluate this integral, we can Taylor expand the free energy at c_0 ($\psi = 0$); the free energy of a spatially homogeneous system is f_0. Moreover, f does also depend on ∇c, $\nabla^2 c$ and higher order derivatives. The Taylor expansion to first order in c, ∇c and $\nabla^2 c$ is

$$f = f_0 + \sum_i L_i \frac{\partial \psi}{\partial x_i} + \sum_{ij} \kappa_{ij}^{(1)} \frac{\partial^2 \psi}{\partial x_i \partial x_j} + \tfrac{1}{2} \sum_{ij} \kappa_{ij}^{(2)} \frac{\partial \psi}{\partial x_i} \frac{\partial \psi}{\partial x_j} + \cdots \tag{3.8}$$

where x_i and x_j represent the spatial variables and

$$L_i = \left. \frac{\partial f}{\partial(\partial\psi/\partial x_i)} \right|_{\psi=0} \tag{3.9a}$$

$$\kappa_{ij}^{(1)} = \left. \frac{\partial f}{\partial(\partial^2\psi/\partial x_i \partial x_j)} \right|_{\psi=0} \tag{3.9b}$$

$$\kappa_{ij}^{(2)} = \left. \frac{\partial^2 f}{\partial(\partial\psi/\partial x_i)(\partial\psi/\partial x_j)} \right|_{\psi=0} \tag{3.9c}$$

Since we will assume that the mixture is isotropic, we will have

$$L_i = 0 \tag{3.10a}$$

$$\kappa_{ij}^{(1)} = \begin{cases} \kappa_1 = \frac{\partial f}{\partial \nabla^2 \psi} & \text{for } i = j \\ 0 & \text{otherwise} \end{cases} \tag{3.10b}$$

$$\kappa_{ij}^{(2)} = \begin{cases} \kappa_2 = \frac{\partial^2 f}{\partial (|\nabla \psi|)^2} & \text{for } i = j \\ 0 & \text{otherwise} \end{cases} \tag{3.10c}$$

This reduces the expansion of f to

$$f = f_0 + \kappa_1 \nabla^2 \psi + \kappa_2 (\nabla \psi)^2 \tag{3.11}$$

By applying the divergence theorem to equation (3.7) and inserting equation (3.8), we obtain the Cahn-Hilliard free energy functional

$$F[\psi(\mathbf{r})] = \int \tfrac{1}{2}(\nabla \psi)^2 + k f_0[\psi(\mathbf{r})] \mathrm{d}\mathbf{r} \tag{3.12}$$

where

$$k = - \left. \frac{\partial^2 f}{\partial \psi \partial \nabla^2 \psi} \right|_{\psi=0} + \left. \frac{\partial^2 f}{(\partial |\nabla \psi|)^2} \right|_{\psi=0}$$

The free energy f has the following properties. It has only one minimum above the critical temperature, and it is located at $\psi = 0$ *i.e.*, above the critical temperature, the system can only be in a homogeneous state. Below the critical temperature, the free energy has two minima which are not located at $\psi = 0$. The free energy f_0 is often assumed to be a Landau free energy near the critical temperature *i.e.*, a free energy in the form

$$f_0[\psi] = f_0(T) + a(T)\psi^2 + b(T)\psi^4 + \cdots$$

Even though the system phase separate, the mass is conserved, which is the same as

$$\frac{\partial \psi}{\partial t} + \nabla \cdot \mathbf{j} = 0 \tag{3.13}$$

where **j** is the flux defined as

$$\mathbf{j} = -M\nabla\frac{\delta F}{\delta\psi} \tag{3.14}$$

The parameter M is a measure of the mobility of the species (similar to diffusion), and $\delta F/\delta\psi$ is the functional derivative of F with respect to ψ. Putting equations (3.12), (3.13) and (3.14) together we obtain the Cahn-Hilliard equation *i.e.,*

$$\frac{\partial\psi}{\partial t} = M\nabla^2\left(\frac{\delta f_0}{\delta\psi} - \nabla^2\psi\right) \tag{3.15}$$

Initial conditions are the homogeneous state *i.e.,* a state where $\langle\psi\rangle = 0$. During the spinodal decomposition patterns are formed, and the final pattern is the equilibrium pattern *i.e.,* phases which are pure in one of the species.

The Cahn-Hilliard equation cannot be solved analytically, but only numerically. In section 3.5 we will discuss how the Cahn-Hilliard equation can be extended in order to include chemical reactions.

3.4.3 Dynamic scaling

Now consider the phase separation process, and let $R(t)$ denote the average domain size. As early as 1961, Lifshitz, Slyozov and Wagner were able to predict that the growth law is algebraic [10] *i.e.,*

$$R(t) \sim t^{1/3} \tag{3.16}$$

This growth law is called the diffusive regime, because the underlying physical model is diffusion-controlled reaction *i.e.,* two domains diffuse together and merge in order to form one large domain. At later times in the phase separation process the growth law can cross over to [10]

$$R(t) \sim t^{2/3} \tag{3.17}$$

The growth law predicted by Lifshitz *et al.* (equation (3.16)) is not the only possible growth law. Equation (3.16) is typically denoted the diffusive regime which the underlying model is a diffusion-controlled reaction. Other regimes include the viscous and the inertial regime.

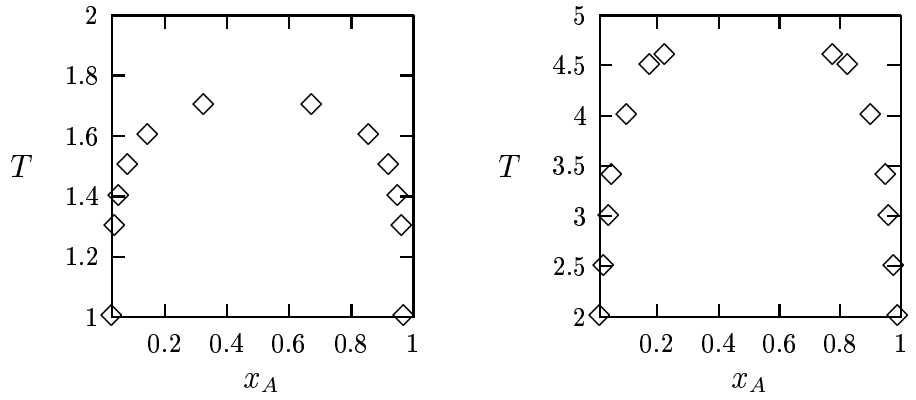

(a) 2 dimensions (b) 3 dimensions

Figure 3.4: The phase diagram of a binary mixture of two- and three-dimensional Lennard-Jones liquids. The data point are found using MD simulation. The density is $0.8\sigma^2$ and $0.8\sigma^3$ in the two cases. From [79].

3.4.4 The Lennard-Jones liquid

The mixture of Lennard-Jones liquids is a good system to study when we wish to understand the kinetics of phase separation.

The phase diagram of a binary Lennard-Jones fluid has been published by Toxværd *et al.* [79, 81]. The phase diagram is shown in figure 3.4

Furthermore, Toxværd *et al.* show that the growth of the domains at late times is algebraic. They find the exponent to be $2/3$ when the particle fraction of each component is $\frac{1}{2}$ while the exponent is $1/3$ when one of the components is dominating.

Going to three-component systems, we see a major difference. Laradji *et al.* [47] find that the growth exponent is $1/3$ for a system where the particle fraction of each component is equal.

3.5 Chemistry

The phase separation discussed in the previous section was a physical process. During the 1990s a number of papers have been published on how chemical reactions might influence the phase separation process.

The Cahn-Hilliard equation (3.15) can be modified in order to include chemical

reactions. Christensen *et al.* [15] and Glozter *et al.* [28] have simple modifications. Consider the reaction $A \leftrightarrows B$. The forward and the reverse rate constants are denoted k_f and k_r, respectively. The modified Cahn-Hilliard equation including these two reactions is

$$\frac{\partial \psi}{\partial t} = M\nabla^2 \left(\frac{\delta f_0}{\delta \psi} - \nabla^2 \psi \right) - k_f \psi + k_r (1 - \psi) \tag{3.18}$$

where ψ is the local mole fraction of A. Both Christensen *et al.* and Glozter *et al.* set $k = k_f = k_r$. The modification of the Cahn-Hilliard equation is simple: we have added the velocity field coming from the chemical reactions.

The average domain size R scales with the time as

$$R(t) \sim t^{\alpha} \tag{3.19}$$

Without the competing chemical reactions, the exponent α is initially $1/3$ and $2/3$ at late times [21, 85]. From a dimensional analysis Glotzer *et al.* [28] find that the average domain size scales as

$$R \sim \left(\frac{1}{k} \right)^{\alpha} \tag{3.20}$$

At low reaction rates ($k \approx 0$) Christensen *et al.* and Glotzer *et al.* finds that the exponent α is approximately $1/3$. At larger reaction rates Christensen *et al.* find that the exponent is $1/4$.

Monte Carlo simulations of an Ising model with competing reactions ($A \leftrightarrows B$) have been performed by Glotzer *et al.* [29]. They find that the exponent $\alpha = 0.22 \pm 0.02$ which is consistent with the result by Christensen *et al.* . Toxværd, on the other hand, has performed Molecular Dynamics simulations of a Lennard-Jones mixture undergoing phase separation competing with chemical reactions. At low reaction rates the growth exponent is approximately 0.33 while it is lower at higher reaction rate.

Glozter *et al.* and Toxværd observe that the phase separation process is hindered by fast reactions. Toxværd argues that the reason is that the fast reactions destroy the hydrodynamic modes which are essential in the phase separation. A similar observation has been done by Verdasca *et al.* [82] and Christensen *et al.* [15]. They see that chemical reactions might freeze the phase separation. This freezing is only observed at high reaction rates.

Carati *et al.* [14] have recently published a paper on the chemical freezing. The theory presented by Carati *et al.* is based on the Cahn-Hilliard theory. They are able to establish a number of criteria for the freezing *e.g.*, that at least one reaction must be autocatalytic.

CHAPTER 4

Chemical Kinetics

Chemical kinetics is the study of how fast chemical reactions proceed. In this chapter we will review the basic theory of chemical kinetics. The only criteria for selecting the material is that it is going to be applied to the systems studied in the present thesis.

The theories presented in this chapter are of macroscopic nature. The simulations presented in chapter 7 are of microscopic nature. The topic of the thesis is partly to see if the macroscopic description of chemical reaction is valid on a microscopic level.

Many textbooks deal with chemical kinetics, and we will here only mention a few. Pilling *et al.* [67] have recently written an excellent book. It is more experimental oriented than usual textbooks, and it covers many of the new techniques and theories. The book by Cox [18] gives an excellent but short overview of reactions in liquid phase.

4.1 Phenomenological chemical kinetics

We begin our introduction to chemical kinetics in the macroscopic world. The phenomenological approach tries to elucidate the mechanism of a complex reaction by writing down a number of differential equations which are the "equations of motion" of the concentrations *i.e.,* the goal is to find, for each species X, an equation of the form

$$\frac{\mathrm{d}[X]}{\mathrm{d}t} = f([X],[Y],\dots) = \nu v([X],[Y],\dots) \tag{4.1}$$

where $Y,\dots$ represent every other species present in the system, f is a function related to its stoichiometric coefficient ν, and the velocity v of the reaction. The stoichiometric coefficient is positive for products and negative for reactants.

A special class of reactions is the class of *elementary reactions*. For an elementary reaction, the velocity can be written using the law of mass action. Consider the reaction

$$aA + bB + \cdots \xrightarrow{k} xX + yY + \cdots \tag{4.2}$$

where k is a proportionality constant called the rate constant. The velocity of the reaction is

$$v = k[A]^a[B]^b\cdots \tag{4.3}$$

i.e., a product over all reactants. The "equation of motion" of the reactant A is then

$$\frac{\mathrm{d}[A]}{\mathrm{d}t} = -a\cdot v = -ak[A]^a[B]^b\cdots \tag{4.4}$$

while the "equation of motion" of the product X is

$$\frac{\mathrm{d}[X]}{\mathrm{d}t} = x\cdot v = xk[A]^a[B]^b\cdots \tag{4.5}$$

4.2 Temperature dependency

It is well-known that the rate of a reaction depends on the temperature. Often Arrhenius is regarded as the discoverer of the so-called Arrhenius expression. The expression relates the rate constant k and the absolute temperature T as [67]

$$k = Ae^{-E_a/RT} \tag{4.6}$$

where A is the pre-exponential factor, E_a is the activation energy, and R is the gas constant. A plot of $\log k$ versus $1/T$ is referred to as the Arrhenius plot for the given reaction. By applying simple algebra, we see

$$\log k = \log A - \frac{E_a}{R}\frac{1}{T} \tag{4.7}$$

i.e., an Arrhenius plot should be a straight line with slope $-E_a/R$ and intercept $\log A$.

A more general relationship between the rate constant and the temperature can be derived from collision theory, see *e.g.,* Pilling *et al.* [67]. We imagine that the reaction $A + B \rightarrow P$ (in gas phase) consists of three reactions, namely

$$A + B \rightleftarrows C \tag{4.8a}$$
$$C \rightarrow P \tag{4.8b}$$

where C is a collision complex. In words the idea is the following. The reactants A and B, collide and form a collision complex C. If the energy of impact is larger than a certain threshold E_a, the complex will break up and form the product P, otherwise the reactants are reformed. From collision theory, we the obtain the following expression:

$$k = A'\sqrt{T}e^{-\frac{E_a}{RT}} \tag{4.9}$$

where A' is a pre-exponential factor.

We notice that the equation (4.9) differs from equation (4.6) by a factor of $\sqrt{T}$. In a small temperature interval, $A'\sqrt{T}$ is almost constant, and we will recover the Arrhenius expression.

4.3 Diffusion-controlled reactions

Diffusion may play an important role for reactions in a condensed phase. The basic idea is that two species, say A and B, have to diffuse together before reacting. Diffusion in two dimensions is very different from three dimensions, and we will briefly review the results in this section. The problem has been studied by many chemists *e.g.,* Naqvi [62]. We will here use the results obtained by Clegg [17].

Consider the following reactions in a condensed phase:

$$A + B \underset{k_r}{\overset{k_f}{\rightleftarrows}} C \tag{4.10}$$

where k_f is the rate constant of the forward reaction, and k_r is the rate constant of the reverse reaction.

The solvent does not enter the reactions explicitly, and A and B must diffuse together in order to react. Let D_A and D_B denote the diffusion coefficients of A and B, respectively. Moreover, the sum of the diffusion coefficients is denoted D_{AB} *i.e.,* $D_{AB} = D_A + D_B$. The reaction between A and B occurs when the separation is less than R_{reac} *i.e.,* when $\|\mathbf{r}_A - \mathbf{r}_B\| < R_{\text{reac}}$.

In three dimensions, Clegg [17] finds the following expressions for the rate constants:

$$k_f = \frac{4\pi N_{\text{Av}} D_{AB} R_{\text{reac}}}{1000} \tag{4.11a}$$

$$k_r = \frac{3D_{AB}}{R_{\text{reac}}^2} \tag{4.11b}$$

However, in two dimensions the situation is more complicated. According to Clegg [17], the rate constants are given as:

$$k_f = \frac{2\pi D_{AB} N_{\text{Av}}}{\log\left(\frac{R_1(t)}{R_{\text{reac}}}\right)} \tag{4.12a}$$

$$k_r = \frac{2D_{AB}}{R_{\text{reac}}^2 \log\left(\frac{R_2(t)}{R_{\text{reac}}}\right)} \tag{4.12b}$$

where $R_1(t)$ and $R_2(t)$ are two functions of time.

In both cases, the rate constants depend linearly on the sum of the diffusion coefficients. This leads us to the following conclusion: if a reaction is diffusion-controlled, the ratio k/D must be constant (k is the rate constant of the reaction, and D is the diffusion coefficients of the reactants).

4.4 Oscillating reactions

One of the main topics of this thesis is the simulation of oscillating chemical reactions. In this section, we will briefly discuss oscillating chemical reactions.

Recently, Scott [72] has written an excellent (and short) introduction to oscillating reactions. Oscillations are one of the exotic behaviours we can observe in chemical systems. Quasi periodic oscillations and chaos have been observed, and in distributed systems (reaction-diffusion systems) target patterns and spiral waves have been observed.

As already mentioned in section 4.1, to a set of chemical reactions there is an associated set of differential equations. In its most condensed form, the set of differential equations can be written as

$$\frac{\mathrm{d}\mathbf{c}}{\mathrm{d}t} = \mathbf{f}(\mathbf{c}; \mu) \tag{4.13}$$

where $\mathbf{c}$ is a vector consisting of the concentrations of the species, $\mathbf{f}$ is the velocity field, and μ is a set of parameters. On the mathematical properties of differential equations, the monograph by Hirsch *et al.* [41] gives a good and not too mathematical introduction while Perko [66] treats the subject more rigorously.

4.4.1 Conditions for oscillations

If the solution of equation (4.13) is periodic in time *i.e.,* $\mathbf{c}(t + T) = \mathbf{c}(t)$ for all times t, then we have an oscillating reaction. A number of conditions must be fulfilled in order to obtain a periodic solution. Probably the most important condition is that the system must be open (or at least driven). If the system is closed, the system will seek an equilibrium state *i.e.,* the concentrations will become constant. The equilibrium condition is a consequence of the second law of thermodynamics. It turns out that a crucial condition is that at least one reaction must be autocatalytic, see *e.g.,* Clarke [16]. An autocatalytic reaction is the chemical term of feedback. A simple example of an autocatalytic reaction is

$$A + B \xrightarrow{k} 2A \tag{4.14}$$

4.4.2 Stability

If we look at equation (4.13) we can wonder which mathematical properties the solution might have. We have already discussed the oscillatory behaviour from a chemical point of view. In this section, we will be more mathematical than chemical.

The most simple solution of equation (4.13) is a stationary solution. The stationary solution is the same as a constant solution *i.e.,* $\mathbf{c}(t) = \mathbf{c}_{ss}$ where $\mathbf{c}_{ss}$ is a constant vector. This stationary state is the root of the function $\mathbf{f}$ *i.e.,* the solution of

$$\mathbf{f}(\mathbf{c}_{ss};\mu) = \mathbf{0} \tag{4.15}$$

Now, a stationary state can either be structurally stable, stable or unstable. The stability of the stationary state can be evaluated in the following manner. Consider a small perturbation of the stationary state, $\mathbf{c}_p$. The trajectory is the solution of equation (4.13) with $\mathbf{c}_p$ as the initial state. The question of stability is answered as follows.

Structurally stable The stationary state is structurally stable if $d(t) \equiv \|\mathbf{c}(t) - \mathbf{c}_{ss}\| \to 0$ as $t \to \infty$ where $\|\cdot\|$ is a measure of the distance in the concentration space.

Unstable If the function $d(t)$ diverges as $t \to \infty$, we say that the stationary state is unstable.

Stable If $d(t)$ is bounded but does not go to zero as $t \to \infty$ we say that the stationary state is stable. If the chemical reaction is oscillatory, its trajectory in the concentration space is bounded but does not approach the stationary state *i.e.*, an oscillating chemical reaction has a stable stationary state.

The stability can easily be computed. Let $\delta\mathbf{c}$ be defined as $\delta\mathbf{c}(t) \equiv \mathbf{c}(t) - \mathbf{c}_{ss}$. The function $d(t)$ is related to $\delta\mathbf{c}$ as $d(t) = \|\delta\mathbf{c}\|$. If we Taylor expand the velocity field to first order, we obtain

$$\frac{\mathrm{d}\delta\mathbf{c}}{\mathrm{d}t} = \mathbf{J}(\mathbf{c}_{ss}) \cdot \delta\mathbf{c} \tag{4.16}$$

where $\mathbf{J}$ is the Jacobian matrix which elements are given as

$$J_{ij} = \frac{\partial f_i}{\partial c_j} \tag{4.17}$$

Equation (4.16) is a linear ordinary differential equation, and the solution is a textbook example. The solution is

$$\delta\mathbf{c} = \sum_j \mathbf{e}_j e^{\imath\omega_j t} \tag{4.18}$$

where $\mathbf{e}_j$ is the jth eigenvector of the Jacobian matrix and ω_j is the associated eigenvalue. The stability of the stationary point can now be summarised:

Structurally stable If the real part of the any eigenvalue is negative, the stationary point is structurally stable.

Stable The stationary point is stable, if the eigenvalues has zero real parts.

Unstable If one eigenvalue has a positive real part, the stationary state is unstable.

4.4.3 An example

At this point an example would be appropriate. Let us consider the famous reaction mechanism called the Brusselator [69]. The mechanism is

$$A \xrightarrow{k_1} X \tag{4.19a}$$
$$2X + Y \xrightarrow{k_2} 3Y \tag{4.19b}$$
$$B + X \xrightarrow{k_3} Y + C \tag{4.19c}$$
$$X \xrightarrow{k_4} D \tag{4.19d}$$

The species of interest are X and Y, and the concentrations of A and B are assumed to be constant. The phenomenological equations for X and Y can be written down. If we scale them appropriately, we have

$$\frac{\mathrm{d}x}{\mathrm{d}t} = f(x,y) = A - (B+1)x + x^2 y \tag{4.20a}$$
$$\frac{\mathrm{d}y}{\mathrm{d}t} = g(x,y) = Bx - x^2 y \tag{4.20b}$$

where x and y are the scaled concentrations of X and Y, and A and B are the constant concentrations of species A and B. The stationary point (x_{ss}, y_{ss}) can found by solving the set of equations:

$$f(x_{ss}, y_{ss}) = A - (B+1)x_{ss} + x_{ss}^2 y_{ss} = 0 \tag{4.21a}$$
$$g(x_{ss}, y_{ss}) = Bx_{ss} - x_{ss}^2 y_{ss} = 0 \tag{4.21b}$$

The stationary point is $x_{ss} = A$ and $y_{ss} = \frac{B}{A}$. In order to evaluate the stability of the stationary point, we first find the Jacobian matrix. It is:

$$\mathbf{J}(x_{ss}, y_{ss}) = \begin{pmatrix} B-1 & A^2 \\ -B & -A^2 \end{pmatrix} \tag{4.22}$$

The eigenvalues are the solutions of a quadratic equation *i.e.,*

$$\omega^2 + (A^2 - B + 1)\omega + A^2 = 0 \tag{4.23}$$

We see that the stationary point is structurally stable if $A^2 - B + 1 > 0$ and $(A^2 - B + 1)^2 - 4A^2 < 0$. Moreover, we will have a stable stationary point if $A^2 - B + 1 = 0$ and $A^2 - B + 1 < 0$ (which implies $B > 1$). In the stable case the solution close to the stationary point will be oscillatory *i.e.,* under certain conditions ($B > 1$) the Brusselator will be an oscillating reaction.

CHAPTER 5

Inelastic Collisions

Systems consisting of particles undergoing inelastic collisions do have a phenomenology of their own. Inelastic collisions are often used in models of granular media, see *e.g.,* Jaeger *et al.* [44]. This chapter will discuss the physical properties of granular media and how inelastic collisions can be modelled. In chapter 8 simulational results obtained by the author of this thesis and his collaborators can be found.

5.1 Hard particles

Hard or rigid particles move, in the absence of an external field, on straight lines between two collisions. The interaction between the particles are through the collisions only. At the collision of two particles, i and j, the velocity of each particle is changed instantaneously. Let $\mathbf{v}_i$ and $\mathbf{v}_j$ denote the velocity before collision, and $\mathbf{v}_i'$ and $\mathbf{v}_j'$ denote the velocity after the collision of particle i and j, respectively. They are related as:

$$\mathbf{v}_i' = \epsilon\mathbf{v}_i + (1-\epsilon)\mathbf{v}_j \tag{5.1a}$$

$$\mathbf{v}_j' = (1-\epsilon)\mathbf{v}_i + \epsilon\mathbf{v}_j \tag{5.1b}$$

where ϵ is a measure of inelasticity and is related to the coefficient of restitution r, as $\epsilon = \frac{1}{2}(1-r)$. In the case of elastic collisions the value of ϵ is 0, and completely sticky collisions $\epsilon = \frac{1}{2}$.

5.2 Soft particles

The rigid particles which were discussed in the previous section move in straight lines between two collisions. When we turn to soft particles, it is a completely different story. The particles move in a potential field and collisions are not well-defined.

Models for granular media using soft particles have recently been proposed independently by Brilliantov *et al.* [11] and Morgado *et al.* [59]. The purpose here is not to review the complete work by Brilliantov *et al.* and Morgado *et al.* but merely to state a simple model which we will use in chapter 8. Our model is only usable in one dimension.

First, let us define what a collision is for soft particles. Consider two particles with separation r. We will say that the two particles are colliding when the separation is less that a given value r_{coll} *i.e.,* when $r < r_{\text{coll}}$. For soft particles, collisions have a duration *i.e.,* the collisions are not instantaneous as collisions of rigid particles.

Elastic colliding particles move according to given equations of motion *i.e.,* equations in the form:

$$\frac{\mathrm{d}\mathbf{r}_i}{\mathrm{d}t} = \mathbf{v}_i \tag{5.2a}$$

$$\frac{\mathrm{d}\mathbf{v}_i}{\mathrm{d}t} = \frac{\mathbf{F}_i}{m_i} \tag{5.2b}$$

where $\mathbf{r}_i$ is the position of particle i, $\mathbf{v}_i$ the velocity, m_i the mass, and $\mathbf{F}_i$ the force. We will modify the equations of motion so that they include a dissipative term which accounts for the inelastic collisions. The new equations of motion are:

$$\frac{\mathrm{d}\mathbf{r}_i}{\mathrm{d}t} = \mathbf{v}_i \tag{5.3a}$$

$$\frac{\mathrm{d}\mathbf{v}_i}{\mathrm{d}t} = \frac{1}{m_i}\left(\mathbf{F}_i - \mathbf{F}_i^{(\text{coll})}\right) \tag{5.3b}$$

where $\mathbf{F}_i^{(\text{coll})}$ is the dissipative force due to the collisions. The force is given by

$$\mathbf{F}_i^{(\text{coll})} = \sum_{j \neq i} \mathbf{F}_{ij}^{(\text{coll})} \tag{5.4}$$

with

$$\mathbf{F}_{ij}^{(\text{coll})} = \begin{cases} -\gamma v_{ij}\sqrt{r_{\text{coll}} - r_{ij}} & \text{for } r < r_{\text{coll}} \\ 0 & \text{otherwise} \end{cases} \tag{5.5}$$

where $r_{ij} = \|\mathbf{r}_i - \mathbf{r}_j\|$ and $v_{ij} = \|\mathbf{v}_i - \mathbf{v}_j\|$. The parameter γ controls the degree of inelasticity and when $\gamma = 0$ the collisions are elastic.

5.3 The cooling problem

Haff [37] and McNamara *et al.* [54] have investigated the problem of rigid particles undergoing inelastic collisions. At every collision kinetic energy dissipates from the system. The (granular) temperature is closely related to the kinetic energy, namely as

$$\mathcal{T} \equiv \frac{1}{N}\sum_{i=1}^{N} v_i^2 = \frac{2}{m}E_{\text{kin}} \tag{5.6}$$

The definition of the temperature as given by the equation above is not correct according to the statistical-mechanical relation. The deviation is the factor $1/N$. In statistical mechanics one would find that it should be the degrees of freedom which for a one-dimensional system in equilibrium is $N-1$. The definition above is adopted of two reasons. First, it has previously been used in the literature and second, we wish to compare the temperature of simulations of both equilibrium and non-equilibrium systems in chapter 8.

As the energy dissipates the temperature is decreasing. Naively one could imagine that the temperature will decay exponentially but the collision rate (collisions per unit time) does depend on the temperature. After one collision the collision rate is slightly lower and the time until the next collision is larger. This physical behaviour leads to the following cooling law [54]:

$$\mathcal{T}(t) = \frac{\mathcal{T}_0}{(1 + \epsilon\rho\mathcal{T}_0 t)^2} \tag{5.7}$$

where t is the time, $\mathcal{T}_0$ is the temperature at time $t = 0$, and ρ is the density. At late times, $t \gg 1$, the cooling law reduces to

$$\mathcal{T} = at^{-2} \tag{5.8}$$

where a is a parameter which depends on ϵ and ρ.

The cooling law is a theoretical prediction by Haff [37] and McNamara *et al.* [54]. McNamara *et al.* [54, 55] have numerically investigated rigid particles in one and two dimensions, and they find that the cooling law is obeyed. It is important to stress that the cooling law discussed here is valid for rigid particles only. In chapter 8 we will study systems of rigid and soft particles numerically and try to apply a more general cooling law, namely $\mathcal{T} \propto t^{\alpha}$.

5.4 Clustering and inelastic collapse

As discussed in section 5.3 a system of inelastic particles will algebraically cool down. It has been observed by *e.g.*, Goldhirsch *et al.* [31] that in some cases clusters are formed; they refer to this phenomenon as a clustering instability. The physical origin of clustering can be explained as follows: a spontaneous fluctuation in the density occurs. The temperature is uniform, and when the density is locally slightly larger in one region, the collision rate in that region will be larger. The larger collision rate leads to a faster dissipation *i.e.*, the temperature decays faster in this region that the rest of the system. Now, when the temperature is lower, the pressure will be lower. The pressure gradient will attract particles to the region *i.e.*, the density will increase. We see that a fluctuation large enough will lead to an increasing inhomogenity, and the clustering has occured. Goldhirsch *et al.* [31] have performed Molecular Dynamics simulations (in two dimensions) of 2×10^5–4×10^5 rigid particles, and they show that clustering is dependent on the system size.

McNamara *et al.* [54, 55] have observed in one and two dimensions another phenomenon might occur. In some cases inelastic colliding particles might end up in an inelastic collapse. The physics of the inelastic collapse is that three or more particles are aligned with no separation in between. The consequence is that the number of collisions goes to infinity. The collapse depends on the number of particles. If the number of particles exceeds a certain treshold value, N_{min}, the collapse might occur. NcNamara *et al.* estimate the value in the elastic limit to be

$$N_{\text{min}} = \frac{\log(2/\epsilon)}{2\epsilon} \tag{5.9}$$

Du *et al.* [20] discuss breakdown of hydrodynamics for many-particle systems undergoing inelastic collisions. The breakdown reported by Du *et al.* is not an inelastic collapse but close to the clustering instability. It is not too obvious whether the breakdown is exactly the same as the clustering or not because the system

studied by Du *et al.* is coupled to a thermostating device. In chapter 8 we will analyse the thermostating of inelastic particles more closely, and present our own simulational results.

5.5 Closing remarks

Granular media have an interesting and odd phenomenology, and it is not an exaggeration to say that granular media are a state of matter distinct from the ordinary three states.

Many problems are still open. Granular media can in many cases be regarded as a liquid, but no fluid dynamics has been developed. Of course a number of attempts has been made, see *e.g.*, Haff [37] and Jenkins *et al.* [45], but no complete theory exists yet. The mixing and transport of grains and powders are heavily used in industrial processes, and therefore a development of a fluid mechanics for granular media is important for the design, optimisation, and control of industrial processes.

CHAPTER 6

Numerical Techniques

The results presented in the present thesis are based upon numerical simulations. The simulational techniques used are the "experimental setup" which has been used. All simulation programs which have been designed and implemented, are of the Molecular Dynamics (MD) type. This chapter describes the MD techniques.

The core of the chapter is about soft particles *i.e.,* systems where the particles interact through a smooth potential. The simulation of hard spheres are discussed in section 6.6.

In the last decade a number of monographs on computer simulations has been published. Allen *et al.* [2] have written the most well-known and cited monograph. It is now a bit out-of-date. While the monograph by Allen *et al.* dealt with both Molecular Dynamics and Monte Carlo techniques, the book by Rapaport [71] is considering MD only. Smith *et al.* [23] have recently written a book about molecular simulations, and it is more focused on the physics behind the simulations while Rapaport is more concerned with the algorithms.

6.1 Naive algorithm

In chapter 2 classical mechanics was discussed. The naive idea behind Molecular Dynamics is to solve the equations of motion of N particles *i.e.,* it is a numerical technique which enable us to solve

$$\frac{\mathrm{d}\mathbf{r}_i}{\mathrm{d}t} = \mathbf{v}_i \tag{6.1a}$$

$$\frac{\mathrm{d}\mathbf{v}_i}{\mathrm{d}t} = \frac{\mathbf{F}_i}{m_i} \tag{6.1b}$$

where $\mathbf{r}_i$ is the position of particle i, $\mathbf{v}_i$ the velocity, $\mathbf{F}_i$ the force, and m_i the mass. We will assume that the force is pairwise additive *i.e.*,

$$\mathbf{F}_i = \sum_{j=1}^{N} \mathbf{F}_{ij} \tag{6.2}$$

where $\mathbf{F}_{ij}$ is the force between particle i and j.

The naive algorithm is:

Algorithm 1 A naive MD program

for $i = 1$ to M **do** $\{M$ is the number of time steps$\}$
  `CalcForce`($\mathbf{r}_1, \ldots, \mathbf{r}_N, \mathbf{F}_1, \ldots, \mathbf{F}_N$)
  `Integrate`($\mathbf{r}_1, \ldots, \mathbf{r}_N, \mathbf{v}_1, \ldots, \mathbf{v}_N, \mathbf{F}_1, \ldots, \mathbf{F}_N$)
end for

where the two procedures `CalcForce` and `Integrate` are given as algorithm 2 and algorithm 3, respectively.

Algorithm 2 A naive force calculation algorithm, `CalcForce`

Require: $\mathbf{r}_1, \ldots, \mathbf{r}_N, \mathbf{F}_1, \ldots, \mathbf{F}_N$
for $i = 1$ to N **do**
  $\mathbf{F}_i \leftarrow \mathbf{O}$
end for
for $i = 1$ to N **do**
  for $j = 1$ to N **do**
    $\mathbf{F}_i \leftarrow \mathbf{F}_i + \mathbf{F}_{ij}(\mathbf{r}_i, \mathbf{r}_j)$
  end for
end for

In algorithm 3 the equations of motion are solved in a very primitive way. We have approximated the derivatives by the well-known approximation

$$\frac{\mathrm{d}y}{\mathrm{d}x} \approx \frac{y(x+h) - y(x)}{h} \tag{6.3}$$

Algorithm 3 A naive integration algorithm, `Integrate`

Require: $\mathbf{r}_1, \ldots, \mathbf{r}_N$, $\mathbf{v}_1, \ldots, \mathbf{v}_N$, $\mathbf{F}_1, \ldots, \mathbf{F}_N$
  for $i = 1$ to N **do** $\{h$ is the length of the time step$\}$
    $\mathbf{v}_i \leftarrow \mathbf{v}_i + h \times \frac{1}{m_i}\mathbf{F}_i$
    $\mathbf{r}_i \leftarrow \mathbf{r}_i + h \times \mathbf{v}_i$
  end for

where h is a small number.

The algorithm has one major problem: its time consumption. We see that there are two loops in `CalcForce` - both of length N. The time complexity is $\mathcal{O}(N^2)$, and in a later section we will address this problem.

6.2 Integrator

The integrator in an MD program is the part where the positions and velocities are updated as done by the procedure `Integrate` in algorithm 1.

The equations of motion in classical mechanics are time reversible *i.e.,* there is no distinction between the past and the future. Furthermore, the equations of motion are symplectic *i.e.,* the total energy is conserved, see *e.g.,* Arnold [4] and Goldstein [32].

The two properties mentioned above must be incorporated into the algorithm since it will make the algorithm more (numerically) stable, see *e.g.,* Martyna *et al.* [53], Miller [57] and Toxværd [77].

6.2.1 NVE simulations

The equations of motion as given by equation (6.1) conserve the total energy and is characterised by a constant number of particles N, volume V and energy E.

In order to derive a suitable algorithm, we begin by Taylor expanding equation (6.1a) to first order *i.e.,*

$$\begin{aligned} \mathbf{r}_i(t + \tfrac{1}{2}h) &= \mathbf{r}_i(t) + \tfrac{1}{2}h\mathbf{v}_i(t) \\ \mathbf{r}_i(t - \tfrac{1}{2}h) &= \mathbf{r}_i(t) - \tfrac{1}{2}h\mathbf{v}_i(t) \end{aligned}$$

where h is a small number (called the length of the time step). By subtraction we obtain

$$\mathbf{r}_i(t + \tfrac{1}{2}h) = \mathbf{r}_i(t - \tfrac{1}{2}h) + h\mathbf{v}_i(t)$$

A similar expansion is done for (6.1b) and we obtain

$$\mathbf{v}_i(t + h) = \mathbf{v}_i(t) + \frac{\mathbf{F}_i(t)}{m_i}h$$

The equations above leads us to a suitable algorithm for integrating the equations of motion which is found in algorithm 4.

Algorithm 4 Integration of the NVE ensemble

Require: $\mathbf{r}_i, \mathbf{v}_i, \mathbf{F}_i$
  for $i = 1$ to N **do**
    $\mathbf{r}_i \leftarrow \mathbf{r}_i + h\mathbf{v}_i$
    $\mathbf{v}_i \leftarrow \mathbf{v}_i + \frac{\mathbf{F}_i}{m_i}h$
  end for

6.2.2 NVT simulations

In the previous section we discussed how to integrate the equations of motion of a general many-body system. The equations of motion conserve the total energy *i.e.,* the sum of the potential and kinetic energy. This is not what we want in many cases - often we wish to be able to control the temperature. As discussed in section 2.4 the Hamiltonian must be modified in order to simulate the canonical ensemble, and Nosé [63] has proposed such an extension. The proposed Hamiltonian $\mathcal{H}$ is

$$\mathcal{H} = \mathcal{H}_{NVE} + \overbrace{\sum_{i=1}^{N} \frac{\mathbf{p}_i^2}{2m_i s^2} + gk_BT\log s + \frac{p_s^2}{2Q}}^{\text{the Nosé-thermostat}} \tag{6.4}$$

where $\mathcal{H}_{NVE}$ is the NVE Hamiltonian, g the degrees of freedom (plus one), s and p_s represent the "thermostat", Q is the relaxation time, and T is the temperature. Hoover [42] has extended this further and refined the argumentation. Hoover notices that the Nosé-Hoover thermostat is unique *i.e.,* any extension expect the Nosé-Hoover extension will not relax to a canonical equilibrium. The idea behind the thermostat is that all particles are coupled to a heat reservoir which is simulated through two extra variables s and p_s.

A more practical form is [76]

$$\frac{\mathrm{d}\mathbf{r}_i}{\mathrm{d}t} = \frac{\mathbf{p}_i}{m_i} \tag{6.5a}$$

$$\frac{\mathrm{d}\mathbf{p}_i}{\mathrm{d}t} = \mathbf{F}_i - \eta\mathbf{p}_i \tag{6.5b}$$

$$\frac{\mathrm{d}\eta}{\mathrm{d}t} = \left(\sum_{i=1}^{N}\frac{\mathbf{p}_i^2}{m_i} - gk_BT\right)/Q \tag{6.5c}$$

where $Q = gk_BT\tau^2$ and τ is the relaxation time. In order to derive a discrete version of the equations above, we Taylor expand equation (6.5a):

$$\mathbf{r}_i(t+h) = \mathbf{r}_i(t+\tfrac{1}{2}h) + \tfrac{1}{2}h\frac{\mathbf{p}_i(t+\frac{1}{2}h)}{m_i} \tag{6.6a}$$

$$\mathbf{r}_i(t) = \mathbf{r}_i(t+\tfrac{1}{2}h) - \tfrac{1}{2}h\frac{\mathbf{p}_i(t+\frac{1}{2}h)}{m_i} \tag{6.6b}$$

These expansions may not be obvious at first glance; by subtraction and rearrangement we obtain

$$\mathbf{r}_i(t+h) = \mathbf{r}_i(t) + h\frac{\mathbf{p}_i(t+\frac{1}{2}h)}{m_i} \tag{6.7}$$

Admitted - this might not have enlightened the reader, but we proceed. Taylor expansions of equation (6.5b) to first order give

$$\mathbf{p}_i(t+\tfrac{1}{2}h) = \mathbf{p}_i(t) + \tfrac{1}{2}h(\mathbf{F}_i(t) - \eta(t)\mathbf{p}_i(t)) \tag{6.8a}$$

$$\mathbf{p}_i(t-\tfrac{1}{2}h) = \mathbf{p}_i(t) - \tfrac{1}{2}h(\mathbf{F}_i(t) - \eta(t)\mathbf{p}_i(t)) \tag{6.8b}$$

Subtracting the second equation from the first, we obtain

$$\mathbf{p}_i(t+\tfrac{1}{2}h) - \mathbf{p}_i(t-\tfrac{1}{2}h) = h(\mathbf{F}_i(t) - \eta(t)\mathbf{p}_i(t)) \tag{6.9}$$

We do not know the momentum $\mathbf{p}_i$ at time t but we use a simple relation to compute it, namely

$$\mathbf{p}_i(t) = \frac{\mathbf{p}_i(t+\frac{1}{2}h) + \mathbf{p}_i(t-\frac{1}{2}h)}{2}$$

Inserting this relation into equation (6.9) and rearranging it a bit, we obtain

$$\mathbf{p}_i(t+\tfrac{1}{2}h) = \frac{h\mathbf{F}_i(t) + (1-\tfrac{1}{2}h\eta(t))\mathbf{p}_i(t-\tfrac{1}{2}h)}{1+\tfrac{1}{2}h\eta(t)} \tag{6.10}$$

We still need to derive a suitable expression for the thermostat *i.e.*, the variable η and equation (6.5c). Two Taylor expansions result in

$$\eta(t+h) = \eta(t+\tfrac{1}{2}h) + \tfrac{1}{2}h\left(\sum_{i=1}^{N}\frac{\mathbf{p}_i^2(t+\tfrac{1}{2}h)}{m_i} - gk_BT\right)/Q \tag{6.11a}$$

$$\eta(t) = \eta(t+\tfrac{1}{2}h) - \tfrac{1}{2}h\left(\sum_{i=1}^{N}\frac{\mathbf{p}_i^2(t+\tfrac{1}{2}h)}{m_i} - gk_BT\right)/Q \tag{6.11b}$$

By subtraction and a bit of rearrangement we obtain

$$\eta(t+h) = \eta(t) + h\left(\sum_{i=1}^{N}\frac{\mathbf{p}_i^2(t+\tfrac{1}{2}h)}{m_i} - gk_BT\right)/Q \tag{6.12}$$

We are now ready to give an algorithm which updates the positions and momenta of N particles in the canonical ensemble. The algorithm is shown as algorithm 5.

Algorithm 5 Integration of the NVT ensemble using the Nosé-Hoover thermostat

Require: $\mathbf{r}_i$, $\mathbf{p}_i$, $\mathbf{F}_i$, η
  $E_{\text{kin}} \leftarrow 0$
  for $i = 1$ to N **do**
    $\mathbf{p}_i \leftarrow (h \times \mathbf{F}_i + (1 - \tfrac{1}{2}h \times \eta)\mathbf{p}_i)/(1 + \tfrac{1}{2}h\eta)$
    $\mathbf{r}_i \leftarrow \mathbf{r}_i + h \times \mathbf{p}_i/m_i$
    $E_{\text{kin}} \leftarrow E_{\text{kin}} + \mathbf{p}_i^2$
  end for
  $\eta \leftarrow \eta + h \times (E_{\text{kin}}/m_i - gk_BT)/Q$
  $E_{\text{kin}} \leftarrow E_{\text{kin}}/2$

6.3 Optimisation of force calculation

The computation of the force contributions is the most time consuming part of an MD program: this is the part of algorithm 1 that gives the square dependency of

the number of particles. Of course the computations can be reduced by a factor of 2 by applying the rule $F_{ij} = -F_{ji}$. But a factor of two is not changing the $\mathcal{O}(N^2)$ complexity.

One very simple optimisation of the force calculation is to truncate the potential. In the system investigated in the present thesis, the potential is short-ranged *i.e.*, the interaction is very weak between two particles with large separation. The truncated potential $\tilde{u}(r)$ is

$$\tilde{u}(r) = \begin{cases} u(r), & \text{for } r \leq r_c, \\ 0, & \text{otherwise} \end{cases} \tag{6.13}$$

where $u(r)$ is the original potential. The choice of the truncation distance r_c is not unique and is a compromise. On one hand we want a value as small as possible because this will lead to fewer calculations. On the other hand we want a larger value, because it will lead to a smaller truncation error. The number of particles in a circle[1] of radius r_c is $\pi r_c^2 \rho$ where ρ is the density of the system. When simulating Lennard-Jones liquids a typical value for r_c is 2.5σ and consequently the number of neighbours within this distance is about 15.

The truncation of the potential leads to an (almost) constant number of force calculations per particle, and the time complexity is apparently linear. This linearity is not true, since we still have to check the distance between all pairs of particles which gives us a square time complexity.

The optimisation discussed above is not enough if Molecular Dynamics simulations are going to be a practical tool for investigating many-body systems. Many techniques have been proposed but here we will only discuss one of them.

The basic idea is shown in figure 6.1. The simulation cell is partitioned into a number of equally sized boxes. The edge length r_b, is larger than the truncation length r_c discussed previously. The particles is each box may interact (the maximum distance between two particles is $\sqrt{2}r_b$ which is larger than r_c). In the near future *i.e.*, a low number of time steps (typically 10), the particles will remain in the same square. The particles in the black square in figure 6.1 may also interact with the particles in the four shaded squares. Of course the particles may also interact with particles in the four other neighbouring squares but this is included because $F_{ij} = -F_{ji}$. Therefore we construct a list of pairs of possibly interacting particles and use this list in the near future when computing the force. It has been observed by Morales *et al.* [58] that this optimisation trick reduces the time complexity to $\mathcal{O}(N \log N)$ where N is number of particles.

The optimisation strategy discussed above can be expressed as algorithm 6.

[1] Remember that we are mainly interested in systems with two spatial dimensions.

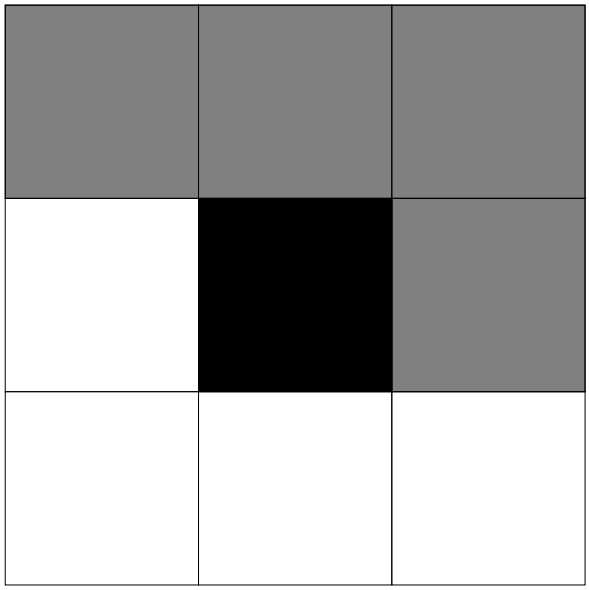

Figure 6.1: The simulation is partitioned into a number of squares. The particles in the four shaded squares may interact with the ones in black square.

Algorithm 6 Optimerised force calculation

for $p = 1$ to M **do** $\{M$ is the number of time steps$\}$
  if $\mod(p, N_{\text{update}}) = 1$ **then**
    `PutInBox`($\mathbf{r}_k$, r_b, H, L)
    `MakeList`($\mathbf{r}_k$, r_b, H, L, $\{i, j\}$)
  end if
  `CalcForce`($\mathbf{r}_k$, $\mathbf{F}_k$, $\{i, j\}$)
  `Integrate`($\mathbf{r}_k$, $\mathbf{v}_k$, $\mathbf{F}_k$)
end for

The procedure `PutInBox` sorts the particles into boxes according to their positions. The algorithm is given by algorithm 7. The function $\lceil x \rceil$ returns the largest integer i, that fulfills $i \leq x$, where x is a real number.

Algorithm 7 `PutInBox`: Sort particles

Require: $\mathbf{r}_k$, r_b, L
  for $i = 1$ to C^2 **do** $\{C$ is the number of cells in each direction$\}$
    $H_i \leftarrow 0$ {Head of list for each cell}
  end for
  for $i = 1$ to N **do**
    $j \leftarrow 1 + \lceil x_i/r_b \rceil \times C + \lceil y_i/r_b \rceil \times C^2$ $\{\mathbf{r}_i = (x_i, y_i)\}$
    $L_i \leftarrow H_j$ $\{L$ is a collection of linked-list of particles$\}$
    $H_j \leftarrow i$
  end for

The procedure `MakeList` makes a list, $\{i, j\}$, with N_p elements which is a list of potentially interacting pairs of particles. The algorithm is given as algorithm 8. For simplicity, we have in algorithm 8 neglected the loop over the neighbouring boxes.

Algorithm 8 `MakeList`: Make a list of potentially interacting pairs

Require: $\mathbf{r}_k$, r_b, H, L, N_p, $\{i, j\}$
  $N_p \leftarrow 0$ {N_p is the number of pairs}
  for $k = 1$ to C^2 **do**
    $i \leftarrow H_k$
    while $i \neq 0$ **do**
      $j \leftarrow H_i$
      while $j \neq 0$ **do**
        if $\|\mathbf{r}_i - \mathbf{r}_j\| \leq r_b$ **then**
          $N_p \leftarrow N_p + 1$ {A new pair}
          $\{i, j\}_{N_p} \leftarrow (i, j)$
        end if
        $j \leftarrow L_j$
      end while
    end while
    $i \leftarrow L_i$
  end for

Finally, the force calculation procedure, `CalcForce`, can be redesigned so that it takes advantage of the list of potentially interacting pairs. The algorithm is shown

as algorithm 9. The function `Force` calculates the force between two particles at a given distance.

Algorithm 9 `CalcForce`: the core of the force calculation

Require: $\mathbf{r}_k$, $\mathbf{F}_k$, N_p, $\{i, j\}$
  for $m = 1$ to N **do** {Reset forces}
    $\mathbf{F}_i \leftarrow \mathbf{0}$
  end for
  for $m = 1$ to N_p **do** {Loop over all pairs}
    $(i, j) \leftarrow \{i, j\}_m$
    $\Delta\mathbf{r} \leftarrow \mathbf{r}_i - \mathbf{r}_j$
    if $\|\Delta\mathbf{r}\| < r_c$ **then**
      $\mathbf{f} \leftarrow$ `Force`$(\Delta\mathbf{r})$
      $\mathbf{F}_i \leftarrow \mathbf{F}_i + \mathbf{f}$
      $\mathbf{F}_j \leftarrow \mathbf{F}_j - \mathbf{f}$
    end if
  end for

Figure 6.2 shows the execution time as function of the number of particles for an MD program written by the author. We see that the execution time grows almost linearly but this might come from the fact that the data can easily be contained in the second-level cache.

6.4 Simulating chemical reactions

One of the main interests in the work behind the present thesis is chemical reactions. Traditionally, chemical reactions have not been simulated by Molecular Dynamics, but a number of papers exist, see *e.g.*, Diebner *et al.* [19], Heinrichs *et al.* [40], and Ortoleva *et al.* [64]. The emphasis in these papers has been on the chemical reactions and their properties. The work presented here is of another nature - we wish to investigate the interplay between phase transitions and oscillating chemical reactions.

In Nature two different types of reactions exist: uni- and bimolecular reactions. Unimolecular reactions involve one molecule only. A typical reaction of this type is the relaxation of an excited molecule which might dissociate it. Two molecules are involved in the bimolecular reactions - a simple picture may be that two molecules collide and something (the reaction) happens.

We have chosen two very simple strategies in order to simulate uni- and bimolecular reactions. The unimolecular reaction ($A \rightarrow P$) is a change in the label

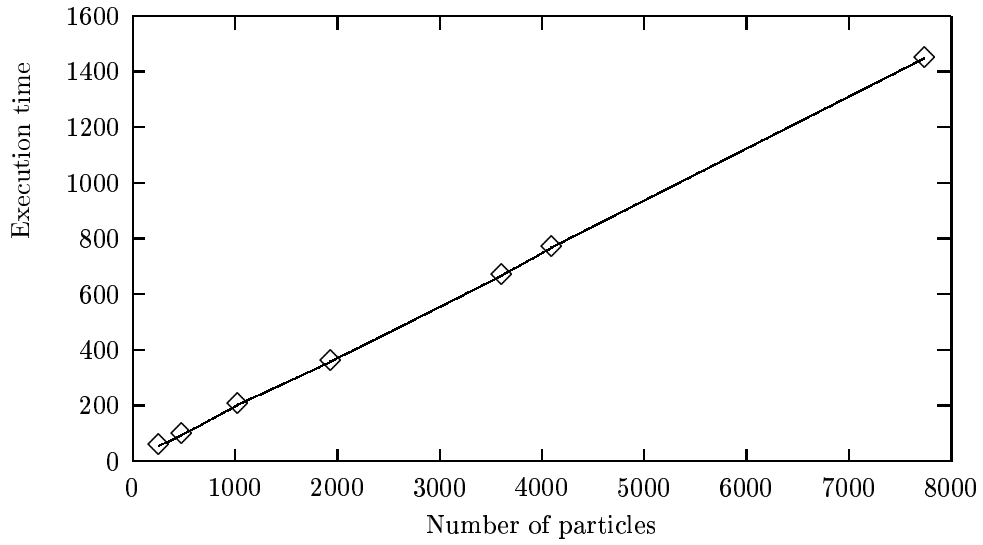

Figure 6.2: The execution time (in seconds) versus the number of particles. The density is $0.8\sigma^2$, and the temperature is $2\epsilon/k_B$. The execution time is the mean of 5 runs. The test was performed on an IBM RS/6000 Model 390 running AIX version 4.0. The compilation was performed using the `xlf` compiler.

or colour of the particle. We modify the colour with a given probability P_r. The algorithm is shown below.

Algorithm 10 Performs the reaction $A \rightarrow P$

```
for i = 1 to N do
  p ← RandUnit {Returns a uniformly distributed random number}
  if p ≤ P_r then {P_r is the reaction probability}
    Alter i's label from A to P
  end if
end for
```

A bimolecular reaction involves two molecules. The general reaction is $A + B \rightarrow P + Q$. The naive idea is to let the reaction occur when A and B collide, but since most of the work presented here is from studies of Lennard-Jones particles, collisions are not a well-defined term. We *define* a collision to be the event where two particles i and j are close *i.e.*, the distance is less than a given number R_{reac}. Moreover, we let the reaction happen with a given probability P_r only. The algorithm shown below uses the list of potentially interacting pairs coming from algorithm 6 since we know that these particles will also be the potentially reacting particles.

Algorithm 11 Performs the reaction $A + B \rightarrow P + Q$

Require: $\{i, j\}_k$
  for $k = 1$ to N_p **do**
    $(i, j) \leftarrow \{i, j\}_k$
    $\Delta r \leftarrow \|\mathbf{r}_i - \mathbf{r}_j\|$
    if $\Delta r \leq R_{\text{reac}}$ **then**
      $p \leftarrow$ `RandUnit`
      if $p \leq P_r$ **then**
        Modify the labels of particles i and j
      end if
    end if
  end for

The parameters, R_{reac} and P_r, introduced above define the reaction rate. The rate of a reaction is, in traditional chemical kinetics, measured by the rate constant; see section 6.7.1 for details about the measurement of the rate constants. One of the most successful theories of reaction rate is the collision theory, see *e.g.*, Pilling *et al.* [67]. The idea behind the collision theory of reaction rates is that two reactants, X and Y, collide and form an encounter pair, C. The encounter pair will either form the reactants again or a product, P. In terms of reactions, the reaction $X+Y \rightarrow P$ is the overall reaction of the three subreactions $X+Y \rightleftarrows C \rightarrow P$. Let $\mathbf{r}_X$ and $\mathbf{r}_Y$ denote the centre of mass of the two reactant molecules, respectively. A collision is then the event that $\|\mathbf{r}_X - \mathbf{r}_Y\| \leq R_{\text{reac}}$ *i.e.*, the distance between the reactants is less than some predefined value, R_{reac}. When the reactants are closer to each other that R_{reac}, they form the encounter pair C. The encounter pair will - as already mentioned - form either the products or the reactants. The probability of forming the product is P_r, and the probability of a non-reactive collision (forming the reactants) is $1 - P_r$.

6.5 Parallelisation

The modern supercomputer is a parallel computer, and the use of these computers becomes more and more popular. Two different approaches to the parallel computer exist; distributed and shared memory computers, see *e.g.*, Tanenbaum [73]. The characteristics are:

Shared memory A number of processors (cpus) are using the same pool of storage (or memory) and system resources *e.g.*, I/O units. A computer of this type is PowerChallenger (Silicon Graphics Inc.). If processor i needs a

piece of data, it can read it at any time in the storage independent of what processor j is doing.

Distributed memory Each processor has a private storage and often private I/O units. When processor i needs data stored in processor j's storage, a communication link is established. The communication is slow compared to direct access to the storage, and communication must be minimised. This type of parallel computer can be built by a number of connected workstations. Typical high-end solutions are RS/6000 SP (International Business Machines) and T3E (Cray Research).

We have had access to an RS/6000 SP computer situated at Uni•C[2] and in the following we will describe our parallelisation strategy.

Systems simulated by Molecular Dynamics are spatial by their nature. It is "obvious" to let a number of processors simulate a region of the simulation cell each. This is the idea behind the parallelisation strategy called domain decomposition, see *e.g.*, Brown *et al.* [12]. Figure 6.3 shows a simulation cell which has been divided into four domains. The particles which are situated in a given domain, are simulated by a given processor *i.e.,* each processor simulates a region of the simulation cell. When a particle moves out of the domain of one processor and into the domain of the neighbouring processor, its position and velocity is sent to the new processor.

In section 6.3 we discussed an optimisation strategy, namely dividing the simulation cell into a number of boxes. The boxes are much smaller than the simulation cell, and even with the domain decomposition many boxes will reside on each processor. Of course we can still use the box idea, and even better, we can use it for optimising the domain decomposition. At each time step in principle each processor needs to know the positions of all particles in order to calculate the forces. But the idea behind the optimisation trick in section 6.3 is that particles far from each other will not interact. Therefore only particles which are located in the subcells close to the boundaries of a processor's domain will interact with the particles situated on the neighbouring processor. Then, only the positions of these particles have to be communicated.

Figure 6.4 shows the execution times for a Molecular Dynamics program which has been parallelised by the domain decomposition. We do not see a linear speed-up but up to 8 processors we only "pay" 25 percent of the execution time for parallelisation.

[2]The Danish Computing Centre for Research and Education. The home page of the computer is `http://www.sp2.uni-c.dk`.

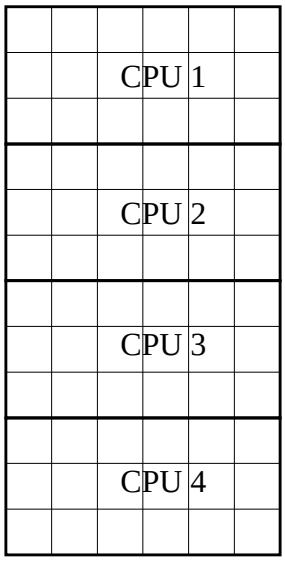

Figure 6.3: The simulation is divided into a number of domains - one for each processor. The subcell structure is also shown.

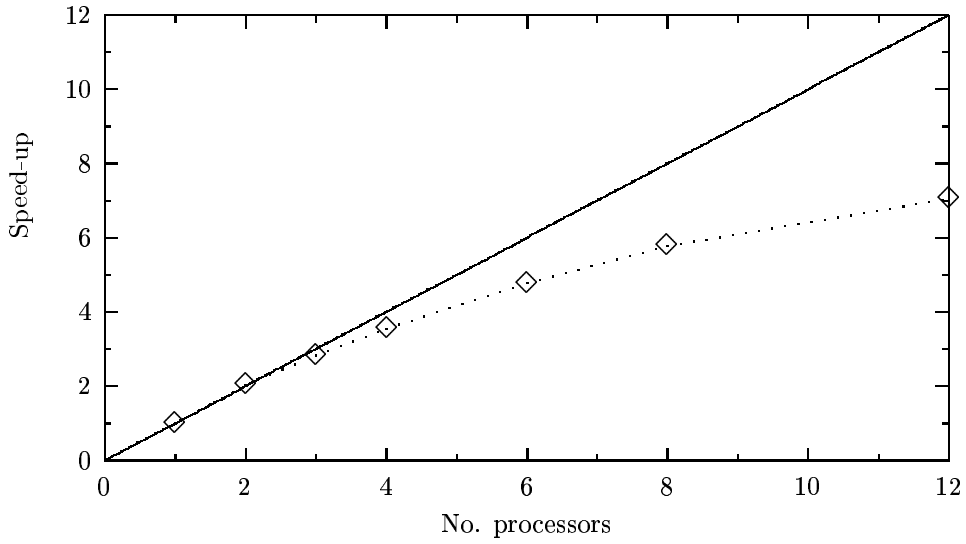

Figure 6.4: The speed-up of a parallel Molecular Dynamics program. The number of Lennard-Jones particles is 65536, the density is $0.8\sigma^2$ and the temperature is $2.0\epsilon/k_B$. The scale is relative to one processor (the serial program). The line with slope 1 is the linear speed-up which is the maximum speed-up which can be achieved.

6.6 Hard spheres

Systems consisting of hard spheres are very different from simulation of Lennard-Jones systems. The interaction potential is fundamentally different because it is discontinuous *i.e.*,

$$u(r) = \begin{cases} \infty & \text{for } r \leq 2\sigma \\ 0 & \text{otherwise} \end{cases} \tag{6.14}$$

where σ is the radius of the particles.

As the potential indicates, the hard spheres cannot overlap. The only interactions between the particles are through collisions, and between collisions the particles move in straight lines (no external field is applied). These observations show that we cannot apply the same simulation strategy as the one for Lennard-Jones particles.

Let us in the following discussion assume that all hard spheres have the same radius σ, and mass m. Typically, we will set the mass to unity.

6.6.1 The main loop

The main loop of a hard sphere simulation program is simple. Since the only interactions are the collisions, we have to find the next collision, update the positions and velocities and start all over again. Algorithm 12 shows the main loop.

Algorithm 12 The main loop of a hard sphere program

```
t ← 0
while t ≤ t_end do
   Find next collision {Δt is the time until the next collision}
   Update positions and velocities
   Collect data
   t ← t + Δt
end while
```

6.6.2 Updating positions and velocities

Since there is no external field, the hard spheres move in straight lines between collisions. The positions of the particles are easily updated; this is done by applying

$$\mathbf{r}_i(t + \Delta t) = \mathbf{r}_i(t) + \Delta t \mathbf{v}_i(t) \tag{6.15}$$

for $i = 1, \ldots, N$. The time difference Δt is smaller (or equal) to the time between two collisions. In practice we choose Δt to be the time until the next collision - see section 6.6.3.

The velocities are only changed at collisions, and only the velocities of the two spheres colliding are changed. It is convenient to introduce a measurement of the inelasticity of the collisions, which we denote ϵ. The quantity ϵ is related to the restitution coefficient r as $\epsilon = \frac{1-r}{2}$. When $\epsilon = \frac{1}{2}$ a collision is completely inelastic, and $\epsilon = 0$ is the completely elastic case. The velocities are updated as

$$\mathbf{v}_i' = \epsilon \mathbf{v}_i + (1 - \epsilon)\mathbf{v}_j \tag{6.16a}$$
$$\mathbf{v}_j' = (1 - \epsilon)\mathbf{v}_i + \epsilon \mathbf{v}_j \tag{6.16b}$$

where $\mathbf{v}_i$ and $\mathbf{v}_j$ are the velocities before the collision, and $\mathbf{v}_i'$ and $\mathbf{v}_j'$ are the velocities after.

6.6.3 Tracking collisions

The discussion of simulation of hard spheres has so far been independent of the spatial dimension. The essential part of a hard sphere simulation program is to find the next collision. Of course we could derive an algorithm for finding the next collision independent of the spatial dimension, but the one-dimensional case can be optimised so easily, that it is worth doing. In this section we will only describe the one-dimensional problem.

The one-dimensional case is different from systems in higher dimensions. The reason is very simple: hard spheres in one dimension cannot exchange their relative position *i.e.*, if initially $x_i > x_j$ where x_i and x_j are the positions of sphere i and j, this inequality will remain true through the whole simulation.

Let us develop the following picture of our one-dimensional system: the spheres are placed on a horizontal line, and the labeling of the spheres is done so that i is placed to the left of j if $i < j$. Then sphere i can only collide with sphere $i - 1$ and $i + 1$. This observation reduces the search for the next collision by one order of magnitude. Moreover, we notice that if sphere i collide with sphere $i + 1$, then sphere $i + 1$ will collide with sphere i. More precisely; we only have to check the neighbour to the right for collisions.

Now consider two spheres, i and $i + 1$, at time t. The equations of motion are

$$x_i(t+\Delta t) = x_i(t) + \Delta t v_i(t) \tag{6.17a}$$
$$x_{i+1}(t+\Delta t) = x_{i+1}(t) + \Delta t v_{i+1}(t) \tag{6.17b}$$

The time until the next collision is Δt. Remembering that $x_i < x_{i+1}$ the condition of collision is $x_{i+1} - x_i = 2\sigma$ where σ is the radius of the spheres. The condition is rewritten to be

$$x_i(t) - x_{i+1}(t) + \Delta t(v_i(t) - v_{i+1}(t)) = 2\sigma \tag{6.18}$$

which can easily be solved, and we obtain

$$\Delta t = \frac{x_i(t) - x_{i+1}(t) - 2\sigma}{v_{i+1}(t) - v_i(t)} \tag{6.19}$$

Obviously we only have physical solutions if $v_{i+1}(t) - v_i(t) \neq 0$ and $\Delta t \geq 0$. Finally, we are able to write down an algorithm which finds the next collision, see algorithm 13.

Algorithm 13 Tracks the next collision in a one-dimensional system

Require: x_i, v_i
  $\Delta t \leftarrow \infty$
  for $i = 1$ to N **do**
    $\delta v \leftarrow v_{i+1} - v_i$
    if $\delta v \neq 0$ **then**
      $\delta t \leftarrow (x_i - x_{i+1} - 2\sigma)/\delta v$
      if $\delta t \leq \Delta t \wedge \delta t \geq 0$ **then**
        $\Delta t \leftarrow \delta t$
        $k \leftarrow i$
      end if
    end if
  end for

6.7 Calculating thermodynamic quantities

The present thesis is concerned with many-particle simulations *i.e.,* we simulate systems with a finite number of particles and a finite volume. But the thermodynamical quantities are all given in the thermodynamical limit *i.e.,* as $N, V \to \infty$.

The purpose of the following sections is to discuss how to calculate thermodynamical quantities from data obtained from a numerical solution of the classical-mechanical equations of motion.

6.7.1 Rate constants

In section 6.4 we discussed how to simulate chemical reactions. In this section we discuss how to measure the rate constant for a reaction simulated by MD. There is no trivial relation between the reaction parameters, P_r and R_{reac}, introduced in section 6.4 and the second-order rate constant.

In this section we will discuss the calculation of the rate constant of a second-order reaction from MD simulations. We will approach the problem through the collision theory [67].

Consider a bimolecular reaction, $A + B \rightarrow P$. The velocity of the reaction is $v = k[A][B]$ where k is the rate constant, and $[A]$ and $[B]$ are the concentrations of A and B. The phenomenological equation describing the evolution of $[A]$ is

$$\frac{\mathrm{d}[A]}{\mathrm{d}t} = -k[A][B] \tag{6.20}$$

From collision theory we can obtain an expression for the evolution of the number of A particles, N_A. The expression is

$$\frac{\mathrm{d}N_A}{\mathrm{d}t} = -2x_A x_B \Gamma P_r \tag{6.21}$$

where x_A and x_B are the particle fractions of A and B respectively, Γ is the collision rate and P_r is the probability of a reactive collision. The number ΓP_r is easily measured during a MD simulation: it is the number of reactions per time unit, and we denote it N_R. The particle fraction of a component is given as $x_A = \frac{N_A}{N}$ where N_A is the number of A particles and N is the total number of particles. Dividing equation (6.21) by N we obtain

$$\frac{\mathrm{d}x_A}{\mathrm{d}t} = -\frac{2x_A x_B N_R}{N} \tag{6.22}$$

The concentration of $[A]$ is related to its particle fraction as $[A] = x_A \rho$. Equation (6.22) can now be rewritten as

$$\frac{\mathrm{d}[A]}{\mathrm{d}t} = -\frac{2[A][B]N_R}{N\rho} \tag{6.23}$$

We can now compare equation (6.20) and (6.23), and we see that the rate constant, k, is proportional with the number of particles N. In other words, the instantaneous rate constants that we measure during the MD simulations will increase with the number of particles. In order to obtain a rate constant which is independent of the number of particles, we have to divide it by the number of particles.

6.7.2 Diffusion coefficients

Diffusion coefficients can be calculated in two different ways; using the velocity autocorrelation function or mean square displacement, see *e.g.*, Hansen *et al.* [38]. The mean square displacement method is easy to implement in an MD program, and we have therefore chosen to use it.

We are aware of the dispute in the literature on the existence of the diffusion coefficient in two dimensions, see *e.g.,* van der Hoef *et al.* [80] and references therein. Even though we do many simulations in two dimensions, we are not interested in participating in this dispute. The diffusion coefficient which we measure is the coefficient on the time scale and length scale of our systems and we are not interesting in the hydrodynamic modes as time goes to infinity.

The Einstein relation for the diffusion coefficient (for a tagged particle) in d dimensions is [38]

$$D = \lim_{t\to\infty} \frac{1}{2dt} \langle \|\mathbf{r}(t) - \mathbf{r}(0)\|^2 \rangle \tag{6.24}$$

where $\mathbf{r}(t)$ is the position at time t and $\mathbf{r}(0)$ is the initial position. Using the equation above to calculate the diffusion coefficient requires a few modifications of an ordinary Molecular Dynamics program.

Most often the MD simulations are performed using periodic boundary conditions. If the periodic boundary conditions are applied, a particle will never move longer than the length of a simulation box. The solution of this problem is simple. We count the number of boxes the particle has traveled *i.e.,* everytime a particle crosses a boundary we either increase or decrease a counter depending on which direction the particle is moving. We are then at any time able to calculate the displacement by modifying $\|\mathbf{r}(t) - \mathbf{r}(0)\|$ to $\|\mathbf{r}(t) - \mathbf{r}(0) + \mathbf{n}L\|$ where $\mathbf{n}$ is a vector containing the counter and L is the length of the simulation box. By applying

simple algebra to equation (6.24) and using the modification just mentioned we obtain

$$2dtD = \langle \|\mathbf{r}(t) - \mathbf{r}(0) + \mathbf{n}L\|^2 \rangle \tag{6.25}$$

Of course the statistics of the equation above become better if we use all particles instead of just one tagged particle. The equation then becomes

$$2dtD = \frac{1}{N} \sum_{i=1}^{N} \|\mathbf{r}_i(t) - \mathbf{r}_i(0) + \mathbf{n}_i L\|^2 \tag{6.26}$$

where N is the number of particles. The diffusion coefficient D can be found by fitting the mean (with respect to the number of particles) square displacement.

CHAPTER 7

The Extended Lotka Scheme

Oscillating chemical reactions have intrigued chemists and many others in the last 2–3 decades. The best known example is the reaction first investigated by Belousov [6] and Zhabotinsky [86]. One can only be fascinated by seeing the solution in the reaction vessel changing colour every minute from deep blue to red and back to blue again.

In this chapter we will look at simulations performed on a very simple chemical mechanism, which is able to exhibit oscillations in the concentrations as function of time. The mechanism is simulated by Molecular Dynamics, and it is therefore a simulation with a finite number of particles. It should be regarded as a prototype of an oscillating chemical reaction.

The chapter is based upon the results described in two papers by the author of the present thesis, Eigil L. Præstgaard, and Søren Toxværd [26, 27] which are enclosed as appendix B and appendix C

7.1 A brief outline of previous studies

The simulation of chemical reactions by Molecular Dynamics is not a new approach. As early as 1975, Portnow [68] simulated a simple chemical reaction by Molecular Dynamics. Portnow studied the fluctuations in the number density of the species *i.e.*, the concentration. The simulated particles were hard spheres.

Ortoleva and coworkers [64] were the first to do MD simulations of chemical instabilities more than two decades ago. The simulated mechanics was:

$$\begin{aligned} X + Y &\rightarrow 2X \\ X &\rightarrow Y \\ Y &\rightarrow X \end{aligned}$$

The last two reactions are introduced in order to prevent that Y is converted to X. Ortoleva *et al.* imagined that the two reactions were radiation processes so that the system can be far from equilibrium but without a mass flux *i.e.*, the system is energetically driven. The individual particles were hard spheres, and Ortoleva *et al.* simulated up to 450 particles.

Boissonade [9] studied almost two decades ago the fluctuations in the concentration in two simple mechanisms ($A + C \rightarrow X + C, 2X \rightarrow 2N$ and $A + C \rightarrow X + C, 2X \rightarrow X + N$). The system was two-dimensional and the particles were hard disks. The simulation results are compared with a master-equation approach.

In 1983 Heinrichs *et al.* [40] performed simulations on another oscillating reaction. The scheme was:

$$\begin{aligned} A + B &\rightarrow C \\ C + B &\rightarrow D + B \\ D &\rightarrow 2B \end{aligned}$$

In order to simulate an open system, Heinrichs *et al.* introduced an inflow and an outflow of particles *i.e.*, the species A, B, C and D are created and removed randomly. Furthermore, there is an inert species, X. If there are any inert species present in the system, an X particle is converted to one of the other species which mimics an open system. If no inert species are present, a new particle is created at a randomly chosen position. The first reaction creates an inert particle, because the reaction really is $A + B \rightarrow C + X$. In the third reaction a new particle (of type B) is created. If the number of inert particles is larger than a certain value, some of them are removed. All particles are hard spheres. It is hard to tell exactly which ensemble Heinrichs *et al.* were simulating.

Recently, Diebner *et al.* [19] simulated a very simple mechanism. The mechanism is the same as we will present in section 7.2. The particles interact through a long-ranged potential; basically a repulsive Coulomb potential. The main result is that the mechanism is oscillatory even on the microscopic level. In a very different context, Frachebourg *et al.* [22] have studied the same mechanism as Diebner *et al.*[1] Moreover, Gorecki *et al.* [34] have studied the same mechanism using hard

[1] Frachebourg *et al.* call the mechanism the cyclic Lotka-Volterra mechanism.

sphere Molecular Dynamics and a master equation. They conclude that the spatial correlation functions oscillate in time, and that the correlations are longer than for a stationary system.

Mansour *et al.* [52] have recently written a very detailed paper about the simulation of chemical reactions on a microscopic level. The primary objective is to investigate complex mechanisms, including oscillating reactions. The simulation technique is *not* Molecular Dynamics in the context of this thesis, but is based upon Bird's algorithm [8] which is a numerical solution of the Boltzmann equation. The particles considered by Mansour *et al.* are hard spheres, and all reactions are binary.

To the best of our knowledge, only Toxværd [78] has considered reactions simulated by Molecular Dynamics in competition with a phase transition (in that case, a spinodal decomposition). The simulated system was a binary mixture of Lennard-Jones particles, and the reaction scheme was $A \rightleftarrows B$. The result from these simulations is that chemical reactions have a strong influence on the kinetics of the spinodal decomposition. In the last years an number of papers has been published on which influence chemical reactions may have on the phase separation process, see *e.g.,* Glotzer *et al.* [28, 29], Christensen *et al.* [15], and Verdasca *et al.* [82]. The papers mainly investigate the problem by modifying the Cahn-Hilliard equation to include chemical reactions, and then solve it numerically. Recently, Carati *et al.* [14] have contributed to the theoretical understanding by analysing a such a Cahn-Hilliard based model. The work of Carati *et al.* is mainly analytically, and their theoretical predictions have not been be verified by *e.g.,* Molecular Dynamics simulations.

7.2 The scheme

Lotka was one of the pioneers in the field of oscillating chemical reactions. His work dates back to 1910s and 1920s, and his work was purely theoretical - he himself was not convinced that oscillating chemical reactions could occur in the real world. At the end of a paper from 1910, Lotka wrote [50]:

> No reaction is known to follow the above law [oscillatory], and as a matter of fact the case here considered was suggested by the consideration of matters lying outside the field of physical chemistry.

His famous scheme from 1920 is [51]:

$$A + X \rightarrow 2X \tag{7.1a}$$
$$X + Y \rightarrow 2Y \tag{7.1b}$$
$$Y \rightarrow P \tag{7.1c}$$

The scheme above gives raise to oscillations in concentrations of X and Y when certain conditions are fulfilled.

Lokta's scheme takes place in an open system; there is a constant inflow of the species A so that the concentration can be assumed to be constant. Moreover, there is a constant outflow of the product P.

Our scheme is very simple; it consists of three reactions and three species only. We call it the extended Lotka scheme since it resembles the Lotka scheme, and it is:

$$X + Y \xrightarrow{k_1} 2Y \tag{7.2a}$$
$$Y + Z \xrightarrow{k_2} 2Z \tag{7.2b}$$
$$Z + X \xrightarrow{k_3} 2X \tag{7.2c}$$

where k_1, k_2, and k_3 are the rate constants. We choose to let the total concentration $[X] + [Y] + [Z]$ be constant and denoted K, because we simulate a system where the total number of particles is conserved. The scheme above violates the Wegschleider conditions [19]. This means that the extended Lotka scheme is energetically driven, and the system will therefore always been far from equilibrium.

From the reactions above, we are able to derive phenomenological equations that describe the evolution of the concentrations. We obtain three equations from the scheme given above:

$$\frac{\mathrm{d}[X]}{\mathrm{d}t} = -k_1[X][Y] + k_3[X][Z] \tag{7.3a}$$
$$\frac{\mathrm{d}[Y]}{\mathrm{d}t} = k_1[X][Y] - k_2[Y][Z] \tag{7.3b}$$
$$\frac{\mathrm{d}[Z]}{\mathrm{d}t} = k_2[Y][Z] - k_3[X][Z] \tag{7.3c}$$

The differential equations above is an initial value problem, and given the initial values of the concentrations of the three species, the solution is unique. We have in principle three differential equations but since the total concentration is constant, the solution will be in a two-dimensional subspace of the three-dimensional

concentration space spanned by $[X]$, $[Y]$ and $[Z]$. A two-dimensional ordinary differential equation cannot have chaotic solutions; this observation is a consequence of the Poincaré-Bendixson theorem [41, chapter 11].

7.3 Linear stability

The solution of the three phenomenological equations given in the previous section will give us the evolution of concentrations of the three species. But it is not possible to find an analytical solution.

Instead of an analytical solution, we are able to obtain an approximate solution. We will apply the technique of linear stability of stationary points. The technique is introduced in section 4.4.

To begin, we find the stationary point *i.e.*, a point in the concentration space where the differential is zero *i.e.*, we wish to solve the set of equations:

$$\frac{\mathrm{d}[X]}{\mathrm{d}t} = -k_1[X][Y] + k_3[X][Z] = 0 \tag{7.4a}$$

$$\frac{\mathrm{d}[Y]}{\mathrm{d}t} = k_1[X][Y] - k_2[Y][Z] = 0 \tag{7.4b}$$

$$\frac{\mathrm{d}[Z]}{\mathrm{d}t} = k_2[Y][Z] - k_3[X][Z] = 0 \tag{7.4c}$$

Let the stationary point be denoted (x_{ss}, y_{ss}, z_{ss}). At the stationary point, the condition $K = x_{ss} + y_{ss} + z_{ss}$ must be fulfilled. Solving equation (7.4) we obtain

$$x_{ss} = \frac{K k_2}{k_1 + k_2 + k_3} \tag{7.5a}$$

$$y_{ss} = \frac{K k_3}{k_1 + k_2 + k_3} \tag{7.5b}$$

$$z_{ss} = \frac{K k_1}{k_1 + k_2 + k_3} \tag{7.5c}$$

Close to the stationary point, we can linearise the ordinary differential equations and solve the linear equations. The approximative solution close to the stationary point is then

$$\begin{pmatrix} [X] \\ [Y] \\ [Z] \end{pmatrix} = \begin{pmatrix} x_{ss} \\ y_{ss} \\ z_{ss} \end{pmatrix} + \sum_i \mathbf{e}_i e^{\lambda_i t} \tag{7.6}$$

where $\mathbf{e}_i$ is the ith eigenvector (scaled appropriately) and λ_i is the ith eigenvalue of the Jacobian matrix. We are only interested to see whether the extended Lotka scheme is oscillatory, so we only calculate the eigenvalues. The extended Lotka scheme has one zero eigenvalue and two complex conjugated which are

$$\lambda = \pm \frac{K\sqrt{k_1 + k_2 + k_3}}{\sqrt{k_1 k_2 k_3}} \imath \tag{7.7}$$

We conclude that the stationary state is stable, and the motion (close to the stationary state) is a harmonic oscillation.

7.4 Molecular details

The extended Lotka mechanism as analysed in the previous sections, can be simulated by Molecular Dynamics. In this section we discuss the molecular details. The three species, X, Y and Z, are chosen to be atoms. The interaction potential is the Lennard-Jones potential *i.e.*,

$$u_{\mathrm{LJ}}(r) = 4\epsilon \left[\left(\frac{\sigma}{r} \right)^{12} - \left(\frac{\sigma}{r} \right)^{6} \right] \tag{7.8}$$

where ϵ is the minimum of the potential (and the fundamental energy unit), and σ is the characteristic length. The minimum of the potential is easily[2] found to be $\sqrt[6]{2}\sigma$.

We have simulated two different systems. They are:

System 1 All the particles are identical *i.e.*, the difference is only the "colour" of the particles. The "colour" represent the species *i.e.*, in our case there are three "colours". The potential is $u_{\mathrm{I}}(r) = u_{\mathrm{LJ}}(r)$.

System 2 The particles of the same "colour" interact through the Lennard-Jones potential given by equation (7.8). Particles of different "colours" *e.g.*, the X-Y interaction, is non-attractive. In order to simulate this, we use the following potential

$$u_{\mathrm{II}}(r) = \begin{cases} u_{\mathrm{LJ}}(r) & \text{for } r \leq \sqrt[6]{2}\sigma \\ 0 & \text{otherwise} \end{cases} \tag{7.9}$$

[2]Differentiate $u_{\mathrm{LJ}}(r)$ with respect to r, set it equal to zero and solve with respect to r.

A system like System 2 is known to phase separate below a certain critical temperature [47, 79].

As mentioned in section 6.4, the simulation of chemical reactions requires two parameters for a binary reaction. The first parameter is the sum of radii of two colliding particles, R_{reac}. In most cases we set $R_{\text{reac}} = 0.96116\sigma$ which ensures that only particles with a large relative velocity might be counted as colliding particles. The algorithms presented in chapter 6 are applied, and the temperature is controlled by the Nosé-Hoover thermostat.

7.5 Steady and oscillatory states in the microscopic system

In section 7.3 we found the stationary state for the extended Lotka scheme. A stationary state is a state where the concentrations are constant. If the phenomenological equations (7.3) represent the microscopic details of the system, the steady state given by equation (7.5) must be reproducible by the MD simulations.

Consider a system where $k_1 = k_2 = k_3$. The steady state is then $x_s = y_s = z_s = \frac{K}{3}$. We set up a simulation with $1/3$ of the particles of each species. Figure 7.1 shows the result. From the figure it is obvious that a steady state exists for the finite system. The fluctuations in the concentration (measured by the particle fraction) decrease with the number of particles.

We also know from section 7.3 that the extended Lotka scheme is oscillatory. Figure 7.2 shows the particle fraction of X. We see that the concentration of X oscillates. The oscillations are not regular but this is due to the fact that the system consists of 1024 particles only..

7.6 Phase transitions and mechanisms

Mixtures of Lennard-Jones particles, which interact as described in section 7.4 (System 2) are known to phase separate, see *e.g.*, Laradji *et al.* [47] and Toxværd *et al.* [79]. Above a certain critical temperature T_c, the system will be homogeneous *i.e.*, the density of each component is constant through the system. Below the critical temperature, we will see domains of each components. For a two-component system, the equilibrium distribution of components is that there are two large domains consisting of one component only. For three- and four-component systems, the formation of domains is more complex.

We have simulated a three-component Lennard-Jones system. It is easy to see

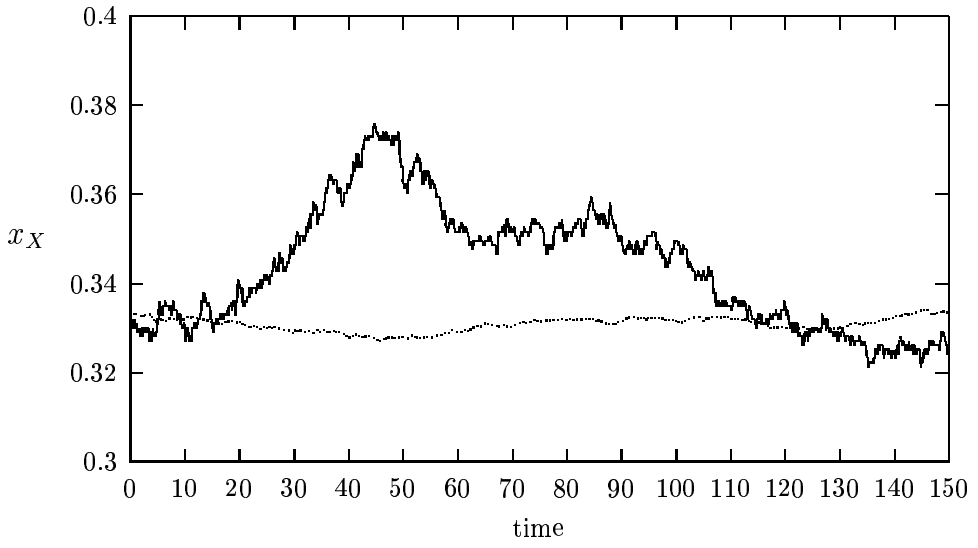

Figure 7.1: The particle fraction of X versus time. The simulation parameters are: $\rho = 0.8\sigma^2$, $T = 2.0\epsilon/k_B$, $P_r^{(1)} = P_r^{(2)} = P_r^{(3)} = 10^{-3}$, and $R_{\text{reac}} = 0.969116\sigma$. The line with the large fluctuations is for a system of 1024 particles while the other line is for a system of 65536 particles.

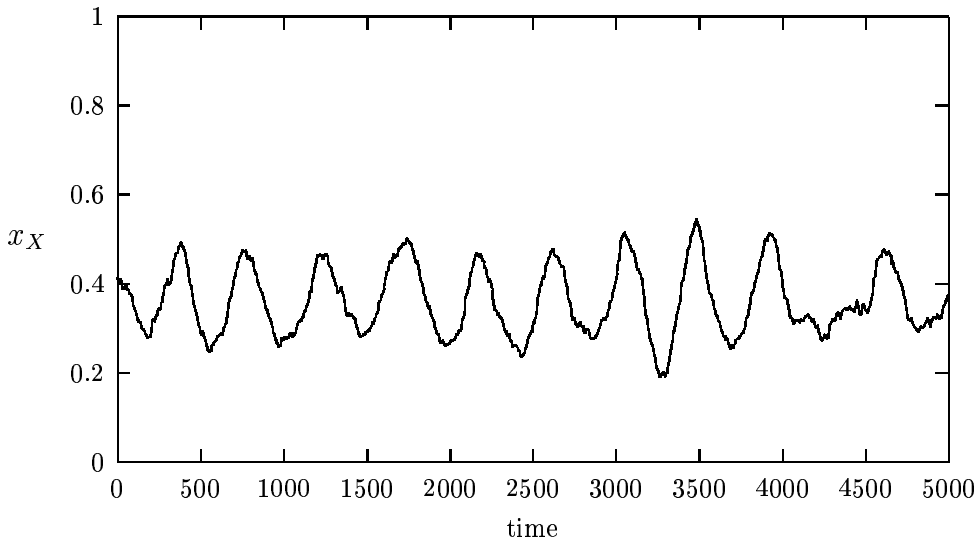

Figure 7.2: The particle fraction of X versus time. The simulation parameters are the same as in figure 7.1 except that the number of particles is 1024 and $P_r^{(2)} = 1.1 \cdot 10^{-3}$.

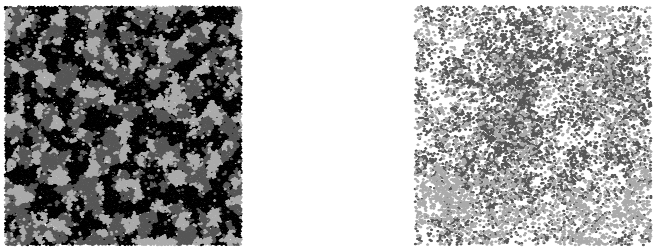

(a) $T < T_C$ (b) $T > T_C$

Figure 7.3: (a) shows the positions of the particles at temperature $T = 1.0\epsilon/k_B < T_c$, while the (b) is taken at temperature $T = 2.5\epsilon/k_B > T_c$. The number of particles is 16386 and the density is $0.8\sigma^2$ in both cases.

whether a phase separation has occurred at a given temperature. This is done by looking a the positions of the particles by the naked eye. Figure 7.3 shows two examples; one above and one below the critical temperature.

We measure the (time averaged) rate constants from the simulations. Figure 7.4 shows the Arrhenius plot for both System 1 and 2 with 1024 particles, and System 2 with 4096 particles. It is clear that at $T_c = 1.7\epsilon/k_B$ there is a cross-over for System 2. This is the phase separation we see. Below T_c System 2 is phase separating while above T_c it behaves essentially as System 1.

As discussed in section 4.3 the ratio k/D must be constant if the reaction is diffusion-controlled (k is the rate constant, and D is the diffusion coefficient). Figure 7.5 shows the k/D ratio versus temperature for System 2. We see that above T_c the ratio is - within the statistical error - constant. This clearly indicates that the reactions are diffusion-controlled above the critical temperature, while below T_c the mechanism is different. Below the critical temperature the mechanism changes to a surface-driven reaction because below T_c domains are formed. The domains are pure *i.e.,* they consist of one species only. Therefore the only place where the reactions can occur is at the boundaries of two domains.

7.7 Concluding remarks

In this chapter we have presented results from microscopic simulations of the extended Lotka scheme. It is clearly demonstrated that the technique of MD can

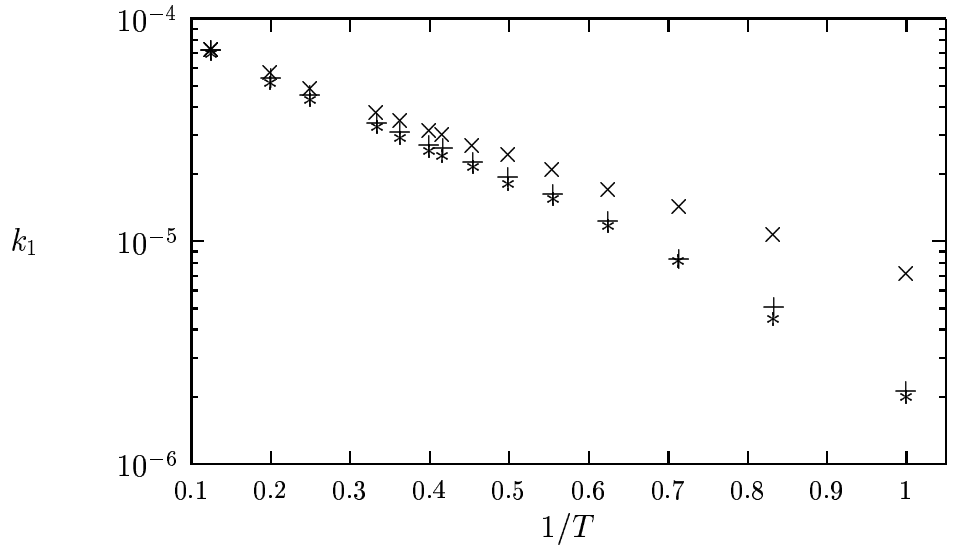

Figure 7.4: The Arrhenius plot for System 1 ($\times$, $N = 1024$), System 2 ($+$, $N = 1024$), and System 2 ($*$, $N = 4096$). The density is $0.8\sigma^2$. The reaction parameters are $P_r^{(1)} = P_r^{(3)} = 1.0 \cdot 10^{-3}$, $P_r^{(2)} = 1.1 \cdot 10^{-3}$, $R_{\text{reac}} = 0.969116\sigma$.

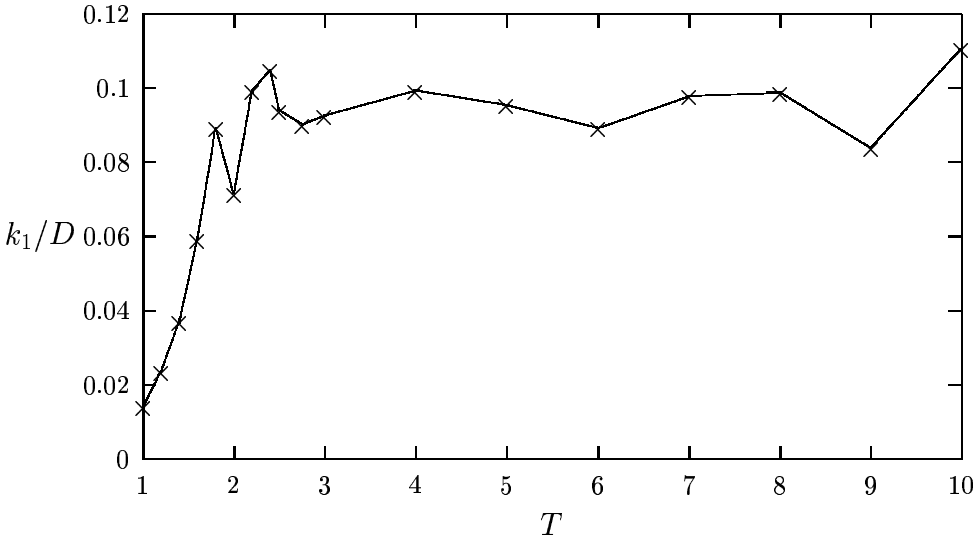

Figure 7.5: The ratio k_1/D versus the temperature. The simulation parameters are the same as in figure 7.4.

be used to simulate chemical reactions.

The simulations presented in the chapter show that macroscopic phenomena can be reproduced by microscopic simulations *e.g.*, the steady state of a complex mechanism. We are able to probe spatial phenomena like pattern formation from a very simple point of view which require only few and simple assumptions.

We also see that simple theoretical considerations can be applied with success. For example the theory of diffusion-controlled reactions can easily be applied.

The chapter clearly demonstrates that a phase transition may alter the underlying chemical mechanism. Lately this subject has attracted some attention, see *e.g.*, Carati *et al.* [14]. By using MD we would be able to investigate theoretical predictions by Carati *et al.* . We have performed a few number of simulations of a simple scheme, namely $2A \rightleftarrows A + B \rightleftarrows 2B$. Our initial simulations show that this mechanism is able to freeze the spinodal decomposition as predicted by Carati *et al.* .

CHAPTER 8

Controlling the Temperature in One Dimension

Inelastic collisions were discussed in chapter 5. In this chapter we will discuss our results obtained from simulations of rigid and soft particles undergoing inelastic collisions. The results presented here are based upon a paper by the author, Paz Padilla, Eigil L. Præstgaard, and Søren Toxværd [25] which is enclosed as appendix D.

The investigation of the inelastic collisions began by reading a paper by Du *et al.* [20]. The results presented by Du *et al.* did seem very odd, and a desire of understanding emerged. Du *et al.* find that when the collisions are inelastic, and even when the particles are coupled to a thermostatting device, the particles get clamped. One can easily imagine the clamping when there is no thermostatting device, and it has been rigorously shown by Haff [37] - see also chapter 5 for a more detailed discussion on inelastic collisions. We do not reveal too much of the conclusions of this chapter by saying that we find that the "extraordinary" state found by Du *et al.* is an artifact of the model they used.

The simulation cell in one dimension is a line. We have two walls at $-\frac{L}{2}$ and $\frac{L}{2}$ where L is the length of the system (typically $L = 1$). One peculiarity of one-dimensional systems is that no scattering occurs *i.e.,* if two particles, i and j, initially are situated so that $x_i > x_j$ then this inequality holds through the complete simulation.

The rigid particles used in this chapter are all point particles *i.e.,* the radii of the particles are set to zero. Moreover, the mass is set to 1. The soft particles interact

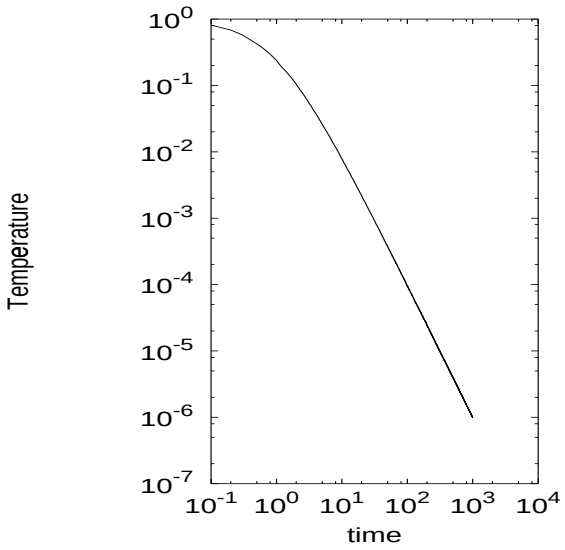

Figure 8.1: A log-log plot of the granular temperature as function of time. The number of rigid, point particles is 100 and $\epsilon = 0.005$. The length of the system is 1.0. During the simulation 38467 collisions occurred.

through the WCA potential, see Weeks *et al.* [83]. The potential is

$$u(r) = \begin{cases} 4\epsilon \left[\left(\frac{\sigma}{r}\right)^{12} - \left(\frac{\sigma}{r}\right)^{6} \right] + \epsilon & \text{for } r \leq \sqrt[6]{2}\sigma \\ 0 & \text{otherwise} \end{cases} \tag{8.1}$$

where r is the inter-particle separation, σ and ϵ are the Lennard-Jones parameters. The details on how the inelastic collisions are modelled can be found in section 5.2.

8.1 Semi-closed system

We will analyse a system consisting of N particles undergoing inelastic collisions. The system is closed in the sense that no energy flows into the system, while energy is dissipated through the collisions.

Figure 8.1 shows the granular temperature, $\mathcal{T} = \frac{1}{N}\sum_{i=1}^{N} v_i^2$, as function of time. We see that after a transient period the temperature decays algebraicly. The slope can easily be found, and we find that Haff's prediction of the decay is correct.

Figures like figure 8.1 can be obtained from simulations of rigid particles with a radius larger than zero and various densities. The transient period depends on the

density and the degree of inelasticity. In the case of soft particles the exponent in Haff's cooling law is not -2. The value of the exponent ranges from -1.16 to -1.90.

8.2 Thermostatting devices

Systems consisting of particles undergoing inelastic collisions dissipate kinetic energy. This implies that the velocity of the particles is decreasing as function of time. Obviously we have that $\mathcal{T} \to 0$ as $t \to \infty$. We therefore have to introduce a thermostatting device in order to control the temperature in this situation.

Thermostats (as we usually call thermostatting devices) have been used in Molecular Dynamics simulations for more than two decades. For soft systems *e.g.,* Lennard-Jones particles, the Nosé-Hoover thermostat (see section 6.2.2 for details) is a well-known thermostat. In the case of rigid particles a few attempts can be found in the literature. In the following we will introduce those thermostats we have implemented, and present simulations on rigid and soft particles coupled to the thermostats. In order to check the functionality of the thermostats we couple them to systems where the collisions are elastic *i.e.,* no energy dissipates. A perfectly working thermostat is a device that on average ensure that the temperature of the system is the same as the temperature of the thermostat.

The coupling between the thermostat and the particles is constructed in the following way: when a particle collides with the left wall, the velocity of the particle is changed according to the thermostat.

8.2.1 The Gaussian wall

The Gaussian wall returns the particles with a new velocity which is drawn randomly from a Gaussian distribution *i.e.,*

$$P(v) = \frac{m}{k_B T_{\text{wall}}} \exp\left(-\frac{mv^2}{2k_B T_{\text{wall}}}\right) \tag{8.2}$$

where T_{wall} is the desired temperature. The wall has been used by Du *et al.* [20]. At first thought this kind of thermostatting device comes natural since the initial velocity distribution of the particles is Gaussian, and by choosing velocities from a Gaussian distribution, one would think that it will preserve the velocity distribution.

The argument above is not correct which is illustrated by figure 8.2. The desired temperature of the thermostat, T_{wall} is set to 1.0. The temperature of the system

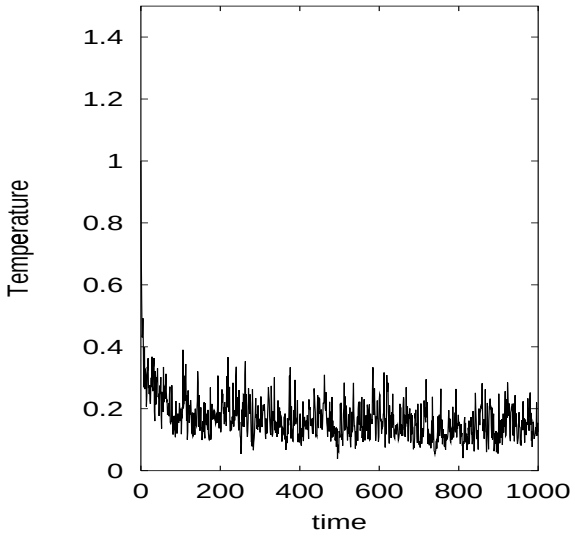

Figure 8.2: The granular temperature versus the time. The system consists of 100 particles and the length of the system is 1. The left wall is a Gaussian wall.

drops quickly to values lower than the thermostat, and the steady state value is 0.15 ± 0.05. If we turn to the soft particles, we see a similar behaviour. The steady state temperature is 0.62 ± 0.02.

8.2.2 The constant wall

The thermostat which we denote the constant wall, is indeed very simple. When a particle hits the wall, the velocity is always set to the same value, namely $\sqrt{T_{\text{wall}}}$. This corresponds to the probability distribution

$$P(v) = \begin{cases} 1 & \text{for } v = \sqrt{T_{\text{wall}}} \\ 0 & \text{otherwise} \end{cases} \tag{8.3}$$

A thermostatting device like the one described above is very odd seen from a physical point of view. It has been used by Du *et al.* [20] and Rapaport [70]. Figure 8.3 shows the granular temperature as it evolves during a simulation. We see that at first the temperature drops but then recovers, and at late times it is T_{wall}. So far everything seem to work perfectly.

A correct steady state temperature is not enough to ensure a perfectly working thermostat - the velocity distribution must be correct as well which means that it

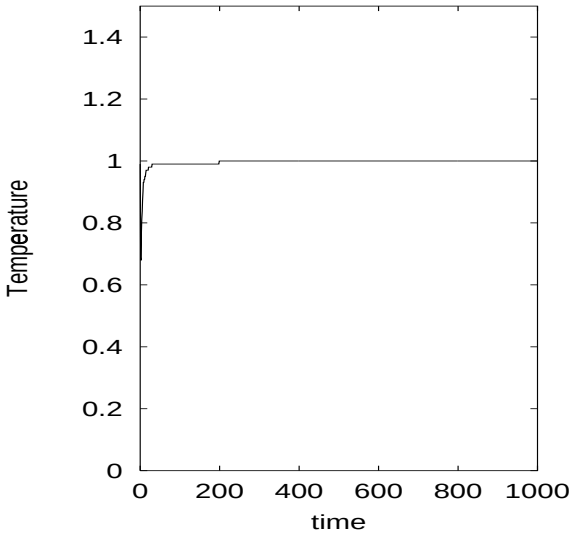

Figure 8.3: The granular temperature versus the time. The system consists of 100 particles and the length of the system is 1. The left wall is a constant wall.

has to be a Maxwell-Boltzmann distribution. The distribution obtained from the constant wall is *not* a Maxwell-Boltzmann distribution - only two velocities are possible (for the rigid particles): $\pm\sqrt{T_{\text{wall}}}$. It is not difficult to understand. When the collisions are elastic the particles will exchange velocities only.

For the soft particles the steady state temperature is incorrect (0.51 ± 0.01), and it is then easy to see that the constant wall does not work in this case neither.

8.2.3 The frequency device

We have implemented yet another thermostat in the following way: at certain time intervals the velocity of the left-most particle is changed. The new velocity is chosen randomly from a Gaussian distribution. The left wall is now a reflecting wall. We have coined the term frequency thermostat for this implementation. This thermostatting device has - to our knowledge - never been suggested or implemented before.

As indicated by figure 8.4 the frequency thermostat is able to set the temperature to the correct value (1.00 ± 0.13). Moreover, the velocity distribution is also correct.

The frequency thermostat seems to work perfectly for rigid particles independently of the frequency. This is not true for soft particles; at high frequencies the thermostat is not able to produce the correct equilibrium value. The origin of this

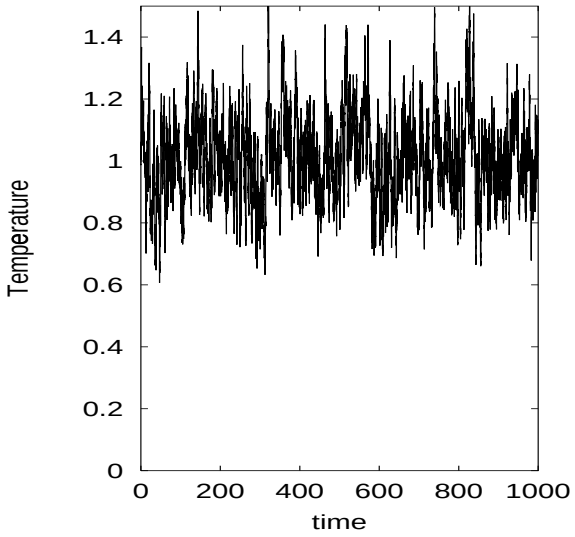

Figure 8.4: The granular temperature versus the time. The system consists of 100 rigid particles and the length of the system is 1. The thermostatting device is the so called frequency thermostat, and the frequency is 41.15.

problem is that equipartition takes time, and when the kinetic energy of one particle is changed too often, the system does not have time to relax to equilibrium.

8.2.4 The stochastic wall

If one digs into the literature one finds a very useful thermostatting device. It is due to Lebowitz *et al.* [48, 49] who investigated the transport properties of a Knudsen gas and a Lorentz gas two decades ago but it has been proposed much earlier. Later Tenenbaum *et al.* [74, 75] have used it in MD simulations of Lennard-Jones fluids. Tenenbaum *et al.* use the term "stochastic boundary conditions" and we adopt it and use the term "stochastic wall".

The velocity of the particle colliding with the walls (in our case the left wall only) is changed and the new velocity is drawn from the distribution

$$P(v) = \frac{vm}{k_B T_{\text{wall}}} \exp\left(-\frac{mv^2}{2k_B T_{\text{wall}}}\right) \tag{8.4}$$

The thermostatting device described above works perfectly for rigid and soft particles as figure 8.5 clearly shows. The equilibrium temperature is 1.00 ± 0.14 for rigid particles and 0.98 ± 0.02 for soft particles.

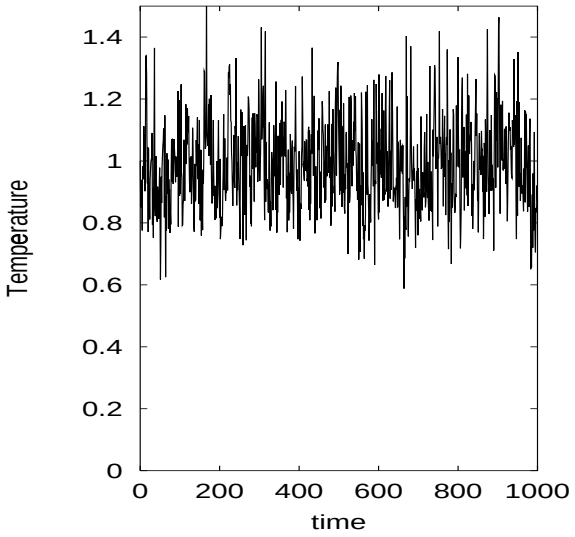

Figure 8.5: The granular temperature versus the time. The system consists of 100 rigid particles and the length of the system is 1. The thermostat applied is the stochastic wall.

8.2.5 Nosé-Hoover

For more than a decade the Nosé-Hoover thermostat has been used frequently; see section 6.2.2 for details. The Nosé-Hoover approach is an extension to the equations of motion. Similar to the thermostatting device discussed in the previous sections, we implement a Nosé-Hoover thermostat at the left wall. The implementation is as follows: instead of the left wall we have a particle tethered to the point $x_0 = -\frac{L}{2}$ by the potential $u(x) = \frac{1}{2}k(x - x_0)^2$ where x is the position of the particle and k is the force constant. This single particle is coupled to a Nosé-Hoover thermostat, and the rest of the particles are not. Figure 8.6 shows the temperature as function of time.

As figure 8.6 shows the thermostat sets the temperature correctly. The equilibrium value of the temperature is 0.99 ± 0.01.

8.2.6 Concluding remarks

As the results reported above show it is important to use a thermostatting device that actually can control the temperature correctly. For the rigid particles we see that the stochastic wall as described in section 8.2.4 is the best candidate. For the soft particles both the stochastic wall and the Nosé-Hoover inspired device can be used. For system in higher dimensions than one, it is easier to implement the

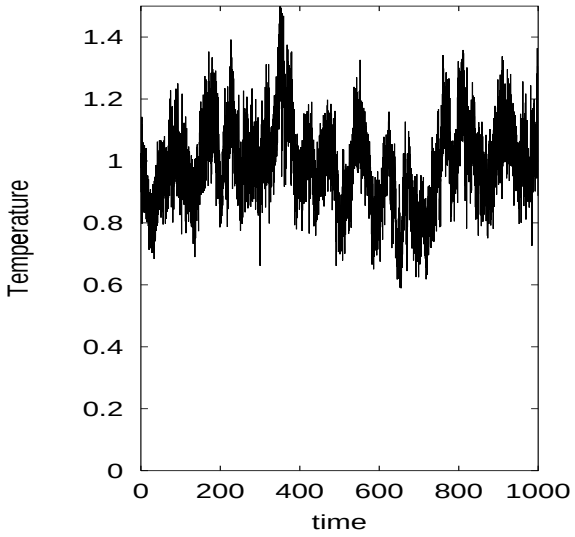

Figure 8.6: The granular temperature versus the time. The system consists of 100 soft particles, the length of the system is 1 and the force constant of the left-most particle is set to 100 in reduced units. The thermostat applied to the left particle is a Nosé-Hoover thermostat.

stochastic wall for the soft particles. The use of any other thermostat than the stochastic wall seems to us to be questionable.

It is not too difficult to understand why the stochastic wall works well, and why the Gaussian wall does not. Consider a three-dimensional system: the probability of a particle with velocity $\mathbf{v}$ arriving at a wall is [36]

$$P_{\text{wall}}(\mathbf{v}) = \mathbf{v} \cdot \mathbf{n} f(\mathbf{v}) \tag{8.5}$$

where $\mathbf{n}$ is a vector normal to the wall, and f is the velocity distribution which, in equilibrium, is a Maxwell-Boltzmann distribution. In order to preserve the velocity distribution, the particles leaving the wall must have the velocities distributed as the incoming particles, and the thermostat must return the particles according to equation (8.5).

8.3 Breakdown of hydrodynamics

As mentioned in the beginning of the chapter the study of inelastic colliding particles was inspired heavily by the paper by Du *et al.* [20]. The main conclusion of

Du *et al.* is that it is possible to observe a breakdown of hydrodynamics when we try to thermostat inelastic particles in one dimension.

The situation in the paper by Du *et al.* [20] is as this: they simulate N rigid point particles in one dimension. The collisions are inelastic; typically they set $\epsilon = 0.005$. Moreover, they have a Gaussian wall at the left wall while the right wall is reflecting. Independent of the initial positions of the particles an "extraordinary" state develops. The "extraordinary" state is that the particles get clamped *i.e.,* the particles are to be found at the right side of the simulation box.

Now the clamping is not a completely unexpected for inelastic systems. McNamara *et al.* [54, 55] have shown numerically that systems (with a thermostatting device) in one and two dimensions might collapse and Goldhirsch *et al.* [31] have shown that a clustering instability is possible for dissipative gases. Moreover, for one-dimensional systems McNamara *et al.* have shown analytically that the collapse will occur if the number of particles exceed a certain threshold; see section 5.4 for further details. But for the chosen degree of inelasticity, Du *et al.* do not exceed this threshold. Furthermore, Du *et al.* report that the clamping does not disappear as $\epsilon \to 0$ *i.e.,* in the elastic limit. Du *et al.* refer to the clamping as the breakdown of hydrodynamics.

We have simulated 100 rigid point particles but instead of the the Gaussian wall we use the stochastic wall. To measure whether the particles will get clamped we use the mean position (which in our case is the same as the centre of mass) *i.e.,* we compute $\langle x \rangle = \frac{1}{N}\sum_{i=1}^{N} x_i$ during the simulation. Figure 8.7 shows the mean position for simulations with three different values of ϵ. Figure 8.7a shows the case of elastic collision, and the mean position fluctuates around zero as we would expect. The value $\epsilon = 0.005$ is the same value as chosen by Du *et al.* [20]. The figure indicates a clamping of the particle, but as we decrease the degree of inelasticity, the clamping disappears; see figure 8.7c. We strongly believe that the conclusion by Du *et al.* is due to an artifact of their thermostat.

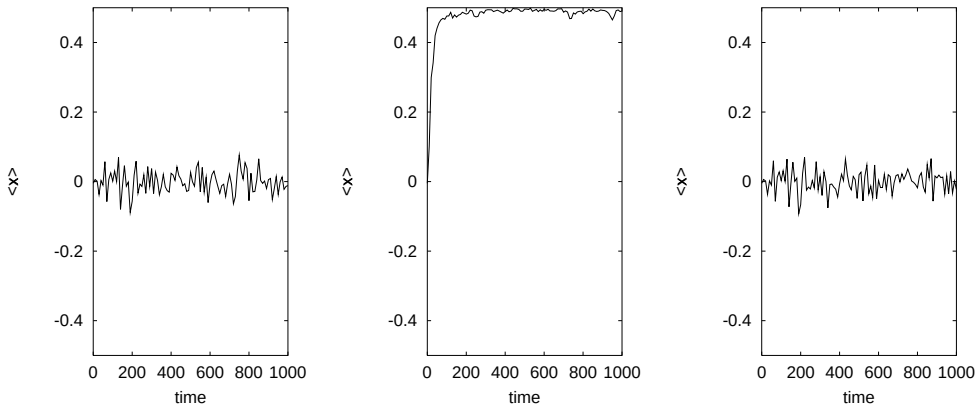

(a) $\epsilon = 0.0$ (b) $\epsilon = 0.005$ (c) $\epsilon = 10^{-7}$

Figure 8.7: The mean position $\langle x \rangle$ versus time. The systems consist of 100 rigid point particles, and the left wall is the stochastic wall.

CHAPTER 9

Discussion and Conclusion

We have in this thesis presented simulational results of two very different systems: oscillating chemical reactions and dissipative gases/ganular media. Both systems have two things in common: they are in a non-equilibrium state, and they have been investigated by Molecular Dynamics.

The systems studied in this thesis are “simple”. They are simple in the underlying physical model, but the phenomenology is indeed not simple. Even though the models are simple, we strongly believe that these models are able to capture some of the phenomena seen in the Nature.

Molecular Dynamics is an invaluable tool when many-particle systems are studied. Two special-purpose MD programs have been designed and implemented by the author; one for Lennard-Jones particles and one for rigid particles. The advantage of MD is that a MD program can be used in equilibrium and non-equilibrium situations. We see Molecular Dynamics as the link between the advanced theories and the complicated experiments. General-purpose Molecular Dynamics programs exist but they have an orientation toward biological problems (proteins in aqueous solution). MD programs for simple liquids (short-ranged potentials *e.g.*, the Lennard-Jones potential) and rigid particles are typically written by the chemist/physicist who is going to use them. But no chemist can keep up with the pace of development of computers, especially not the new parallel computers. An important project would be to implement - using modern software engineering methods - novel algorithms on state-of-the-art computers. Moreover, it is important to design and implement a number of tools which can analyse data, and an easy-to-use graphical user interface (GUI) is essential.

The rich phenomenology of dissipative gases and granular media has surprised us. In order to be able to model granular media, we will need macroscopic descriptions analoguous to fluid mechanics and thermodynamics. As far as we see it, Molecular Dynamics is at the moment the only reliable tool which can model granular media. The validation of a fluid mechanics can therefore only be done with the help from MD.

Using Molecular Dynamics to study chemical reactions is not a new idea; in fact it is more than two decades ago since the first simulations were performed. We have clearly demonstrated in this thesis that the macroscopic phenomena can be reproduced in a finite system using MD. In other words, MD is able to reproduce the macroscopic world, and even better than that: the idea behind MD is so naive that it is much easier to understand the physical model.

The interest in the interplay of (energetically driven) chemical reactions and phase separation has increased in recent time (measured by the number of papers per year). Almost all studies have so far been carried out on a mesoscopic level (Hilliard-Cahn theory). Molecular Dynamics is in this context an invaluable tool because the number of simplifying assumptions is limited. Simulations of phase separation and chemical reactions are computer intensive. In order to see pattern formation we need a large number of particles (often $5 \cdot 10^5$) and follow the system over long time scales. The simulations presented in this thesis are not exhausting in the sense that they are only the beginning. We have demonstrated that a phase separation is able to change the underlying mechanism of chemical reactions. The theoretical predictions have not yet been verified by simulations, and moreover, the theory has to be extended to three- and four-component system in order to be more applicable.

APPENDIX A

Geisshirt [24]

Computerens rolle i moderne kemi

Kenneth Geisshirt

7 juni 1996

Indledning

Computere er nutildags blevet allemandseje Elektronik - og derved også computere - er en af de få varer, der gennem tiden har fået større ydelse samtidig med at prisen er faldet Som tommelfingerregel kan man sige, at computere bliver dobbelt så hurtige i løbet af 18–24 måneder uden at prisen stiger!

Udviklingen af computere tog for alvorlig fart i 1950'erne, hvor de store amerikanske forskningslaboratorier (f eks Los Alamos) brugte dem Meget hurtigt kunne fysikere og kemiker drage nytte af disse maskiner

I denne artikel vil jeg forsøge at give et indblik i hvordan jeg opfatter brugen af computere i kemien Jeg tænker ikke på almindelig tekstbehandling eller litteratursøgning, men på - til tider tunge - beregninger Langgård [13] har her i bladet skrevet om de mange kemiprogrammer, som findes til pc'ere, og han gjorde især noget ud af programmer til molekylær modellering Denne artikel handler ikke om specifikke programmer, men mere om de muligheder, man får med computeren

Metafysiske bemærkninger

Naturvidenskaben var i sit udspring spekulativ [7] I antikken opfattede man ikke eksperimenter som noget, der var værd at give sig i kast med Vi kender nok alle Zenons paradoks om Achilleus og skildpadden, som betød at kinematikken stod i stampe i mange hundrede år Naturvidenskaben er først i 1400-tallet blevet rigtig naturvidenskabelig i den forstand, at naturfilosoffer begyndte at lave eksperimenter for at be- eller afkræfte deres teorier Det vil sige, at der skete en deling af naturvidenskaben, i stedet for kun en gren (teori) fik vi to grene (teori og eksperimenter)

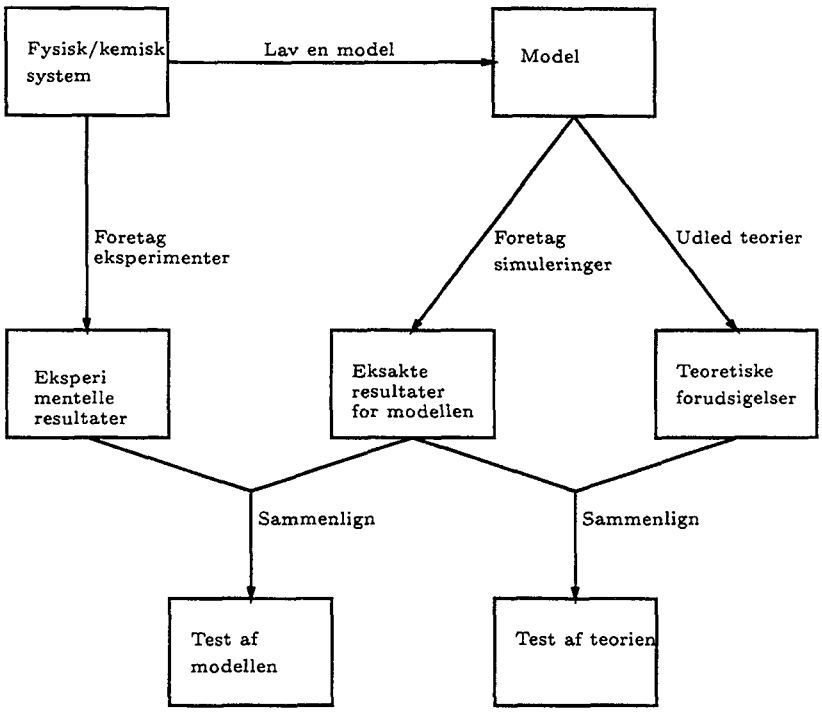

Figur 1 Naturvidenskabens tre-deling Inspireret af figur 1 2 i [1]

Vi står nu i en historisk situation naturvidenskaberne er igen ved at dele sig Den tredie gren er brugen af computeren [14] Jeg vil vælge at tale om beregningsvidenskab som en dansk oversættelse for det engelske "computational science"[1] Beregningsvidenskaben indtager en ganske interessant plads mellem den teoretiske og den eksperimentelle Den er hverken teoretisk eller eksperimentel, men ligger et sted midt mellem de to andre grene På sin vis er beregningsvidenskab meget naiv i forhold til teoretisk kemi eller fysik I stedet for at udvikle en stor flot (men approksimativ) teori for et eller andet system, beregner beregningskemikeren diverse egenskaber direkte fra de simpleste ligninger, han eller hun kender De eneste approksimationer han foretager er den, som ligger i, at computeren regner med endelig nøjagtighed og naturligvis den der ligger i modellen eller ligningerne Figur 1 forsøger at opsummere ovenstående ideer

Man kan spørge sig selv om det er Naturen vi genfinder i et computerprogram Det er det efter min opfattelse Som Wolfram skrev i Scientific American [17]

> It is presumably true that any physical process can be described by an algorithm, and so any physical process can be represented as a computational process Perhaps most significant, it [the use of computers] is introducing a new way of thinking in science

Scientific laws are now being viewed as algorithms A new paradigm has been born

Kemisk kinetik

At ville skrive om computerens rolle i kemisk kinetik er nok et lidt for ambiøst emne, og jeg vil da også begrænse mig til et par eksempler

Pseudo-stationaritet

Beskrivelsen af kemisk kinetik er en beskrivelse af, hvordan koncentrationerne af diverse kemiske forbindelser udvikler sig i tid Den naturlige form er sædvanlige differentialligninger, dvs vi har et begyndelsesværdiproblem af typen

$$\frac{\mathrm{d}\vec{c}}{\mathrm{d}t} = \vec{f}(\vec{c}) \tag{1}$$

hvor $\vec{c}$ er koncentrationerne samlet i en vektor og $\vec{f}$ er hastighedsfeltet Ovenstående ligning kan løses i enkelte - og simple - tilfælde Allerede i 1913 foreslog Chapman og Underhill [9] pseudo-stationaritetsprincippet (PSP), som siger at koncentrationen af et intermediat efter nogen tid ikke ændrer sig I matematiske termer betyder det, at

$$\frac{\mathrm{d}[X]}{\mathrm{d}t} \simeq 0$$

hvor X er et intermediat Ved hjælp af PSP kan vi reducere vores differentialligningsproblem For hvert intermediat, hvor vi benytter PSP får vi en algebraisk ligning, samtidig med at vi får en differentialligning mindre Det var på denne måde Bodenstein og Lütkemeyer i 1925 [8] var i stand til at vise, at deres mekanisme for syntesen af hydrogenbromid stemte overens med deres eksperimenter

Naturligvis giver brugen af PSP problemer, idet det er en approksimation Man kan derfor spørge sig, om man får det samme resultat, som hvis man løste differentialligninger uden nogen approksimation Det spurgte Farrow og Edelson sig om i 1974 [10], og i de systemer de så på, kunne de konstatere at man ikke fik samme resultat! Deres undersøgelser var foretaget vha computere, med hvilke de havde løst både de eksakte ligninger og de approksimerede ligninger[2]

Det kræver naturligvis mere regnetid at simulere det fulde system end det PSP approksimerede system Men her må det bemærkes, at simuleringen

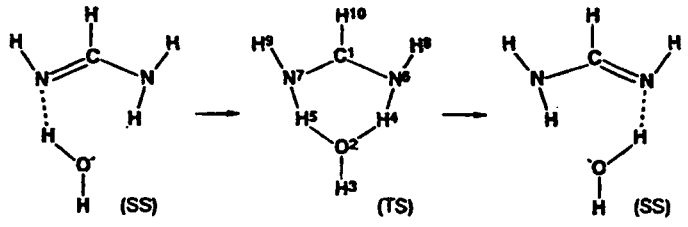

Figur 2 Proton-overførsel i formamidin Molekylet i midten er et "transition-state" kompleks Tallene nummererer atomerne Reproduceret efter [6]

af kemisk kinetik for selv store systemer ikke er mere tidskrævende end at det kan gøres på en almindelig pc'er Kinetikerne kan med andre ord bruge computeren til noget, det drejer sig især indenfor emner hvor man ser på store mekanismer, som f eks atmosfærekemi og oscillerende reaktioner

I fænomenologiske del af den kemiske kinetik er det nok mere de mere eksperimentelt orienterede kemikere end de teoretiske, som har glæde af den nye gren af kemien

Proton-overførselsreaktioner

Det er svært at vælge en artikel blandt de mange, der omhandler simuleringer af kemiske reaktioner Jeg har valgt at beskrive et enkelt arbejde Det drejer sig om Nagaoka, Okuno og Yamabe [6] der har undersøgt reaktionen som er illustreret i figur 2

De har set på hvordan de enkelte atomer i formamidin og vand bevæger sig De har antaget at disse bevægelser følger klassisk mekanik I matematiske termer kan klassiske bevægelsesligninger skrives som

$$\begin{aligned} \frac{\mathrm{d}\vec{r}_i}{\mathrm{d}t} &= \vec{v}_i \\ \frac{\mathrm{d}\vec{v}_i}{\mathrm{d}t} &= \frac{\vec{F}_i}{m_i} \end{aligned}$$

hvor $\vec{r}_i$ er atom i's position, $\vec{v}_i$ hastigheden, $\vec{F}_i$ den kraft som atomet er påvirket af og m_i dets masse Kraften $\vec{F}_i$ er givet ved potentialerne mellem de forskellige atomer og disse har Nagaoka *et al* fundet vha *ab initio* beregner Ved at løse de klassiske bevægelsesligninger var Nagaoka *et al* i stand

til at "se" proton-overførelsen De observerer at afstanden mellem atom nr 4 (hydrogen) og nr 2 (oxygen) bliver mindre med tiden, hvilket viser at hydrogen-atomet nu indgår i vandmolekylet og ikke formamidin

Dette arbejde viser hvad computer-simuleringer kan betyde for kinetikken Det er muligt at undersøge dynamikken af et "transition-state" kompleks helt ned på det atomare niveau Naturligvis kan simuleringerne ikke laves på en formiddag (denne type simuleringer bruger megen regnetid) men det viser hvilke muligheder den fysisk-organiske kemi har til rådighed

Statistisk termodynamik

Den statistiske termodynamik forsøger at udregne termodynamiske størrelser ud fra mikroskopiske tilstande En termodynamisk størrelse kunne f eks være temperaturen som viser sig at være den gennemsnitlige kinetiske energi

Simuleringen af mange-partikel systemer er en måde hvorpå vi kan forbinde det mikroskopiske niveau med det makroskopiske niveau Historisk set var netop dette område et af de første, som fysikere og kemikere undersøgte vha computere i 1950'erne I termodynamik er det af store interesse at finde et systems tilstandsligning, som beskriver hvordan forskellige termodynamiske størrelser er relateret Den mest kendte er idealgasligningen

$$PV = nRT$$

hvor P er trykket, V er rumfanget, n stofmængden, T temperaturen, og R er gaskonstanten Denne tilstandsligning gælder for en gas, hvor de enkelte partikler ikke vekselvirker, dvs de hverken frastøder eller tiltrækker hinanden

Empirisk ved man, at ikke alle systemer opfører sig som ideale systemer Det har man forsøgt at efterrationalisere gennem virialudviklinger, dvs at tilstandsligningen for gassen er

$$PV = nRT\left(1 + \sum_{i=2}^{\infty} B_i P^{i-1}\right) \tag{2}$$

hvor B_i er den i'te virialkoefficient Eksperimentelt finder man så mange koefficienter, som det er muligt ud fra ens data

Ideale gasser er det simpleste system vi kan forstille os Det næste system er hårde kugler Hårde kugler er ikke andet end små kugler, der bevæger sig rundt i en beholder - et billardbord er en god to-dimensional analogi Den

eneste måde, partiklerne vekselvirker er gennem kollisioner Når de støder sammen, ændrer de kurs og hastighed gennem et elastisk stød Teoretikere har brugt megen tid på at udlede tilstandsligningen, dvs finde virialkoefficienterne

Simulering af systemer af hårde kugler er ikke særlig kompliceret, og det er muligt at skrive meget hurtige programmer Ved hjælp af et sådan program kan vi finde sammenhørende værdier af tryk, temperatur og tæthed (tætheden er $\frac{n}{V}$), og derefter lave en kurvetilpasning til ligning 2 og finde så mange virialkoefficienter som vores beregnede data tillader Tabellen nedenfor viser virialkoefficienterne ($b = B_2$) fundet ved simuleringer og udregnet vha HNC-teorien [12] HNC-teorien er bygget op omkring integralligingen

$$\log g(\vec{r}) + \beta v(\vec{r}) = \rho \int (g(\vec{r} - \vec{r}') - 1)(g(\vec{r}') - 1 - \log g(\vec{r}') - \beta v(\vec{r}'))\mathrm{d}\vec{r}'$$

hvor $\beta = 1/k_B T$, $g(\vec{r})$ er den radiale fordelingsfunktionog $v(\vec{r})$ er potentialet, som ved hårde kugler er simpelt HNC-teorien giver et lukket udtryk for virialkoefficienterne

$$B_n/b^{n-1} = 2(2 + 3n(n-1))4^{-n}$$

Som det ses af tabellen, giver HNC-teorien gode værdier for de første virialkoefficienter, men de sidste er gale

virial koefficient	Simulering	HNC
B_2/b	1 0000	1 0000
B_3/b^2	0 6250	0 6250
B_4/b^3	0 2861	0 2092
B_5/b^4	0 1103	0 0493
B_6/b^5	0 0386	0 0281

Simuleringsteknikkerne udviklet omkring statistisk mekanik ser ud til - for mig - at koncentrere sig mere om teoretiske studier (idealiserede modeller) end om koblingen til eksperimenter Det mener jeg ikke, at der er noget galt i, det viser bare at beregningskemi indtager en væsentlig plads mellem teoretiske og eksperimentelle aspekter af kemien Simuleringer af mange-partikel systemer er interessante, fordi de giver os mulighed for at koble den mikroskopiske verden med den makroskopiske verden Det er svært at sige, hvor stort et typisk system er Verdenrekorden ligger omkring 250 millioner partikler, men det er nok mere almindeligt at simulere mellem 500 og 100000 partikler

I det sidste årti er der fremkommet en række mere eller mindre kommercielle programmer til undersøgelse af store biologiske molekyler, f eks proteiner Med mere eller mindre kommerciel mener jeg programmer som er gratis at bruge for undervisnings- og forskningsinstitutioner, mens private virksomheder nå betale for dem Jeg tænker på programmer som Gromacs [16], DL_POLY [11], etc Programmer benytter de samme numeriske algoritmer som benyttes i statistisk termodynamik Det, folk kan være interesseret i, er et proteins struktur i vandig opløsning Ved hjælp af en simulering af de enkelte atomers bevægelser finder man ligevægtstrukturen Det drejer sig her ofte om mere eksperimentelle folk som ønsker at trække ny information ud af deres eksperimentelle data fra f eks Röntgen-diffraktion eller NMR-spektroskopi

Kvantekemi

Kvantekemi er nok den gren af kemien, som langt de fleste forbinder med supercomputere og tunge beregninger, dvs det er her, man forventer at finde beregningskemikere Det er da heller ikke forkert

Den første opgave i en kvantekemisk beregning er at opstille og løse Hartree-Fock ligningerne, dvs [15]

$$\left(-\frac{\hbar}{2m}\nabla^2 - \frac{Ze^2}{r}\right)\varphi_i(\vec{x}) + \int \frac{e^2}{|\vec{x}-\vec{x}'|}\sum_j \varphi_j^*(\vec{x}')\left[\varphi_j(\vec{x}')\varphi_j(\vec{x})\varphi_j(\vec{x})\varphi_j(\vec{x}')\delta_{m_{s_i},m_{s_j}}\mathrm{d}\vec{x}'\right] = \epsilon_i\varphi_i(\vec{x})$$

hvor φ_i er den i'te atomorbital, ϵ_i dens energi, Z er ladningen af kernen for det pågældende atom og s_i er spintilstanden Molekylorbitaler dannes som en linearkombination af atomorbitaler

Gennem de sidste 3–4 årtier er der udviklet mere og mere sofistikerede numeriske metoder, som løser Hartree-Fock ligninigerne for et givet molekyle Gennem løsningen finder vi molekylets elektroniske tilstande og egenskaber, og det giver os desuden mulighed for at udregne forskellige termodynamiske størrelser som f eks dannelsesenthalpi

Der findes flere kommercielle programmer, som arbejder indenfor det kvantekemiske område Langgård [13] har her i bladet beskrevet et par af dem, man kan købe til pc'ere (Gaussian, Mopac, HyperChem) Naturligvis er selv en hurtig pc'er ikke hurtig nok til at undersøge meget store systemer, når det drejer sig om *ab initio* beregninger

Jeg vil ikke her opremse alle *ab initio* beregninger der er fortaget i verden (Dansk Kemi kunne sikkert fyldes hver måned med referencer til de nyudkomne artikler) Jeg vil kort nævne et enkelt arbejde af Ho *et al* [4] I sin korthed omhandler det beregning af dannelsesenthalpier af $SiCl_n$, SiH_n og SiH_nCl_m forbindelse Motivationen for Ho *et al* er at SiH_nCl_m-forbindelserne er termisk ustabile hvilket betyder at de eksperimentelle data er noget usikre Tabellen nedenfor viser de beregnede enthalpier og de eksperimentelle (som er fra JANAF [3]) ved $T = 298K$ Enheden er kcal mol^{-1}

Forbindelse	Ho *et al*	JANAF
SiH_3Cl	$-32\,2$	$-33\,0 \pm 2$
SiH_2Cl_2	$-74\,5$	$-76\,6 \pm 3$
$SiHCl_3$	$-117\,0$	$-118\,6 \pm 1$
$SiHCl$	$17\,0$	
SiH_2Cl	$7\,8$	
$SiHCl_2$	$-34\,3$	

Som det ses af tabellen er der god overensstemmelse mellem de beregnede og de eksperimentelle værdier for de tre første forbindelse For de sidste tre forbindelser foreligger der ingen eksperimentelle værdier Det er her *ab initio* beregningerne efter min mening kommer til deres ret Der er ingen idé i at reproducere naturen, men der kan være til stor hjælp at give eksperimentalister en idé om hvad de manglende data er Det kan havde stor betydning i tolkningen af eksperimenter

Symbolske programmer

I de sidste 10–15 år er der fremkommet en meget speciel type programmer, nemlig programmer, som er i stand til at manipulere med matematiske udtryk og strukturer på en eksakt måde De metoder, som jeg har beskæftiget mig med i de foregående afsnit var alle numeriske, løsningerne er ikke eksakte, men givet af en computer som regner med endelig præcision De symbolske programmer (Mathematica, Maple, Macsyma, Reduce, etc) gør det samme, som vi mennesker gør, når vi sidder med et stykke papir og en blyant og løser en ligning, finder egenværdier for en matrix, etc Med andre ord er disse programmer i stand til at reducere $x^2 + y^2 + 2xy$ til $(x + y)^2$, uden at vide andet end at x og y er to variable Selvfølgelig kan symbolske programmer meget mere - de kan finde egenværdier for vilkårlige matricer, løse algebraiske ligninger og meget andet

De symbolske programmer er endnu ikke så udbredte, men jeg er overbevist om, at når først mere teoretisk orienterede kemikere opdager mulighederne i at bruge symbolske programmer, vil de få stor betydning Naturligvis kan programmer ikke andet end vi mennesker kan - hvis en ligning ikke kan løses eksakt, kan programmerne ikke hjælpe os Men det er vigtigt at huske, at hvor vi mennesker hurtigt får svært ved at overskue komplicerede matematiske udtryk, er det ikke et problem for en computer, bare dens bruger har tålmodighed Og hvem kan lige huske at[3]

$$\sum_{n=1}^{\infty} \frac{1}{n^6} = \frac{1}{945}\pi^6$$

eller

$$\int_0^{2\pi} \exp(x)\sin(x) = -\frac{1}{2}e^{2\pi} + \frac{1}{2}$$

Mit kendskab til symbolske programmer er begrænset til Mathematica og Maple Både Mathematica og Maple er i sig selv programmeringssprog som er konstrueret med matematiske anvendelser for øje For disse to programmer ligger styrken ikke i, at det er muligt i udregne ovenstående to eksempler, men det at det er muligt at skrive lange programmer i det indbyggede programmeringssprog

Et godt eksempel, som dog ikke så vidt jeg ved er blevet realiseret, er undersøgelser af gittermodeller i statistisk mekanik Den simpleste er Ising modellen, og her er det muligt at finde faseovergange ved håndkraft Men det kunne være interessant om det også var muligt for andre modeller, f eks en Potts model[4] Det er ganske givet umuligt at gøre i hånden, men et program til f eks Mathematica ville måske være i stand til at gøre det

Der er dog i de senere år fremkommet nogle eksempler på hvordan symbolske programmer kan bruges i teoretisk fysik og kemi Lad mig her nævne et par eksempler med kemisk relevans Det første er et arbejde af Ageev og Sanctuary [2] De har vha Maple udregnet NMR liniers intensiteterne for systemer med spin $\frac{7}{2}$ Som de skriver i deres resumè

> Developments in computer algebra have prompted us to reconsider earlier intractable problems

Et andet arbejde er af Cox, Smith og Sutcliffe [5] De har skrevet programmer til Maple som kan løse Schrödinger ligningen for tre-legeme problemer under bestemte forhold Det skal bemærkes, at uddata fra det symbolske program bruges i et program, der regner videre numerisk, altså en mere traditionel metode

Afslutning

Jeg har i denne artikel forsøgt at beskrive nogle af de områder i kemien hvor computere har en vigtig rolle at spille Beregningskemien må altid søge inspiration hos den eksperimentelle kemi, men samtidig kan beregningskemien inspirere eksperimentalister i tolkningen af målinger og i design af eksperimenter

Noter

1 Det er værd at bemærke, at der er forskel på "computational science" og "computer science" Det sidste er hvad vi på dansk kalder datalogi

2 Jeg vil ikke forsvare den holdning, at PSP helt skal opgives, idet det har stor betydning i mere teoretiske overvejelser

3 Værdien af rækken og integralet er fundet vha Maple

4 En Potts model er en generaliseret Ising model

Litteratur

[1] M P Allen and D J Tildesley *Computer Simulation of Liquids* Clarendon Press, 1987

[2] S Z Ageev B C Sanctuary Analytical solutions for spin 7/2 line intensities in solid sate NMR *Molecular Physics*, 84(5) 835–844, 1995

[3] D R Stull H Prophet JANAF thermochemical tables United States Department of Commerce National Bureau of Standards, 1981

[4] P Ho M E Coltrin J S Binkley C F Melius A theoretical study of the heats of formation of SiH_n, $SiCl_n$, and SiH_nCl_m compounds *Journal of Physical Chemistry*, 89 4647–4654, 1985

[5] H Cox S J Smith B T Sutcliffe An application of the computer algebra system Maple for the calculations on atomic and molecular system *Computer Physics Communications*, 84 186–200, 1994

[6] M Nagaoka Y Okuno T Yamabe Chemical Reaction Molecular Dynamics simulation and the energy-transfer mechanism in the proton-transfer reaction of formanidine in aqueous solution *Journal of Physical Chemistry*, 98(48) 12506–12515, 1994

[7] J Avery *Science and society* University of Copenhagen

[8] M Bodenstein and H Lütkemeyer Die photochemie Bildung von Bromwasserstoff und die Bildungsgeschwindigkeit der Brommolekel aus den Atomen *Zeitschrift fur Physicalische Chemie*, 124 208–236, 1925

[9] D L Chapman and L K Underhill The interaction of chlorine and hydrogen The influence of mass *Journal of the Chemical Society*, 103 496–508, 1913

[10] D Edelson and L A Farrow The steady-state approximation fact or fiction? *International Journal of Chemical Kinetics*, 6 787–800, 1974

[11] T R Forester and W Smith *The DL_POLY 2 0 User Manual* Daresbury Laboratory, december 1995

[12] J P Hansen and I R McDonald *Theory of simple liquids* Academic Press, 2 edition, 1986

[13] Morten Langgård Molekylær modellering på en PC *Dansk Kemi*, (11) 13–17, november 1995

[14] O G Mouritsen Computeren som værktøj i statistisk fysik *Kvant*, pages 19–22, april 1993 In Danish

[15] F Schwabl *Quantum Mechanics* Springer-Verlag, 2 edition, 1991

[16] D van der Spoel, H J C Berendsen, A R van Buuren, E Apol, P J Meulenhoff, A L T M Sijbers, and R van Drunen *Gromacs User Manual* University of Groningen, 1995

[17] Stephen Wolfram Computer Software in Science and Mathematics *Scientific American*, 251(3) 140–151, 1984

APPENDIX B

Geisshirt *et al.* [27]

Oscillating Chemical Reactions Simulated by Molecular Dynamics

K Geisshirt[1], *E Praestgaard*[1], *and S Toxvaerd*[2]

[1]Department of Life Sciences and Chemistry, Roskilde University, DK-4000 Roskilde, Denmark

[2]Department of Theoretical Chemistry, University of Copenhagen, DK-2100 Copenhagen, Denmark

We outline how chemical reactions can be simulated by Molecular Dynamics, and we apply our technique to an oscillating chemical reaction scheme; a modified Volterra-Lotka scheme We observe deviations from the phenomelogical equations in the phase separating temperature region

1 Introduction

The phenomenon of oscillating chemical reactions is fairly new, i e it has been known for the last three or four decades. The development of the theory for oscillating chemical reactions is strongly connected to the theory of nonlinear dynamical systems and nonequilibrium thermodynamics Until now oscillating chemical reactions have experimentally been investigated macroscopicly and the theory used for describing the reactions is phenomelogical. Experimentally studied oscillating reactions are either external driven systems or systems allowed to relax to equilibrium

On the other hand oscillating systems have been investigated numerically as long as oscillating reactions have been known by means of coupled differential equations in the consentrations It is however possible by today's computers to simulate chemical reactions in continious space and on a molecular level by Monte-Carlo (MC) and Molecular Dynamics (MD) simulations It implies that it is possible to investigate realistic systems where also other nonlinear dynamics, like a phase seperation might influence the chemical reaction It was recently shown that chemical reactions have a large effect on phase separation; see e g [4] for a Monte-Carlo study of simple first-order reactions $A \rightleftarrows B$ and Molecular Dynamics study of first- and second-order reactions [5]

2 Chemical kinetics and molecular dynamics

Chemical reactions, on a microscopic level, are usually formulated as coupled elementary reactions We will here only consider coupled bimolecular reactions, i e a reactions where there are two reactants in each reactions.

The usual chemical viewpoint is the transition state theory The basic idea is that the two reactants collide and form an activated complex ($C^{\ddagger}$), which can either break into the reactants again or into the products The quantum mechanical details in this reversible dynamics are, however, believed to be of no

Springer Proceedings in Physics, Volume 82
Computer Simulation Studies in Condensed Matter Physics IX
Eds : D P Landau K K Mon, H. -B Schüttler

importance for the overall kinetics of oscillating reactions The main feature is that the exchanges of covalent bonds occur with a certain probability when the reactants are separated at a short molecular distance The reaction rate is typically given by an Arrhenius expression where the rate depends exponentially on the activation energy in units of the kinetic energy (the temperature) Experimentally, reactions with small activation energy are difficult to follow because they are fast In Molecular Dynamics, however, we are in the opposite situation With today's computers we are able to simulate of the order 10^5 (simple) molecules in of the order 10^6 time steps, which correspond to reaction times of only nanoseconds For this reason the transition energy is taken to be of the order T which automatically implies that the reaction takes place on a time scale equal to the mean collision time Futhermore, a chemical reaction appears in an open system, i e without a conserved energy and fixed number of reactant On the other hand a traditional MD system consists of a fixed number of particles and with a well-defined Hamiltonian, which makes it to a non-trivial task to reformulate the dynamics in open systems with chemical reactions The actual implementation and its impact on the dynamics is described in in more details in Ref [5] In summary the reaction dynamics is implemented into the MD by spontaneously and with a certain probability, to relabel the colliding particles Futhermore, in order not to introduce large force gradients into the system by this reaction dynamics we only consider reactions between particles with almost the same excluded volumes, i e the chemical individualities of the reactants are given by their long range forces and not by their short range forces This feature is certainly unrealistic from a chemical view point; but it is believed to be of no importance for the qualitative behavior of the chemical reaction dynamics as will be demonstrated

3 A particular example: MD simulations of the modified Volterra-Lotka reaction

We have chosen a particular oscillating system as our system It consists of three species and three reactions The reactions are:

$$A + X \xrightarrow{k_1} 2X \tag{1}$$

$$X + Y \xrightarrow{k_2} 2Y \tag{2}$$

$$Y + A \xrightarrow{k_3} 2A \tag{3}$$

To minimise the number of parameters in our model, we have chosen to set k_3 to the same value as k_1

This reaction scheme is a simple modification of the Volterra-Lotka equation for a homogeneous (in space) oscillating reaction [6] [7] In a traditional chemical reaction experiment the system is fed by a reactant A which through a consecutive set of unimolecular reactions is transformed into the product B In our case and for an open MD system of particles in a volume with periodical

boundaries it is, however, convenient to equal reactant and product and thus to recover A through reaction 3 It is the only modification of the traditional reaction scheme for the oscillating reaction and the flow through the system is obtained, as usual by only forward elementary reactions without reverse reactions This corresponds to that the reactant has a significant higher (free) energy than the product

From these three reactions, one can easily derive three phenomelogical equations describing the concentrations of the three species The equations are:

$$\begin{aligned}\frac{d[A]}{dt} &= -k_1[A][X] + k_1[A][Y] \\ \frac{d[X]}{dt} &= k_1[A][X] - k_2[X][Y] \\ \frac{d[Y]}{dt} &= k_2[X][Y] - k_1[A][Y]\end{aligned}$$

where [ ] means the concentration The phenomelogical equations are only valid in the complete homogeneous case, which experimentally is realised by stirring the contents of the chemical reactor

We have three coupled ordinary differential equations which are impossible to find an analytical solution to In general, we have equations of the type.

$$\frac{d\vec{x}}{dt} = \vec{f}(\vec{x})$$

We can first find a stationary solution to the problem above, i e find an $\vec{x}_0$ which satisfies $\vec{f}(\vec{x}_0) = \vec{0}$ Then we can linearise the differential equation at this stationary point and obtain

$$\frac{d\delta\vec{x}}{dt} = \mathbf{J}(\vec{x}_0)\delta\vec{x}$$

where $\mathbf{J}$ is the Jacobian matrix and $\delta\vec{x}$ is the deviation from the stationary point, i e $\delta\vec{x} = \vec{x} - \vec{x}_0$ The linearised system is a linear differential equation. The solution of the linear differential equation is

$$\delta\vec{x} = \sum_i \vec{e}_i e^{\omega_i t}$$

where ω_i is the ith eigenvalue and $\vec{e}_i$ is basically the ith eigenvector which is normalised appropriately

The modified Volterra-Lotka scheme has a stationary solution, which is

$$\begin{aligned}[A]_0 &= C\left(1 - \frac{2k_1}{2k_1 + k_2}\right) \\ [X]_0 &= [Y]_0 = \frac{Ck_1}{2k_1 + k_2}\end{aligned}$$

where C is the total concentration, i e $C = [A] + [X] + [Y]$ which is a constant

We can now linearise the system and calculate the eigenvalues of the Jacobian matrix at the stationary point We get

$$\lambda_1 = \overline{\lambda_2} = \frac{Ck_1\sqrt{k_2}}{\sqrt{2k_1 + k_2}}i$$

which shows us that the system will have sustained oscillations - at least close to the steady-state solution

4 Simulational details

The chemical equations for the Volterra-Lotka reaction expresses a *homogeneous* change in the concentration space of the reactants, which for certain values of the reaction rates, oscillate In a real experiment it means that large concentrations of a certain component is built up for a while and then disappears through a chemical reaction. If the three components are miscible for all concentrations one would expect that the dynamics might be well described by the traditional homogeneous differential equations, whereas a new situation appears if one of the concentrations exceeds the critical value of solubility and a competing phase separation takes place in the oscillating system For this reason we will expect a non-trivial difference between a set of homogeneous chemical reactions and a corresponding MD simulation This is due to the fact that we in an MD system can create a phase separation by a chemical reaction, simply by ensuring that the product has an intermolecular potential which favors phase separation This is ensured in the very same manner as for the chemical reaction by varying the long range attractions between the molecules For details see e g [8]

The system is - as already mentioned - a three-component system The interaction of particles of the same type is a Lennard-Jones potential which is cut at $r = 2\,5$ The interaction between particles of different types is also a Lennard-Jones potential, but it is cut at $r = 1\,0$ meaning that it is replusive only The density of the system is 0 6 At low enough temperature a system with such interactions will phase separate We use the same reaction parameters throughout all our simulations The collision diameter is set to 1 0 (in Lennard-Jones units) The probability of reaction is set to $1\,0\ \ 10^{-3}$ for reactions 1 and 3 while for reaction 2 it is set to $1\,1\ \ 10^{-3}$

All our simulations are performed in the NVT-ensemble using a Nosé-Hoover thermostat to control the temperature and a leap-frog algorithm to integrate the equations of motion [1] The chosen time step is $h = 5\ \ 10^{-4}$ Furthermore, all simulations are done in two spatial dimensions

5 Results and open questions

We have performed a number of simulations at different temperatures with either 1024 or 8192 particles Rate constant for a reaction usually follow Arrhenius' law, i e $k(T) = A\ \ e^{-E_a/RT}$, where E_a is the activation energy, A is a preexponetial factor, and R is the gas constant.

During our simulations we have stored instantaneous values of the concentrations and the number of times the three reactions has occured Figure 1

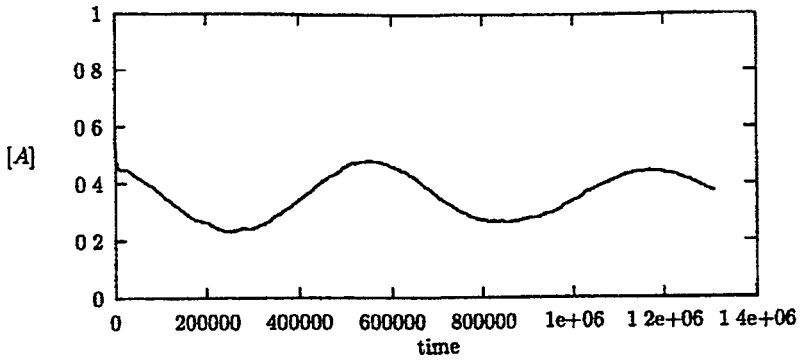

Figure 1: The concentration of A versus time The simulation shown consists of 8192 particles and the temperature is 1 4 The time is measured in unit of time steps

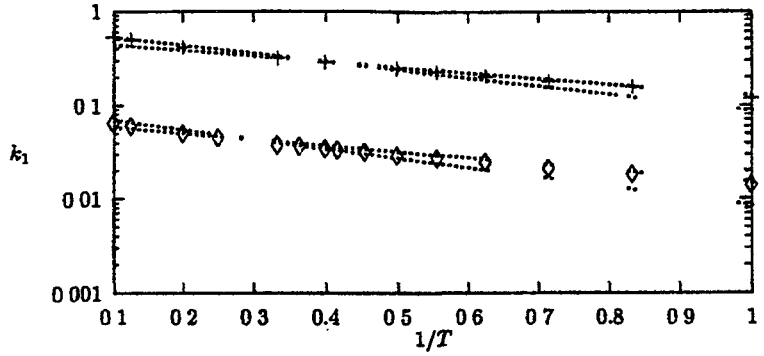

Figure 2: Arrhenius plot for the rate constant for reaction 1 The lower curve is for 1024 particles and the upper one is for 8192 particles Note that the rate constants are not normalised according to the number of particles and therefore the rate constants for the 8192 particle simulations are 8 times larger. The dotted lines are the best fitted lines to the data in that particular temperature region

shows the concentration of A versus time for a typical simulation The number of times a reaction has occured (denoted N_R) is proprotional to the velocity of that reaction and we therefore have a simple relationship for the rate constant, namely $k = \frac{N_R}{[J][J']}$, where J and J' denote the two reactants in the reaction.

Figure 2 shows the rate constant for reaction 1 versus the inverse temperature Similar plots can be made for the two other reactions The estimated error bars are very small. Our estimates are that they are at 4th or 5th significant digit [2]

We notice there is a crossover at $T \approx 3$ The crossover seems not just to be a finite-size effect since we see it at simulations with 1024 and 8192 particles

We believe that this effect comes from the fact that the system goes from being phase separated to a homogeneous phase when we increase the tempera-

ture In the homogeneous phase the three reactions can occur at all places in the simulation box while below the phase separating temperature, the reactions will mainly occur at the boundaries between clusters of, say, X and Y The critical temperature for a similar system of a binary mixture is $T_c \approx 4\,7$ [8] In the critical region the phase separation dynamics is extremely slow; but well below this region two processes will compete: diffusion (to the interfacial reaction zone) and reaction The figure shows that the activation energy in the low temperature region is not the activation energy for the reaction but the activation energy for combined process of diffusion and reaction

Acknowledgements

The authors wish to thank the National Science Foundation (in Denmark) for computing time on the IBM SP2 at the National Computer Centre (Uni-C) We also wish to thank M Laradji for his many advices

References

[1] Toxvaerd, S , 1991, Mol Phys **72**(1), 159

[2] Flyvbjerg, H and Petersen, H G , 1989, J. Chem Phys **91**(1), 461.

[3] Chemical Kinetics, 3rd edition K J Laidler. HarperCollins, 1987.

[4] Glotzer, S C , Stauffer, D , and Jan, N , 1994, Phys Rev Lett **72**(26), 4109.

[5] Toxvaerd, S., 1996, *to appear in* Phys Rev E **53**

[6] Lotka, A , 1910, J Phys Chem **14**, 271

[7] Lotka, A , 1920, J Am Chem Phys **42**, 1593

[8] Toxvaerd, S and Velasco, E , 1995, Mol Phys **86**, 845

APPENDIX C

Geisshirt *et al.* [26]

Oscillating chemical reactions and phase separation simulated by molecular dynamics

Kenneth Geisshirt and Eigil Praestgaard
Department of Life Sciences and Chemistry Roskilde University, 4000 Roskilde Denmark

Søren Toxvaerd
Department of Chemistry, University of Copenhagen 2100 Copenhagen Ø Denmark

(Received 12 May 1997; accepted 4 September 1997)

Molecular dynamics (MD) of stationary chemical kinetics is used to simulate oscillating chemical reactions in a system of N classical mechanical particles with Lotka–Volterra kinetics The MD includes oscillations in a (closed) system with conserved energy and time reversible dynamics as well as oscillating chemical reactions in an open and driven non-equilibrium system, and with and without a competing phase separation of the different components in the reactions The approach allows a detailed investigation of the kinetics and demonstrates on a molecular level, the phenomenon oscillating reactions for various chemical and reaction kinetics details When phase separation takes place during the oscillations the kinetics is no longer simple diffusion driven
 [S0021-9606(97)50846-4]

I INTRODUCTION

Oscillating chemical reactions have been known for many years Lotka was the first to do a theoretical investigation,[1] whereas the first systematic experimental studies were performed by Belousov and Zhabotinsky[2] In the recent years there has been a vast interest in spatial inhomogeneous systems after Zhabotinsky's observations of chemical waves[3] Prigogine and co-worker's investigations of far from equilibrium systems have been of great importance in the theoretical understanding and especially the Brusselator has been a source of inspiration for the chemical community[4,5] Models for chemical reactions are usually formulated in terms of continuous parameters, like the concentrations and free energy density, for the variation in time and space, and do not include the microscopic molecular details of the reactions By molecular dynamics (MD), however, simple chemical kinetic systems can be simulated microscopically by a finite number of particles according to the (classical) equations of motion[6,7] and this approach allows an investigation of the details in the reaction dynamics and domain formation Simulation of chemical instabilities and oscillating chemical reaction by molecular dynamics has in fact been performed for more than two decades[6,8–10] Recently it has been shown that chemical reactions ($A \rightleftharpoons B$) may alter the dynamics of a spinodal decomposition[7] The present work analyzes the interplay between oscillating chemical reactions and a spinodal decomposition into coexisting phases of the different species in the chemical reaction scheme

The outline of this paper is the following: Section II presents the chemical system we have investigated It is a modified version of the old Lotka–Volterra equations Diffusion driven reactions in condensed phases are discussed in Sec III In Sec IV we discuss the molecular details of the open and (energetically) driven reaction scheme and how the bimolecular reactions are implemented in the MD system, and the results obtained from our simulations are discussed in Sec V

II THE CHEMICAL SCHEME

The first step in the present investigation of chemical kinetics is to formulate a chemical reaction scheme which is suitable for simulation by MD The first problem is to set up an open MD system for a stationary state of chemical reactions In chemical kinetics we have in general a consecutive set of chemical reactions in which the reactant(s), A, is transformed into the product(s), D In a stationary flow one ensures a constant flow with respect to the way in which A enters the open reaction cell and correspondingly the way in which the product D leaves In MD this can be done by introducing the A molecules at the positions where the products are taken away, in the most simple case by relabeling the particles This periodic kinetics, however, has the shortcoming that it correlates the position of the reactants directly with the position of the products and moreover, this stationary driven MD system might violate fundamental thermodynamics principles e g the Wegschleider conditions[6] But both shortcomings however are easily circumvented by introducing an activation reaction The complete MD-stationary chemical kinetics technique (MD-SCK) is best described by a specific example (see also Sec III) We shall use a particularly simple autocatalytic oscillating reaction, namely the Lotka–Volterra mechanism,[1] often simulated in deterministic chemical kinetics[6,11] Traditionally this set of consecutive forward reactions is written as

$$A^* + B \xrightarrow{k_1} 2B \tag{1}$$

$$B + C \xrightarrow{k_2} 2C \tag{2}$$

$$C \xrightarrow{k_3} D, \tag{3}$$

where k_1, k_2, and k_3 are the rate constants (The MD kinetics can easily include reverse reactions;[7] but in the stationary driven state far from equilibrium these reactions play no role) Experimentally the reactant A^* is injected and the

 0021-9606/97/107(22)/9406/7/$10 00

product D removed continuously with a constant flow from the reaction cell by fast diffusion In the MD-SCK, however, the stationary kinetics are set up so that the product D is replaced by "precursors" A, of the reactant The extended Lotka scheme is then obtained by introducing an activation reaction

$$A \xrightarrow{k_0} A^*, \tag{4}$$

by which the precursors of the active reactant are energetically activated, e g , experimentally by a photo induced transition and in MD e g , by thermostating some (randomly) selected precursors to a higher temperature The last equation is modified, e g , to

$$C+A^* \xrightarrow{k_3} 2A, \tag{5}$$

whereby the deactivated precursor A is reproduced

In the limit of fast activation ($k_0 \gg k_i$) one can derive phenomenological equations describing the evolution of the concentrations The phenomenological equations are only valid for a homogeneous system, i e , a system where the concentrations are independent of space—at least on a macroscopic scale The three phenomenological equations for the scheme given by reactions (1), (2), and (5) are:

$$\frac{d[A^*]}{dt} = -k_1[A^*][B]+k_3[A^*][C], \tag{6}$$

$$\frac{d[B]}{dt} = k_1[A^*][B]-k_2[B][C] \tag{7}$$

$$\frac{d[C]}{dt} = k_2[B][C]-k_3[A^*][C] \tag{8}$$

It is easy to see that we can only have simple solutions; there are no chaotic solutions The system is two-dimensional since the total concentration is constant, $K=[A^*]+[B]+[C]$ The Poincaré–Bendixson theorem then shows that only simple solutions may exist [12] It is not possible to find an analytical solution, and instead we can find an approximate solution First we find a steady state, i e , a point in the concentration and parameter space (the parameters are the rate constants and the total concentration) where the derivatives of the concentrations with respects to time are zero The steady state is

$$[A^*]_{ss} = \frac{Kk_2}{k_1+k_2+k_3}, \tag{9}$$

$$[B]_{ss} = \frac{Kk_3}{k_1+k_2+k_3}, \tag{10}$$

$$[C]_{ss} = \frac{Kk_1}{k_1+k_2+k_3} \tag{11}$$

The eigenvalues and eigenvectors of the Jacobian matrix are calculated at the steady state and the approximate solution—close to the steady state—is then

$$\mathbf{c}(t)-\mathbf{c}_{ss} = \sum_j \mathbf{e}_j \exp(\omega_j t), \tag{12}$$

where $\mathbf{c}$ is the concentration vector, $\mathbf{e}_j$ the jth eigenvector (normalized appropriately) and ω_j is the jth eigenvalue It turns out that the chemical scheme has one eigenvalue which is zero and two eigenvalues which are imaginary only The latter two form a complex conjugated pair, and the value is

$$\omega = i\frac{K\sqrt{k_1k_2k_3}}{\sqrt{k_1+k_2+k_3}} \tag{13}$$

In other words, the solution close to the steady state is oscillatory

III BIMOLECULAR REACTIONS IN CONDENSED PHASES

In the case of chemical reactions in condensed phases we often see that diffusion may play an important role If we look at the reaction $X+Y \rightarrow Z$ in a condensed phase, the reaction may be split up in two reactions[13]

$$X+Y \xrightarrow{k_f} Z, \tag{14}$$

$$Z \xrightarrow{k_r} X+Y \tag{15}$$

The species Z represents the products while X and Y are the two reactants The rate constants k_f and k_r depend on the spatial dimension, i e , the functional form in two dimensions is very different from the three-dimensional case We will limit ourselves to the two-dimensional case since all our simulations have been performed in two dimensions It turns out that the rate constants are time dependent The two expressions are[13]

$$k_f = 2\pi(D_X+D_Y)\log\left(\frac{R_1(t)}{R_{\text{reac}}}\right) \tag{16}$$

$$k_r = \frac{2(D_X+D_Y)}{R_{\text{reac}}^2}\log\left(\frac{R_2(t)}{R_{\text{reac}}}\right) \tag{17}$$

where R_1 and R_2 are two slowly varying functions, D_X and D_Y are the diffusion coefficients for the two species X and Y, and R_{reac} is the sum of the radii of X and Y We will in Sec IV A define this parameter more precisely

We observe that the two rate constants scale linearly in the diffusion coefficients When we observe an overall rate constant k for the reaction $X+Y \rightarrow Z$, the ratio between k and D_X+D_Y must be constant, if the reaction is diffusion-controlled It is also worth noticing that in our simulations, the diffusion coefficients of the three species are the same, i e $D_X=D_Y$ (The controversy about diffusion in two dimensions[14] concerns diffusion in infinite systems The self-diffusion in the present, finite system is a well defined quantity which can be obtained e g , from the Einstein relation for the mean square distance of the particle diffusion)

IV SIMULATING OSCILLATING REACTION WITH COMPETING PHASE SEPARATIONS BY MD

A Simulating bimolecular reactions by MD

Since we are interested in the general and qualitative properties of MD simulation of chemical kinetics we have chosen simple Lennard-Jones (LJ) intermolecular potentials between the various species in the reaction scheme and with identical short-range repulsion (σ) by which we avoid introducing large force gradients in the (open) MD-system caused by fast kinetics This is also convenient when applying the MD-SCK technique introduced above In fact the MD for continuous space model, in contrary to lattice models, in principle allows the introduction of a (reactant) molecule everywhere and this fact is used e g , for MD simulations of open equilibrium systems by (slowly) scaling up particles at random position With fast reactions, however, this technique will introduce large force gradients into the system and bring it in a deep non-equilibrium state But this problem is overcome by ensuring the same excluded volume of all the species in the reaction scheme, and the heat of reaction is introduced smoothly into the particle dynamics by changing the range of attractions of the pair potentials after a chemical reaction

The phenomenological equations discussed in Sec II do not explain how the reactions proceed on a molecular level We will not try to review the theories of reaction dynamics here but only discuss how we implement chemical reactions in a molecular dynamics simulation

The naive idea about a bimolecular reaction like $A+B\rightarrow P$ is that the two reactants A and B collide, forming a collision complex which breaks up and forms the product P This is the idea behind the collision theory of reactions [15] Writing this idea in reactions we have: $A+B\rightleftharpoons C\rightarrow P$ We have assumed that the collision complex C may also form the reactants and not only the product

Since we are not working with hard spheres but particles with (qualitatively) realistic intermolecular potentials, we have to specify what we mean by a collision in the context of chemical reactions A collision, which might result in a chemical reaction, simply appears when the distance between two particles is less than a given distance R_{reac} determined by the activation energy $\mathscr{E}=u_{LJ}(R_{\mathrm{reac}})$ In order to simulate the "fate" of the collision complex we let the product be formed with a certain probability P_r, i e , we choose which of the two reactions ($C\rightarrow A+B$ or $C\rightarrow P$) to occur by using a random number generator The parameter R_{reac} is the same parameter we used when we discussed diffusion-controlled reactions In the context of diffusion-controlled reactions, the parameter is the sum of the radii of the two reacting species

B Simulating oscillating reaction by MD

A simple molecular dynamics implementation of the modified Lotka–Volterra reaction is indeed very easy set up just by randomly labeling (A^*, B, C) the N identical particles in an ordinary (two-dimensional) MD system The oscillating kinetics in this *closed* system is implemented only by relabeling particles at (high energy) collisions This means that e g , an A^*-particle can be converted irreversibly into a B-particle by collision with a B-particle etc by which the forward reactions in reactions (1), (2), and (5) are performed This corresponds to a spontaneous and constant activation of the precursor to the reaction species, i e , $k_0\gg k_3$ The activation energy at a binary collision, $\mathscr{E}$, as well as the reaction probability, P_r, is easily adjusted[7] and the underlying dynamics of the N identically, but labeled particles, is purely classical and time reversible The concentration of individual labels, however, changes irreversibly and for certain choices of reaction parameters the concentration of e g , A^* particles oscillates with a frequency given by Eq (13)

A simple example of this purely deterministic MD system with oscillating concentrations is given in Ref 6 for MD at constant energy and with Coulomb pair repulsion The system most commonly used in MD, however, consists of Lennard-Jones particles at constant temperature and with a time reversible classical mechanical dynamics [16] This closed system oscillates too, even when the system is not spontaneously activated by a large k_0 in reaction (5), and it demonstrates that the oscillating reactions are insensitive to details in the intermolecular potentials and the activation process

These systems are, however, in an extreme situation seen from an experimental point of view A real system with oscillating chemical reactions is an *open* and driven system far from equilibrium, and it consists of species which differ with respect to their potential interactions, and the kinetics is associated with different heats of reaction We have obtained oscillating reactions for such systems by keeping the activated species A^* at a higher temperature than the product C (and with net forward reactions), as well as by thermostating all the particles and by ensuring the irreversible driven system by the net forward reactions in reactions (1), (2), and (5) The results reported below are for this case

The heat of the chemical reactions implies that local concentration gradients are introduced into the system during the oscillations which now takes place in a non-uniform system This may even result in phase separations and when this happens we shall demonstrate that the bulk diffusion-controlled reaction mechanism switches over to a surface, or interface controlled mechanism As mentioned all particles have the same repulsive (LJ) potential ($u_{LJ}(r)$ for $r<2^{1/6}\sigma$) and the heat of reaction is given by the fact that pairs of species differ with respect to the range of their attractive pair potentials (As a technical consequence of that fact, the chemical reactions do not spontaneously result in any release of heat It is only when the pairs separate smoothly and without any big force gradients after the collision, that the heat of reaction dissipates into the system for $r>2^{1/6}\sigma$)

A mixture will separate into coexisting phases if the gain in energy exceeds the loss of mixing entropy This ability is also simply ensured by having only short-range and repulsive Lennard-Jones forces between particles with different labels Two systems of this kind have recently been considered First, a two-dimensional non-reactive binary mixture was shown to separate slowly and algebraically into coexist-

ing phases for temperatures below $T_c \approx 1.7\epsilon/k_B$ (where ϵ is the energy parameter in the potential and k_B is Boltzmann's constant) [17] The situation, however, is much more complex when the spinodal decomposition is performed together with a competing chemical kinetics A spinodal decomposition in a (2D) binary mixture and with a simple kinetics between the two species was recently investigated by MD [7] In general, the chemical reaction(s) may prevent the coarsening spinodal decomposition and recently Carati and Lefever[18] have derived a series of conditions for the freezing of the Ostwald ripening stage of phase transition in a binary mixture But when it comes to a ternary mixture with several competing chemical reactions the situation is even more complex A ternary mixture with equal concentrations of the three species, and without competing chemical reactions was found to perform a phase separation with a dynamics and a morphology completely different from that of a binary mixture [19] The three species formed separated domains, different from the bicontinious morphology of the (late stage) structure of a binary mixture, and also the growth laws were different from the corresponding growth laws for a binary mixture This behavior, however, is expected as a consequence of the composition of the ternary mixture If, on the other hand, one of the species (e g , A^*) dominates one can expect that it, at a late stage forms a continuous phase and from that time the phase growth of the A^* rich phase is expected to switch over to the growth of a "binary mixture" of A^* and $(B+C)$ since there is no difference between the mixing energies between A^* and $B+C$, respectively

V RESULTS

As already mentioned we have simulated two different kinds of systems In system 1 all particles are identical except for their label while system 2, the interaction between odd and similar pairs is different, i e , two particles of different species e g , B and C are non-attractive while two particles of the same species interact according to the "full ' LJ potential In order to have a non-attractive potential for odd pairs, we truncate the potential at the minimum, i e , at $2^{1/6}\sigma$ In this way, the potential will either be repulsive or zero The bimolecular activation energy $\mathscr{E}/k_B$ (k_B is Boltzmann constant) is given by R_{reac}, which was set equal to 0 9611 in most of the simulations and the reaction probability P_r was adjusted in order to obtain several periods of oscillations within a simulation Since $u(R_{\text{reac}})/k_B = 2.4$ this corresponds to the fact that the chemical reactions only appear at high energy collisions

Figure 1 shows the positions of the particles for some representative simulations The first figure, Fig 1(a) is for the system which undergoes phase separations during the oscillations and it shows the positions of the A^* particles when $[A^*]$ is maximum Also shown on Figs 1(b) and 1(c), are the positions of the B and C particles at the same point of state The sum of the phases, shown in Figs 1(a)–1(c), covers the hole area and represents a condensed liquid mixture at $\rho^* = 0.8$ From the three figures one can see (and it was tested by a cluster-calculation program) that the A^* and the

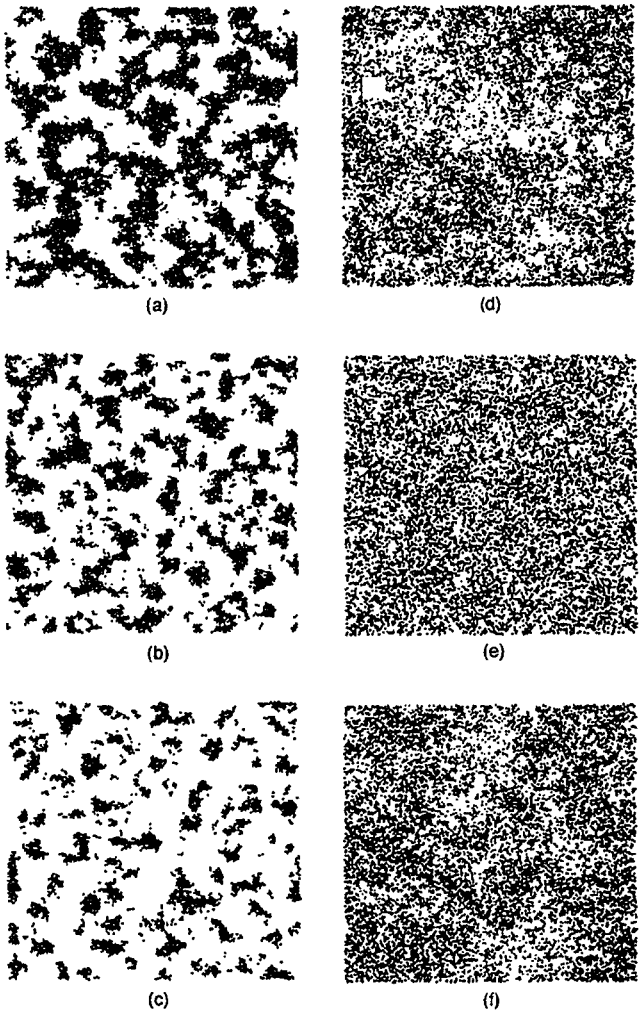

FIG 1 Snapshots of the positions of the individual particles at $T=1.0$ and $T=7.5$ respectively The number of particles is 16384 at density $\rho=0.8$ The pictures are taken when the concentration of A^* was at its maximum The simulation parameters are $R_{\text{reac}}=0.96116\sigma$ $P_r^{(1)}=P_r^{(3)}=10^{-3}$ $P_r^{(2)}=1.1\times10^{-3}$ (a)–(d) are for system 2 whereas (e)–(f) are for system 1 (a)–(c) and (e) are for $T=1$ and (d) and (f) are for $T=7.5$ (a) and (d)–(f) show the positions of A^* particles and (b) and (c) show the corresponding positions of the B and C particles

$(B+C)$ particles perform a bicontinious morphology [Fig 1(a)], whereas the B and C particles are separated in clusters At temperatures above T_c the mixture does not separate during the chemical oscillations The three figures, Figs 1(d), 1(e) and 1(f), show the positions of the A^* particles when $[A^*]$ is at its maximum and are taken at a high temperature [Fig 1(d)] for the same system (system 2) as shown in Figs 1(a)–1(c), and at low and high temperature [Figs 1(e) and 1(f)] for the system 1 without particle attractions and phase separations As it can be seen from the last three figures the distributions of the A^* particles are rather uniform, but with density fluctuations as expected in a continuous (MD) system The distributions of the two other species in the ternary mixture are qualitatively similar

Figure 2 shows the concentration of A^* versus time in a typical simulation of system 2 The concentrations of the

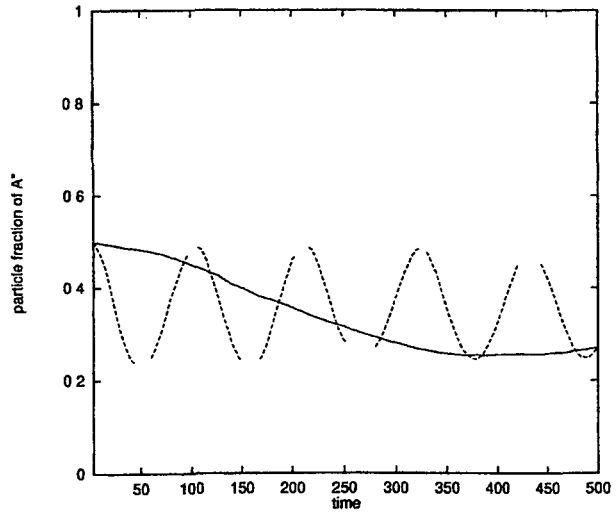

FIG 2 The particle fraction of A^* versus time [in time units $\sigma(m/\epsilon)^{1/2}$ an MD time step is 0 005] for typical simulations of system 1 (identical particles) The parameters are $\rho=0\,8$ $k_BT/\epsilon=1\,8$ $N=1024$

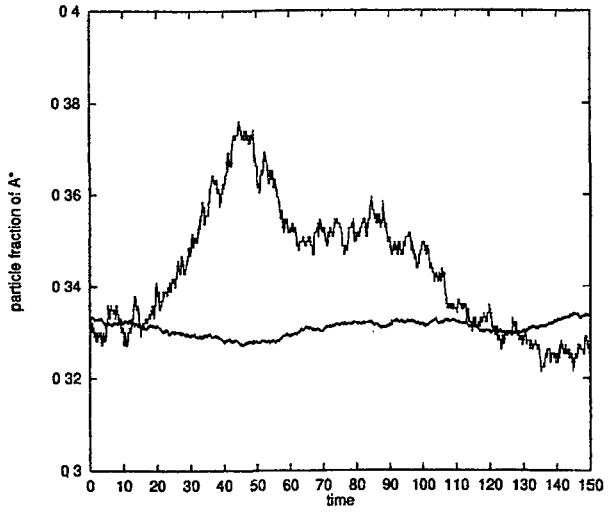

FIG 3 The particle fraction of A^* at the steady state with equal start particle fractions (1/3) of A^* B and C The solid line is for 1024 particles while the dotted line is for 65536 particles The simulation parameters are: $\rho=0\,8$ $R_{reac}=0\,96116\sigma$ $P_r^{(1)}=P_r^{(2)}=P_r^{(3)}=10^{-3}$ $T=2\,0\epsilon/k_B$

three components oscillate easily as long as one chooses the reaction probability to be a small value (less than 10^{-2}) The ratio between the reaction probability of the three reactions must neither be too large nor too small When a reaction is too fast, the number of particles of one type drops to zero and the reactions stop whereas MD gives a "window in time" in the order of nanoseconds, and if we choose a too small value of the different reaction probabilities the oscillation times exceed this window

A good question is whether the steady state found in Sec II exists in a system with a finite number of particles In order to examine this, we performed simulations with 1024 and 65536 particles where the initial concentrations of A^*, B and C were chosen exactly at the steady state with all the particle fractions equal to 1/3 Figure 3 shows the evolution of the concentration of A^* during the two simulations We see that the steady state is indeed a real phenomenon for the finite system and that the concentration fluctuates around the mean value 1/3, but the fluctuations decrease in size with the system size The linear stability analysis in Sec II gave an expression for the frequencies near the steady state, cf Eq (13) In Fig 4 we have plotted the observed frequency versus the calculated frequency The calculated frequency is computed by using the rate constant measured from the simulations performed with systems 1 and 2 (It is unnormalized because the rate constants are unnormalized) We see that the linear stability analysis predicts the frequencies well except for a normalization factor

When chemical reactions appear together with phase separations one observes deviations in the usual Arrhenius behavior [20] Our first test shows how the present phase separation alters the chemical reactions and is summarized in Fig 5 The figure shows two Arrhenius plots, i e , plots of $\log k$ versus $1/T$ where k is the rate constant and T the temperature The number of particles was fixed at 1024 (pluses and crosses) and 4096 (stars), respectively The first observation is that the system 1 (pluses, identical particles) follows simple Arrhenius equation with a small correction at high temperatures The second observation is that the system 2 (crosses odd pairs are non-attractive only) does not follow the Arrhenius equations—there is a cross-over at $k_BT_c/\epsilon \approx 1\,7$ It is worth noting that above and below $k_BT_c/\epsilon \approx 1\,7$ the system behaves according to Arrhenius equation but with different activation energies and pre-exponential factors This indicates that the underlying mechanism is changed The rate constants for the two systems approach each other and in an asymptotically way for high temperatures as expected At this state the oscillating reactions occur in homogeneous mixtures where the long-range pair interactions act as a uniform background, which does not affect the self-

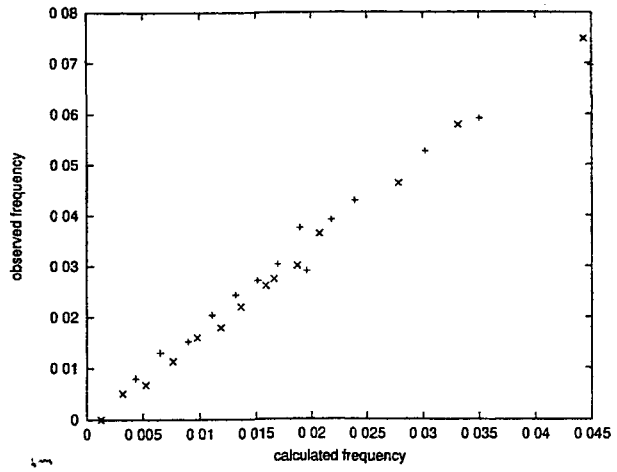

FIG 4 The calculated versus observed frequencies from simulations of system 1 (pluses) and system 2 (crosses) The parameters were $N=1024$ $\rho=0\,8$ $R_{reac}=0\,969116$ $P_r^{(1)}=P_r^{(3)}=10^{-3}$ $P_r^{(2)}=1\,1\times10^{-3}$ The different frequencies are from simulations at different temperatures (in the range from $1\,0\epsilon/k_B$ to $8\,0\epsilon/k_B$)

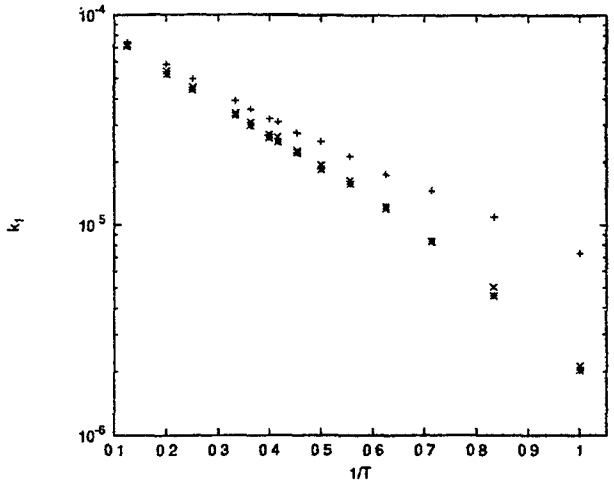

FIG 5 A plot of $\log k$ versus $1/T$ System 1 ($N=1024$) is plotted using pluses (+) while system 2 ($N=1024$) is plotted using crosses (x) and ($N=4096$) stars (*) The simulation parameters are the same as in Fig 4 The rate constants are normalized by dividing the measured rate constant by the number of particles

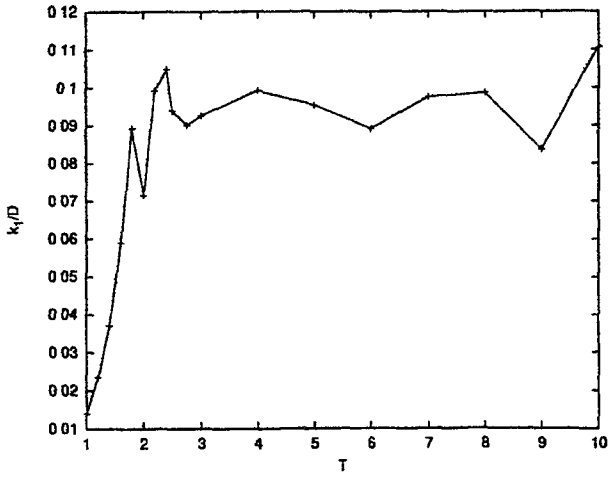

FIG 6 A plot of the ratio k_1/D versus T for system 2 The parameters are the same as in Fig 4 The rate constant is for reaction 1 and is unnormalized

diffusion In order to be sure that the cross-over is not a finite-size effect, we also performed the simulations with 4096 particles (squares) which, however, exhibited the same cross-over behavior and at the same temperature The cross-over temperature agrees with the upper critical temperature for phase separations in a two-dimensional binary mixture of the same kind of particles,[17] indicating the onset of a phase separation for temperatures below $k_BT_c/\epsilon \doteq 1\,7$ At the temperatures below T_c, there are small , but detectable differences between the 1024 and 4096 particles systems, (due to that the domain sizes are of the same order as the area of the system)

If the reactions in the system behave as simple diffusion-controlled reactions, the ratio between the rate constant and the diffusion coefficient must be (almost) constant as previously pointed out in Sec III In a uniform system the long-range attractive forces only change the diffusion marginally They act as a uniform background field We see in Fig 6 that above the critical temperature the ratio is constant within the statistical error while below the critical temperature, the ratio is certainly not constant This is a clear indication that the mechanism changes from a diffusion-controlled scheme to something else at the critical temperature We believe that the mechanism below the critical temperature is surface-controlled By a surface-controlled reaction we simply mean that a reaction like $A+B\rightarrow P$ occurs in the interfaces between A-clusters and B-clusters It is not difficult to see why it must be so: All reactions in the chemical scheme are bimolecular, i e , have the form $X+Y\rightarrow P$

VI CONCLUSION AND DISCUSSION

The chemical reaction scheme we have simulated is the same as found in Ref 6, but the potentials used are very different The potential used in Ref 6 is a long-ranged one ($1/r$) while ours are short-ranged Even though they differ in molecular details, we see oscillations in both This shows, not surprisingly, that it is the chemical scheme rather than the molecular details that determines the oscillating nature The molecular implementation of oscillating chemical reactions agrees with the corresponding macroscopic (continuous, mean-field) formulation, given in Secs II and III We obtain the steady state solution (Fig 3) as well as the same dependency of the frequencies with respect to reaction rate (Fig 4) as predicted by the mean field theory In the case of oscillations without a competing phase separation we obtain, within the accuracy of the computations, a rate constant, k_1, proportional to the selfdiffusion constant, D, (Fig 6) in accordance with the continuous, mean-field theory for bulk-diffusion driven kinetics in 2D

Our results presented in this paper clearly show that a phase separation alters the underlying mechanism of a chemical reaction This gives us a new insight, on a particle level, to the Arrhenius equation and at the same time allows a determination of the mechanism of chemical reactions in competition with phase separations As pointed out in Sec IV the phase growth in a ternary mixture with competing chemical reactions is expected to be very complicated and we have not obtained data like structure factors, etc from which the growth might be determined We believe, however, that the data shown in the paper represents chemical oscillations with spinodal decomposition morphology similar to the morphology of spinodal decomposition in a binary mixture This is based on three facts First we observe a "non-Arrhenius" cross-over behavior of the exponential temperature dependence of the rate constant, $k_1(T^{-1})$, below a temperature $T\approx T_c$ (the upper critical temperature for a binary mixture) Second, we notice that the system separates in subphases below T_c [Figs 1(a)–1(c)] and that a species at its maximum concentration, and the sum of the two other performs a bicontinious morphology [Fig 1(a)], which is characteristic for (late time) spinodal decomposition in a binary mixture, and different from the morphology of domains in a ternary mixture of species with equal concentrations [19]

But even so the growth is complicated since every species (A^*, B, C) might cross several growth regimes with different scaling properties, during an oscillation [21] Third, we notice that the minimum concentrations of the species during the oscillations are significantly larger than the spinodal concentrations[17] which exclude nucleation growth as the mechanism which drives the phase transitions with the present choice of reaction probabilities Finally we observe that whereas the chemical oscillations are bulk-diffusion driven with a proportionality between the rate constant k_1 and the self diffusion constant D, above T_c, the ratio, k_1/D also exhibits a (dramatic) cross-over in the temperature interval $T \approx T_c$ (Fig 6) This cross-over behavior, which is due to a big reduction of the rate constant k_1 below T_c is a consequence of the fact that the bimolecular reaction kinetics is no longer bulk diffusion driven; but now only takes place in the interfaces

It is worth noting that the oscillations persist even for large systems One could wonder whether the oscillations are a local or a global phenomenon The frequency and amplitude of the oscillations seem independent of the number of particles; we have tried with 1024 and 65536 particles and for systems with and without competing phase separations This indicates that there exists a correlation length scale much larger than the system size On this length we imagine that the oscillations locally are somehow synchronized, and a further investigation seems worth doing

Our results presented in this paper are coming from simulations of finite microscopic systems which have a high level of details (e g , we know the trajectory of every particle) Despite the microscopic nature of our simulations we are able to reproduce the phenomena seen in the macroscopic description of the same chemical system: Stationary point, frequencies close to the stationary point and the oscillations The present calculation is performed for two dimensional systems due to computational resources; but the method in general can be applied to more complex reaction schemes and with more realistic chemical kinetics with exchange of covalent bonds; as well as systems in three dimensions and at catalyzing surfaces The advantage of molecular dynamics simulations above other methods is that this simulation technique is for a continuous space and with a dynamics which includes the hydrodynamics modes

ACKNOWLEDGMENTS

The National Science Foundation of Denmark is acknowledged for computer time and P G Sørensen for valuable discussions

[1] A J Lotka, J Am Chem Soc **42** 1593 (1920)
[2] A M Zhabotinsky in *Oscillation processes in biological and chemical systems* edited by G M Franck (Science Moscow 1967) p 252
[3] A N Zaikin and A M Zhabotinsky Nature (London) **255** 535 (1970)
[4] I Prigogine and G Nicolis J Chem Phys **46** 3542 (1967)
[5] I Prigogine and G Nicolis J Chem Phys **46** 3542 (1967); R Lefever and I Prigogine *ibid* **48** 263 (1968)
[6] H H Diebner and O E Rössler Z Naturforsch Teil A **50** 1139 (1995)
[7] S Toxvaerd Phys Rev E **53** 3710 (1996)
[8] P Ortoleva and S Yep J Chem Phys **65** 2045 (1976)
[9] M Heinrichs and F W Schneider Ber Bunsenges Phys Chem **87** 1195 (1983)
[10] J Gorecki and J Gryko Comput Phys Commun **54** 245 (1989)
[11] X G Wu and R Kapral Phys Rev Lett **70** 1940 (1993)
[12] L Perko *Differential equations and dynamical systems* (Springer Verlag Berlin 1994)
[13] R M Clegg J Chem Educ **63(7)** 571 (1986)
[14] See M van der Hoef and D Frenkel Phys Rev Lett **66** 1591 (1991) and references therein
[15] M J Pilling and P W Seakins *Reaction Kinetics* (Oxford University Press New York, 1995)
[16] S Toxvaerd, Mol Phys **72** 159 (1991); Phys Rev E **50** 2271 (1994)
[17] E Velasco and S Toxvaerd, Mol Phys **86** 845 (1995)
[18] D Carati and R Lefever Phys Rev E **56** 3127 (1997)
[19] M Laradji O G Mouritsen and S Toxvaerd, Europhys Lett **28** 157 (1994); Phys Rev E **53** 3673 (1996)
[20] See I Vattulainen J Merikoski T Ala Nissila and S C Ying Phys Rev Lett **79** 257 (1997) and references therein
[21] A J Bray Adv Phys **43** 357 (1994)

APPENDIX D

Geisshirt *et al.* [25]

Controlling the temperature of one-dimensional systems composed of elastic and inelastic particles

Kenneth Geisshirt,[1] Paz Padilla,[2] Eigil Præstgaard,[1] and Søren Toxvaerd[2]
[1]*Department of Life Sciences and Chemistry, Roskilde University, 4000 Roskilde, Denmark*
[2]*Department of Chemistry, University of Copenhagen, 2100 Copenhagen Ø, Denmark*
(Received 31 July 1997)

We have studied systems composed of either elastic or inelastic particles constrained to move in one dimension and confined on a line by using molecular dynamics (MD) simulation techniques We have tested several ways of modeling a boundary that exchanges energy with the system. Furthermore, we have studied one-dimensional granular systems composed of soft particles under cooling and found that the decay in temperature follows a power law $T \propto t^{-\alpha}$ similar to the case of rigid particles, but now, the value of α depends on the density and degree of inelasticity in the system For systems composed of inelastic particles thermostated by one of the boundaries we find that the "extraordinary" state reported by Y Du, H. Li, and L P Kadanoff [Phys Rev Lett. 74, 1268 (1995)] is an artifact introduced by method of providing energy to the system [S1063-651X(98)05202-7]

PACS number(s): 81 05.Rm

I. INTRODUCTION

Granular material flows appear in nature (sand dunes, planetary rings, powders) and are of great technological importance (handling and transport of, e g , seeds and pharmaceuticals) In the dry state, granular materials interact mainly by repulsive forces and there is energy dissipation during collisions due to the excitation of internal modes Thus, in the absence of an energy source the granular medium cools, and the motion of the grains eventually stops One-dimensional models of granular media have been studied in the hope that the origin of phenomena that appear in models for two or three dimensions can be enlightened by results from more "simple" one-dimensional models The dynamics of particles in one dimension, nevertheless, has the peculiarity that their motion is confined between two neighbors, and therefore the transport of physical quantities across the system is very inefficient.

The present investigation was motivated by the work of Du *et al* [1] where they report the appearance of an "extraordinary" state in thermostated systems composed of model granular particles in one dimension. In such a state, the majority of the particles form a clump in the side of the simulation box opposite to the thermostat, and they move at a very low speed The rest of the particles move at a much higher speed between the thermostat and the clump

The first part of this investigation is devoted to analyzing the thermostating devices used in Ref [1] We have tested whether these thermostating devices are able to produce true equilibrium states at a desired temperature With this purpose, we have studied systems composed of rigid and soft particles constrained to move in one dimension We found that the thermostating devices used in Ref [1] either failed in setting the system at the target temperature (which is the assumed temperature of the boundary), or produced a wrong distribution of energies in the systems Therefore, we propose alternative methods that successfully produce equilibrium states at a desired temperature in one-dimensional systems, and test another method due to Ciccotti *et al* [2–4]

In the second part of the paper, we elucidate whether the appearance of the "extraordinary" state is a universal behavior for systems composed of inelastic particles (granular particles) constrained to move in one dimension, or it is an artifact of the model We found that the appearance of the "extraordinary" state depends on how the energy is pumped into the system.

Additionally, we compare the behavior of soft and rigid inelastic particles under cooling, i e , when there is no thermostating device coupled to the system. It has been established [5–7] that the cooling granular medium is not spatially uniform but it shows clusters and voids In the case of inelastic particles in one dimension and in absence of any thermostating device, it is possible to show [5,8] that the temperature of the system will decrease following a power law, i.e , t^{-2}; this is referred to as the cooling problem in granular materials We verify this result for rigid particles, but find that for soft particles, although the dependence of temperature on time is a power law $T \propto t^{-\alpha}$, the value of α depends on the density and the degree of inelasticity in the system. McNamara and Young have numerically verified the cooling problem in one and two dimensions [5,9]

The outline of the paper is the following: Sec II describes the system composed of rigid particles, Sec III presents the system composed of soft particles and describes how inelastic collisions can be introduced The thermostating devices studied in this paper are described in detail in Sec IV In Sec V, we present and discuss the results from the simulations A summary and the conclusions of the investigation are collected in Sec. VI.

II. RIGID PARTICLES

We consider a system of N point particles of equal mass m, which are constrained to move in one dimension and confined in a box The interaction between particles occurs through collisions only If the collisions are elastic, in the particular case of one dimension, a collision simply means

an exchange of momenta between the colliding particles Moreover, it should be noticed that the particles are points make the properties of the system independent of the density of particles in the box The walls confining the system are hard walls of infinite mass In some of the simulations the particles are allowed to exchange energy with one of the walls, which, thus, acts as a thermostat. This is described in detail in Sec IV

Inelasticity is introduced into the system in the same way as in previous simulations [1,5] Let i and j denote the indexes of two colliding particles The velocities after collision, v_i' and v_j', are related to the velocities before collision, v_i and v_j, as

$$v_i' = \epsilon v_i + (1-\epsilon) v_j, \tag{1}$$

$$v_j' = (1-\epsilon) v_i + \epsilon v_j, \tag{2}$$

where $\epsilon = (1-r)/2$ and r is the restitution coefficient. The parameter r is the ratio of the relative velocities right after and just before a collision and provides a measure of how inelastic the collisions are The case $r=1$ the collisions are elastic, and the case $r=0$ the collisions are completely inelastic This model is identical to the one chosen in Ref [1], where the simulation results indicate a breakdown of hydrodynamics for inelastic particles in one dimension.

The temperature of the system is defined as [10]

$$T = \frac{1}{N} \sum_{i=1}^{N} v_i^2, \tag{3}$$

where N is the number of particles The temperature as defined above is used in all simulations

For this model, all the results are reduced with the mass of the particle, m, the length of the simulation box, L, and the time between collisions τ_{coll} Thus, for instance, the units for energy are $mL^2\tau_{\text{coll}}^{-2}$

We have studied systems of $N=100$ particles The simulation program for the rigid particles is simple, and we will describe our program in general terms The program tracks the collisions, advances the position, and changes the velocities Finding the next collision is easy for a one-dimensional system: a particle i can only collide with two particles, namely, $i-1$ and $i+1$ (and we only have to check with one of them) The computational effort is, therefore, clearly $O(N)$ where N is the number of particles

III. SOFT PARTICLES

Our soft particle models are disks of equal mass m constrained to move in one dimension and confined in a box. The interaction between particles is purely repulsive and the shape of the potential is the Weeks-Chandler-Andersen (WCA) potential [11]:

$$u(x_{ij}) = \begin{cases} 4\epsilon\left[\left(\frac{\sigma}{x_{ij}}\right)^{12} - \left(\frac{\sigma}{x_{ij}}\right)^{6}\right] + \epsilon & \text{for } x_{ij} \leq 2^{1/6}\sigma \quad (4) \\ 0 \quad \text{for } x_{ij} > 2^{1/6}\sigma, & (5) \end{cases}$$

where x_{ij} is the distance between the centers of the disks The potential parameters σ, ϵ and the mass m of the particles are the units of length, energy, and mass, respectively All the quantities obtained for this model are presented in reduced units The reduced temperature is defined as $k_B T/\epsilon$ (k_B is Boltzmann's constant) and the reduced time as $\sigma(m/\epsilon)^{1/2}$

Inelasticity can be brought into the system by introducing dissipative forces during collision. In the present model, contrary to rigid particles, collisions have finite duration. We have chosen to let the particles experience dissipative forces whenever the distance between them is less than $2^{1/6}\sigma$, i e , during the whole period of time of the collision The shape of the dissipative force is

$$F_{\text{dis}} = \gamma D^{1/2} \frac{dD}{dt}, \tag{6}$$

where D is a so-called deformation parameter defined as

$$D = 2^{1/6}\sigma - x_{ij} \quad \text{if } x_{ij} \leq 2^{1/6}\sigma, \tag{7}$$

$$D = 0 \quad \text{if } x_{ij} > 2^{1/6}\sigma \tag{8}$$

and γ is related with the degree of dissipative friction in the system. Hence, the dissipative forces depend on the degree of deformation of the grains and the relative velocities between the colliding particles, v_{ij}:

$$F_{\text{dis}} = \gamma D^{1/2} \frac{dD}{dt} \tag{9}$$

$$= -\gamma D^{1/2} v_{ij} \tag{10}$$

The force F_{dis} represents the dissipation that arises from frontal friction between two granular particles This specific form of the dissipative force was recently proposed independently by Morgado *et al* [12] and Brilliantov *et al* [13] To the best of our knowledge, this is the first time it has been implemented in a MD simulation.

Actually, the loss of kinetic energy due to tangential collisions should also be taken into account, but because we are considering the relative motion in one dimension only, tangential collisions will not be considered here

The equations of motion are solved using the leap-frog algorithm [14] Since dissipative forces depend on the relative velocity of a pair of particles, for our one-dimensional system the resolution of the equations of motion involves solving a set of linear equations, where the velocities at time $t+h/2$ (h is the length of the time step) are the unknown quantities The matrix of this set of equations is presented in Appendix A This matrix is tridiagonal, and therefore, the resolution of the system is a fast procedure from a computational point of view [15]. The use of this model of dissipative forces in a system of two or three dimensions will be far more expensive computationally since it will entail an iterative process to compute the forces

The length of the time step was set to 0 002 reduced units of time and systems of $N=100$ and 1000 particles were considered.

IV. THERMOSTATING

As written previously, without any energy supply, the motion of inelastic particles will eventually stop In order to investigate steady states of the flow of granular materials, one needs to pump energy into the system, i e , we have to introduce a thermostating device We have chosen to supply energy into the system from the left boundary (thermal wall), which should basically act as a wall held at constant temperature T_{wall} The right boundary is an insulating wall modeled as a hard wall of infinite mass (reflecting wall) Thus, in our one-dimensional systems, only the left-most particle will exchange energy with the thermal wall In this section we describe a number of ways of doing this In Sec V we will reveal how the different implementations work.

Gaussian wall: When a particle hits a wall (the left-most particle–particle 1), it is sent back with a random velocity drawn from a Gaussian distribution The distribution is a Maxwell-Boltzmann (MB) distribution, corresponding to a temperature T_{wall} This type of thermostat was used in Ref [1]

Stochastic wall: The original idea of a stochastic boundary is due to Lebowitz *et al* [16] and used intensively by Ciccotti *et al* [2–4] In their work, after a particle hits the stochastic wall it comes off with a distribution corresponding to T_{wall} This is done by sampling the value of the velocity component in the direction normal to the wall from the probability density:

$$P(v_n)=\frac{mv_n}{k_BT_{\text{wall}}}\exp\left(-\frac{mv_n^2}{2k_BT_{\text{wall}}}\right) \tag{11}$$

where k_B is Boltzmann's constant, T_{wall} the temperature of the thermal wall, m the mass, and v_n the component of the velocity normal to the wall (we set k_B and m to 1 in our simulations) The rest of the components are sampled from a MB distribution at the temperature of the thermal wall Notice that for a one-dimensional system, the distribution of the velocities of the particles emitted by the Gaussian wall is different than in the present case due to the factor v_n in Eq (11). This is discussed in the next section

Constant velocity wall: After the collision with the wall, the left-most particle is always returned with the same velocity, $\sqrt{T_{\text{wall}}}$ It has been used in previous studies [1,17]

Frequency: This type of thermostat does not involve a collision with a wall Instead, the velocity of the left-most particle is changed with a certain frequency The velocity is drawn from a MB distribution with temperature T_{wall} This way of thermostating the system has, to the best of our knowledge, never been used before

Wall particle coupled to a Nosé-Hoover (NH) thermostat: We substitute the left hard wall by a particle tethered to the point $x_0=0$ by a harmonic potential $U_{\text{wall}}=\frac{1}{2}k_{\text{wall}}(x-x_0)^2$ The value of k_{wall} is set to 100 reduced units The dynamics of this particle is coupled to a Nosé-Hoover thermostat [18] Moreover, the wall particle interacts with the left-most particle of the system through a WCA potential with the same parameters as for the rest of the particles in the system There is no dissipation of energy during the collision of the left-most particle and the wall particle The equations of motion for the wall particle are

$$x=\frac{p}{m}, \tag{12}$$

$$\dot{p}_x=f_x-\zeta p_x, \tag{13}$$

$$\dot{\zeta}=\frac{1}{\tau^2}\left(\frac{p_x^2}{mk_BT}-1\right), \tag{14}$$

where ζ and τ are, respectively, the friction parameter and the relaxation time of the thermostat. The relaxation time of the thermostat was set to 0 15 reduced units

The system composed of rigid particles was thermostated with the first four devices The system composed of soft particles were thermostated with all of them

V RESULTS

A. Elastic particles

We have performed simulations of one-dimensional systems containing rigid and soft particles The results of our simulations will be discussed in this section To begin with, we analyzed the final states obtained with the thermostating devices described above Our goal is to obtain equilibrium states at a temperature T_{wall}

Figure 1 shows the temperature as a function of time for a system composed of rigid point particles undergoing elastic collisions when the different thermostats described in the previous section are coupled to the system The target temperature of the thermostats is $T_{\text{wall}}=1\ 0$ in all the cases The velocities of the starting configuration were drawn from an MB distribution with $T=1\ 0$ Apparently, the only thermostat that fails to maintain the temperature of the system is the Gaussian wall used in Ref [1], which sets the temperature of the system below the target temperature [see Fig 1(a)] However, the constant velocity thermostat [Fig 1(b)] for one-dimensional systems composed of rigid particles produces configurations where the velocities of the particles take the values $\pm\sqrt{T_{\text{wall}}}$ only, and therefore, these configurations are not equilibrium configurations This is due to the fact that in such a one-dimensional system the collisions between particles involve exchange of momenta only, since there is no scattering This introduces an extra peculiarity in the system since equilibrium states can never be reached with the thermostating devices used in this work if the initial configuration includes particles whose velocity is 0 In summary, given an initial configuration where all the velocity of the particles are non-negligible only the stochastic wall [Fig 1(d)] and the frequency thermostat [Fig 1(c)] are able to generate equilibrium states at T_{wall}

We have also performed simulations with hard disks instead of point particles at low (0 01) and high density (0 83) and there is no qualitative difference

The same analysis for the one-dimensional system composed of soft particles (undergoing elastic collisions) yields similar results In Table I, we summarize the temperatures of the final states obtained for both rigid and soft particles The results for soft particles are for a density $\rho=0\ 83$; ρ defined as N/L ($N=100$ and L is the length of the box), the target temperature of the thermostats is 1 0, and the temperature of the system was averaged over 5×10^6 time steps after equili-

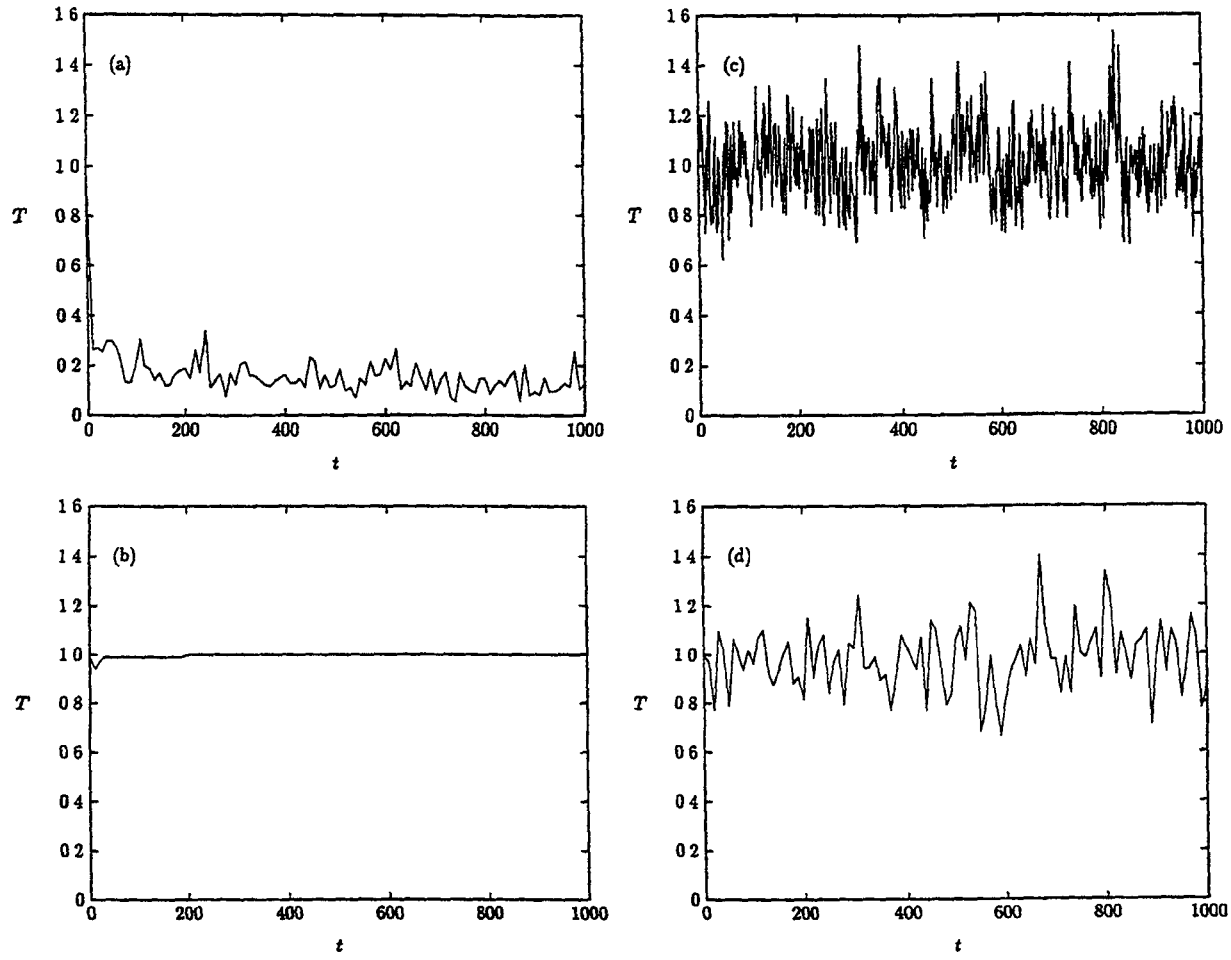

FIG 1 The temperature as a function of time Both quantities are in reduced units System of point rigid particles and elastic collisions is shown The number of particles is 100, and the length of the system is 1 The target temperature of the thermostats is 1 0 (a) Gaussian wall (b) Constant velocity wall (c) Frequency (d) Stochastic wall.

bration for the soft particles As in the case of rigid particles, the Gaussian wall coupled to the system composed of soft particles does not perform well as a thermostat. Furthermore, the constant velocity thermostat and the frequency thermostat at high frequency also fail to set the temperature of the system to the target temperature All three devices set the

TABLE I. Equilibrium temperatures

Thermostat	Hard particles	Soft particles
Gaussian wall	0 15±0 05	0 62±0 02
Stochastic wall	1.00±0 14	0 98±0 02
Constant	1.00±0 03	0.507±0 005
Frequency	1 00±0 13	1 01±0 01 [a]
Frequency	1 02±0 09	0 49±0.02 [b]
Wall particle+NH		0 99±0 01

The velocity of particle 1 is taken from an MB distribution every 00th time step (soft particles) or with frequency 1/0.0243 (rigid articles)

The velocity of particle 1 is taken from a MB distribution every me step (soft particles) or with frequency 1/2 4299 (rigid parcles)

temperature of the soft particle system below the target temperature Moreover for the system composed of soft particles, the final states obtained with these thermostats do not fulfill equipartition, i e , the kinetic energy is not equally distributed among the particles in the systems This is illustrated in Fig 2, where we show the mean kinetic energy (temperature) for each particle in the system for a final state reached with the Gaussian wall The kinetic energy of the left-most particle is significantly lower than the average temperature of the system ($T=0\,62$) This indicates that this is not an equilibrium state but a nonequilibrium steady state

The explanation of why the Gaussian wall proposed in Ref [1] and the constant velocity thermostat do not produce equilibrium states at the target temperature is as follows The principle behind a thermal wall is to change the distribution of velocities of the particles arriving at the wall to the distribution corresponding to the temperature of the wall [16] Let us assume a three-dimensional system, and denote as $\vec{n}$ the unit vector normal to a wall boundary Then the probability that a particle with velocity $\vec{v}$ arrives at the wall (or, in general, crosses a planar surface) is

$$\vec{v}\cdot\vec{n} f(v_x,v_y,v_z)dv_x dv_y dv_z, \qquad (15)$$

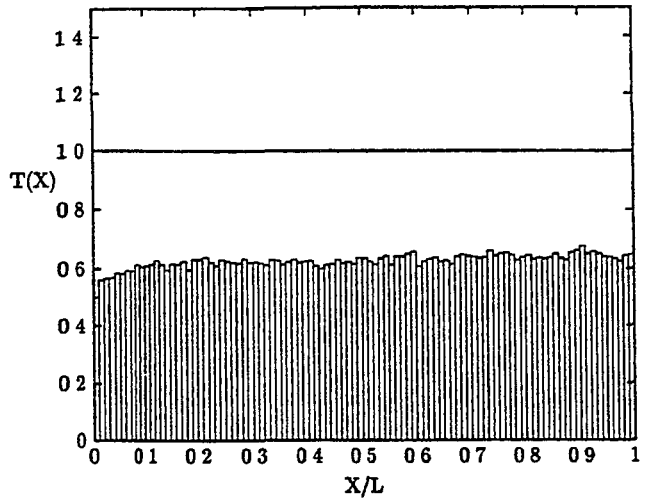

FIG 2 Mean kinetic energy (in reduced units) for each particle of the soft particles system at $\rho=0.83$ when the Gaussian wall thermostat is applied

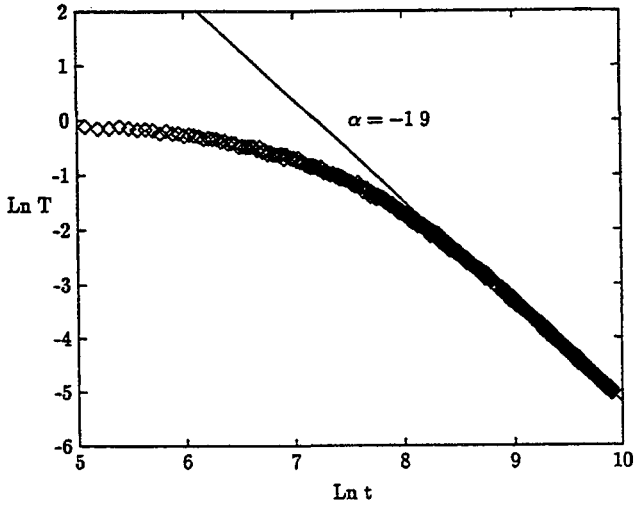

FIG 3 ln$T$ plotted versus ln$t$ The temperature T and the time t are in reduced units Results for a system of soft particles undergoing inelastic collisions and no thermostating device coupled to the system The system is composed of $N=1000$ particles $\rho=0.83$ and $\gamma=0.001$ ◇: simulation results; straight line: least square fit.

where $f(v_x,v_y,v_z)$ is the MB distribution of velocities at the temperature of the fluid. At equilibrium, the probability that a particle with velocity $\vec{v}$ leaves the wall will have the same shape For our one-dimensional system this probability is

$$v_x f(v_x)dv_x \tag{16}$$

This is obviously not the case for the Gaussian wall or the constant velocity wall Furthermore, the distribution of velocities of the particles arriving at these boundaries will be different from that of the particles emitted by these boundaries, and therefore, equilibrium will never be reached

The fact that the frequency thermostat works so well for the system composed of rigid particles is easy to understand Due to the one-dimensional nature of the system, the distribution of velocities remains unchanged when there is no thermostating device coupled to it. This is so because, in the collisions, the particles simply exchange momentum. With the frequency thermostat, a random number generator will ensure that particle 1 has the kinetic energy corresponding to the desired temperature Thus, particle 1 simply provides velocities to the rest of the system sampled from the correct distribution function In the case of the frequency thermostat, the frequency at which particle 1 gets a new velocity from the MB distribution is totally uncorrelated with the previous velocity of the particle In the case of a system composed of soft particles, energy should be distributed among all the potential and kinetic energy of the particles If the velocity of particle 1 is not changed too rapidly by the random number generator, particle 1 will be in equilibrium with the rest of the system because energy will have time to be redistributed among all the degrees of freedom in the system Equipartition will then be fulfilled, and the system will reach the desired temperature, i e., the temperature of particle 1 When the velocity of particle 1 is exchanged at too high frequency the system has not time enough to relax (redistribute the energy) Indeed, our results show nonequipartition of the energy in the system when the frequency is high

The system thermostated with the wall particle coupled to a Nosé-Hoover thermostat works as one should expect, since it is a well-defined system, where the equations of motion can be derived from an extended Hamiltonian [18]

B Inelastic particles

The main purpose of the present investigation is to study the behavior of one-dimensional systems where particles undergo inelastic collisions, since these are models for granular materials

We start looking at the system under cooling (i e , there is no thermostating device coupled to the systems) In Fig 3, the typical behavior of the temperature as a function of time for a system composed of $N=1000$ soft particles is shown After a transient, whose length depends on the density of the system, the temperature decays following a power law $t^{-\alpha}$ For rigid particles, we found similar behavior and a value of the exponent $\alpha=2$ (within the statistical uncertainty) that agrees with theoretical predictions [5,8] and previous simulations [5] For the system composed of soft particles, the value of the exponent seems to depend on the density and the degree of inelasticity in the system The values of the exponent α obtained for different densities and degrees of inelasticity are collected in Table II At sufficiently high density and weak inelasticity the value of the exponent α agrees with the theoretical predictions [5,8] for rigid particles This is interesting in the case of Haff's theory [8] since it was developed for very dense granular systems, where the interparticle distances are significantly smaller than the diameter of

TABLE II Values of the exponent in the cooling law $T\propto t^{-\alpha}$

Density	Inelasticity	α
0.2	Weak	1.16
0.2	Strong	1.39
0.83	Weak	1.90
0.83	Strong	1.59

the particles On the other hand, the theory developed by McNamara *et al* [5] was based in the fact that in one-dimensional granular systems composed of point rigid particles under cooling, a bimodal velocity distribution raises They predict that the temperature will decay as

$$T=\frac{U_0^2}{(1+2\epsilon\rho t U_0)^2}, \tag{17}$$

where U_0 is the mean value of the velocity modulus at $t=0$, ϵ is the friction parameter introduced in Eqs (1) and (2), and ρ is the density Nevertheless, we do not find any trace of a bimodal velocity distribution as the one-dimensional system composed of soft particles cools down.

Finally, we analyze the behavior of one-dimensional systems with inelastic collisions and a thermostat coupled to the system As mentioned, for one-dimensional systems of particles undergoing inelastic collisions an "extraordinary" state was found in Ref [1] In such an "extraordinary" state, the majority of the particles get clamped in a small region of space moving with very low velocities, and few remaining particles travel between one of the boundaries and the group of clamped particles at a much higher speed. In the present investigation, nevertheless, we find that the thermostating devices used in Ref [1] failed to produce equilibrium states for elastic particles Therefore, we have carried out simulations where our one-dimensional systems are coupled to thermostats that we have shown perform well in equilibrium, namely, the stochastic wall and a wall particle coupled to a NH thermostat.

We have repeated the simulations performed in Ref [1] for rigid point particles but now coupling the system to a stochastic wall (the left-side wall) and we have reproduced their main findings In other words, we observe that the "extraordinary" state also appears when a correct thermostating device is used. The appearance of the "extraordinary" state is illustrated in Fig 4(b) for a system composed of $N=100$ particles This figure shows the position of the center of mass, $\langle x\rangle=(1/N)\Sigma_{i=1}^{N}x_i$, as function of time The position of the center of mass of the system moves to the right side of the box and remains there as steady state is reached. For the sake of completeness we also show results without a thermostat in Fig 4(a); the value of $\langle x\rangle$ stays around zero, which shows that the particles are uniformly distributed. This is indeed what we would except with only $N=100$ particles (for $\epsilon=0\,005$ clustering does not occur for a number of particles less than or equal to $N_{\min}=599$ [5]) In Ref [1] it is found that the particles in the clump get squeezed into a smaller space and move with slower speeds, for a fixed number of particles and decreasing ϵ We, on the contrary, find that when the initial distribution of velocities is Maxwellian the formation of the clump disappears This is illustrated in Fig 4(c), where one can see that for $\epsilon=10^{-7}$, the position of the center of mass fluctuates about the center of the simulation box. Furthermore, the density profile shows that, at steady state, the particles remain homogeneously distributed in the simulation box in agreement with the predictions of the hydrodynamic equations Nevertheless, we have also started the simulations with all the particles uniformly distributed, and with only the leftmost particle having nonzero

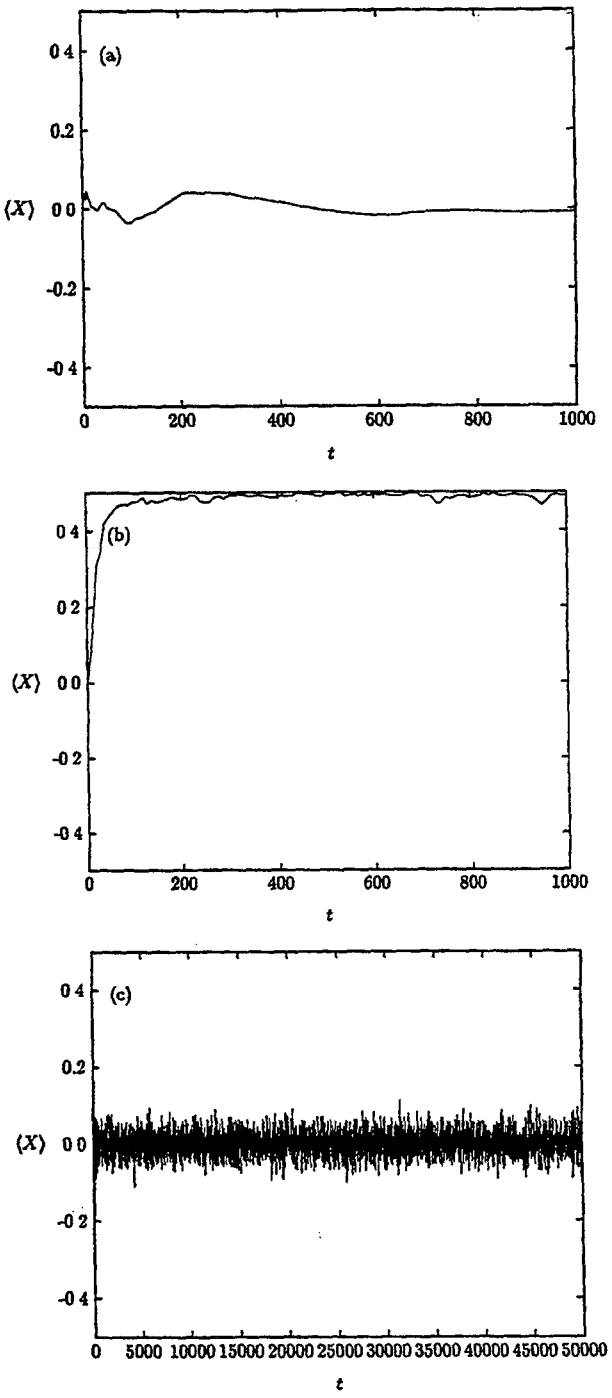

FIG 4 The center of mass position versus time X and t are in reduced units Results for a system composed of rigid point particles undergoing inelastic collisions The length of the system is 1, and the "box" is the interval from $-0\,5$ to 0.5 (a) $\epsilon=0\,005$, reflecting walls (b) $\epsilon=0\,005$, stochastic wall (c) $\epsilon=10^{-7}$, stochastic wall.

velocity In this case, the position of the center of mass oscillates with a greater amplitude and a long period (about 10^6 collision times), and the distribution of particles is not uniform but the system is more dense on the right side, but we do not see the formation of a clear clump Furthermore, the velocities of the particles are smaller than in the previous

case Thus, for $\epsilon \to 0$, we observe a dependence of the final steady state on the initial conditions of the simulations We assume then that the observations from Ref [1] quoted above correspond to our second initial conditions However, even in this case we do not observe that the particles, when $\epsilon \to 0$, get squeezed into a smaller space than for greater values of ϵ

In order to investigate the origin of the "extraordinary" state, we have simulated a similar system composed of soft particles This allows us to use as a thermal boundary a wall particle coupled to a NH thermostat, which is the most realistic way, among those described in Sec IV, of modeling a wall held at constant temperature Moreover, in this case, the exchange of energy between the wall and the left-most particle takes place during a finite time interval, instead of instantaneously

Figure 5 shows the steady state profiles of density and temperature for the soft particle system at $\rho = 0.2$ for different degrees of inelasticity in the collisions (we have chosen three values of the friction coefficient $\gamma = 0\,001$, $0\,01$, and $0\,1$) The density is normalized as $\rho_{nor}(x) = \rho(x)/\rho$ and the X coordinated as x/L The results are for a system coupled either to the wall particle coupled to a NH thermostat or to the stochastic wall At the lowest inelasticity ($\gamma = 0\,001$), the steady states produced by the two thermostats are equal Density and temperature can be considered constant across the system, and the average value of temperature is about 0 9 in both cases [see Figs 5(a) and 5(d)] In the figures, the quasi straight lines in the middle of the density and temperature profiles are the arithmetic mean of those, and one can see that they form a symmetry axis about which the density and temperature profiles are mirror images

For $\gamma = 0\,01$, the steady state density and temperature profiles obtained with the two thermostats also show similar fashion [Figs 5(b) and 5(e)] Now there is no symmetry as we observed at $\gamma = 0\,001$ Moreover, the average temperatures of the two steady states are different, $T = 0\,427(6)$ when the system is coupled to the stochastic wall, and $T = 0\,28(1)$ when it is coupled to the wall particle coupled to the NH thermostat. The shape of the temperature profiles can be assumed as exponentials within the left-hand half of the box, i e , in the side closest to the thermostat. This is illustrated in Fig 6 where the $\ln T$ is plotted versus x/L The straight lines are the least square fits to the simulation data. The exponential decay of temperature is what one could expect from a hydrodynamic approach

Finally, we show the results for $\gamma = 0\,1$ Here, the final steady states obtained with the two thermostats are clearly different. The steady state obtained with the wall particle coupled to the NH thermostat corresponds to a state with an average temperature of $O(10^{-4})$, this means that the particles have practically stopped moving The density profile indicates that the particles are homogeneously distributed in the simulation box [see Fig 5(c)] The steady state obtained with the stochastic wall is very different. The density profile indicates the appearance of a clump of particles in the right-side of the box and mean kinetic energy of these particles is practically zero [see Fig 5(f)] Although the velocities of the rest of the particles close to the thermal wall are very low, they are several orders of magnitude higher than the particles in the clump This steady state is very much like the "extraordinary" state described in Ref [1]

The differences between the steady states created with the two different thermostating devices [Figs 5(c) and 5(f)] should emerge from differences in the way that the two thermal boundaries pump energy into the system. The stochastic wall can be interpreted as a boundary that destroys the arriving particles and emits new ones with a velocity drawn for an MB distribution for the target temperature Thus, the value of the velocity of the outcoming particle is totally independent of the value of the incoming velocity, and therefore the increase in kinetic energy of a particle hitting a stochastic wall can be arbitrarily large On the other hand, when the left boundary is a wall particle coupled to the NH thermostat, the left-most fluid particle will also increase its kinetic energy by the interaction with the wall particle Nevertheless, the magnitude of the velocity of the particle after hitting the wall particle will depend on its incoming velocity and therefore the amount of kinetic energy that the left-most particle can load in this way is limited. Furthermore, we have measured in our simulations for soft particles the amount of energy that a particle loads, in a time step, from a stochastic boundary and found that it is several orders of magnitude greater than from a wall particle coupled to a NH thermostat.

When our one-dimensional inelastic models are coupled to a thermostat in the left-side boundary of the simulation box, as the inelasticity of the model increases (the value of ϵ or γ increases), a temperature gradient appears in the system and the density profiles indicate that the more energetic particles on the left side of the box press the particles on the right side of the box to the right-side boundary We believe that the origin of this "extraordinary" state is due to the great amount of energy that the stochastic wall pumps into the system in the limit of (relatively) high inelasticity, where the temperature of the particles (due to inelastic collisions) is well below the temperature of the boundary Thus, the particles emitted by the stochastic wall have significantly more kinetic energy than the rest of the particles in the system and press them against the other side of the box, where due to their low kinetic energy remain together and form a clump In the same limit of (relatively) high inelasticity, but when the thermal boundary of the system is a wall particle coupled to a NH thermostat, the thermostat will simply not be able to maintain the temperature of the system, and the motion of particles will eventually stop

VI. CONCLUSION

We have tested several models used in the literature for modeling a thermal boundary in one-dimensional systems The results of our simulations indicate that only the stochastic wall, the frequency thermostat, and the wall particle coupled to a NH thermostat are able to generate equilibrium states at the desired temperature of the boundary

We have studied the cooling of one-dimensional models for granular systems, modeled as rigid and soft particles For rigid particles we found that the cooling of the system follows the power law, $T \propto t^{-2}$, which agrees with theoretical predictions [5,8], and previous simulations [5] For soft particles we found a similar power law, $T \propto t^{-\alpha}$, but now, the value of the exponent, α, depends on density and the degree

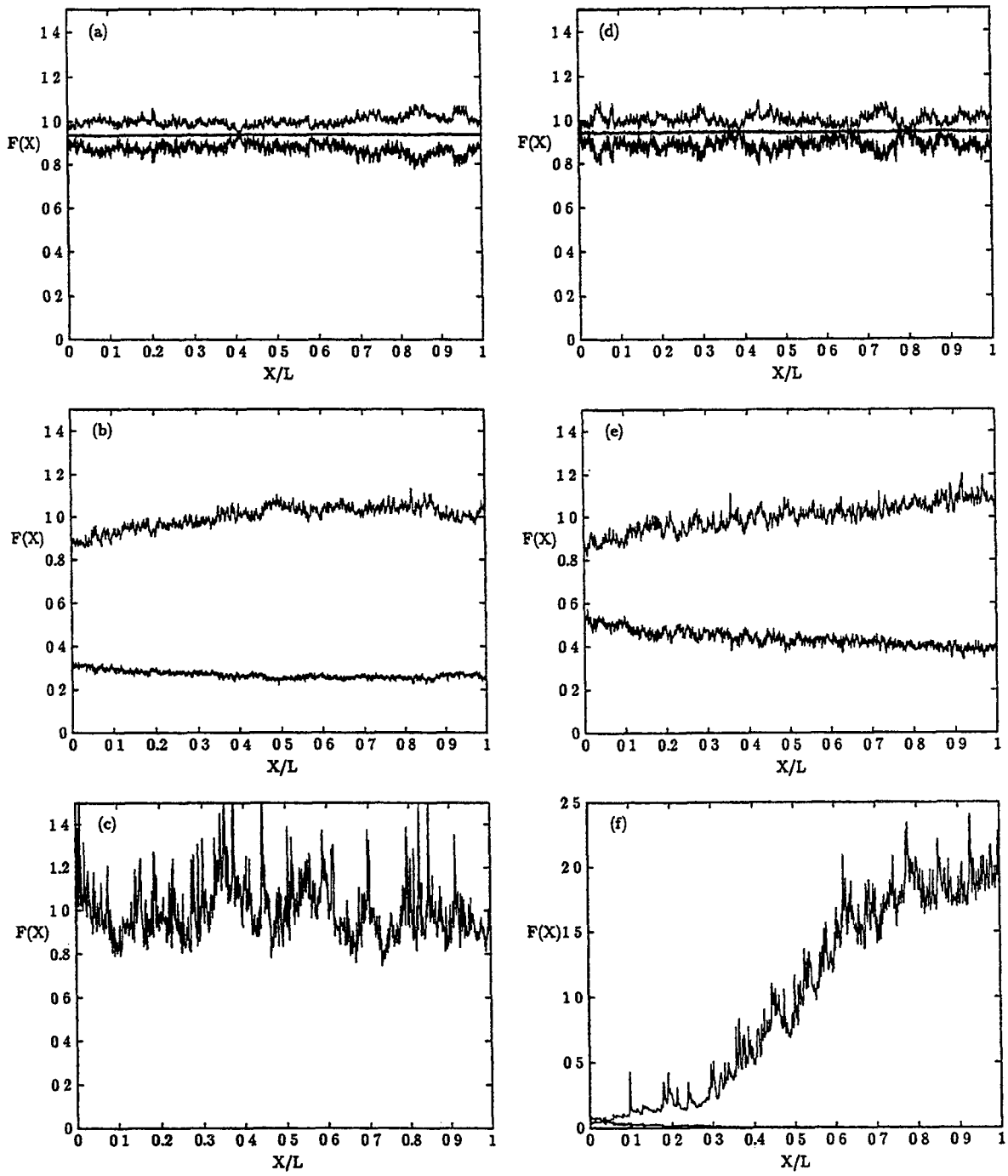

FIG 5 Temperature (in reduced units) and density profiles Density is expressed as $\rho(X)/\rho$ where $\rho(X)$ is the local density and $\rho = N/L$, L being the length of the box. Results for a system of soft particles undergoing inelastic collisions The system is composed of $N = 1000$ particles at a density $\rho = 0\,2$ Thin lines: density profiles, Thick lines: temperature profiles (a) System thermostated with a wall particle coupled to a NH thermostat and $\gamma = 0\,001$, (b) $\gamma = 0\,01$, (c) $\gamma = 0\,1$, (d) System thermostated with a stochastic wall and $\gamma = 0\,001$, (e) $\gamma = 0\,01$, (f) $\gamma = 0\,1$

of inelasticity in the system. In the limit of high density and low inelasticity the value of the exponent for soft particles seems to tend to the value for rigid particles

Finally, we have investigated the appearance of the "extraordinary" state in one-dimensional granular systems thermostated at the boundaries, described in Ref [1] We believe that the origin of such a state is in the way that the thermal boundaries chosen in Ref [1] or the stochastic boundary used by Ciccotti *et al* [2–4] work The interaction with any of these boundaries can be interpreted as an exchange of incoming particles and outgoing particles whose velocity is set to a value totally independent of the incoming velocity In other words, the kinetic energy of the particles after leaving the boundary can be arbitrarily high in comparison with the mean kinetic energy of the rest of the particles in the fluid This is the case when the particles undergo inelastic colli-

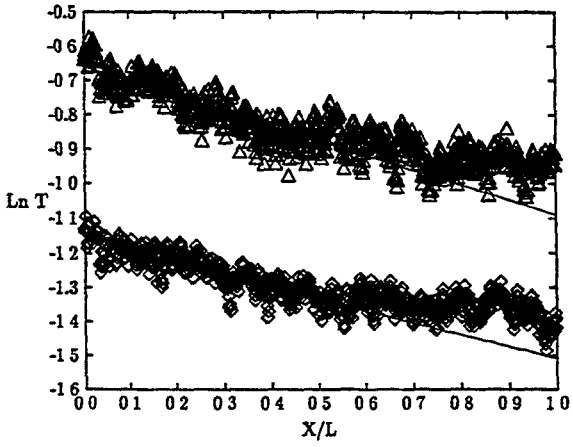

FIG 6 ln$T$ plotted vs X/L The temperature is in reduced units Soft particles undergoing inelastic collisions for $\rho=0.2$ and $\gamma=0.01$ ◇: System thermostated with a wall particle coupled to a NH thermostat. △: System thermostated with a stochastic wall, straight lines: least square fits

sions if the energy dissipated during the collisions is high enough Hence in this case, the particles emitted by the boundary press the majority of the particles in the system against the opposite boundary forming a clump If, on the other hand, the interaction with a thermal boundary is such that the particle hitting the boundary can only load a limited amount of kinetic energy, in the limit of high inelasticity the system will simply cool down until all motion stops

ACKNOWLEDGMENTS

Grant No 11-0065-1 from the Danish Natural Science Research Council is gratefully acknowledged. P.P acknowledges the University of Copenhagen for ~~financial support.~~ a Carne postdoctoral grant

APPENDIX: INELASTIC COLLISIONS FOR SOFT PARTICLES

The equations for the time evolution of velocities for our (one-dimensional) system of soft particles undergoing inelastic collisions are

$$\begin{aligned}
\dot{v}_1 &= a_1 + \gamma D_{12}^{1/2} v_{12}, \\
\dot{v}_2 &= a_2 - \gamma D_{12}^{1/2} v_{12} + \gamma D_{23}^{1/2} v_{23}, \\
v_3 &= a_3 - \gamma D_{23}^{1/2} v_{23} + \gamma D_{34}^{1/2} v_{34},
\end{aligned} \tag{A1}$$

where a_i are the accelerations coming from the conservative forces, and the second term in the right-hand side is the accelerations coming from the dissipative forces due to collisions ($v_{ij}=v_i-v_j$ and γ and D are defined in Sec III) These equations conserve the momentum of the center of mass but kinetic energy is dissipated.

In the leap-frog algorithm scheme, the velocity of the system at time $t+h/2$ (h is the length of the time step) is calculated as

$$v(t+h/2)=v(t-h/2)+ha(t) \tag{A2}$$

and the velocity at time t is approximated as

$$v(t)=\tfrac{1}{2}[v(t+h/2)+v(t-h/2)] \tag{A3}$$

Writing Eq (1) in the leap-frog scheme:

$$\begin{aligned}
v_1(t+h/2) &= v_1(t-h/2)+h[a_1(t)+\gamma'_{12}(t)v_{12}(t)], \\
v_2(t+h/2) &= v_2(t-h/2)+h[a_2(t)-\gamma'_{12}(t)v_{12}(t) \\
&\quad +\gamma'_{23}(t)v_{23}(t)], \\
v_3(t+h/2) &= v_3(t-h/2)+h[a_3(t)-\gamma'_{23}(t)v_{23}(t) \\
&\quad +\gamma'_{34}(t)v_{34}(t)],
\end{aligned} \tag{A4}$$

where for the sake of compactness we rename the product $\gamma D_{ij}^{1/2}(t)$ as $\gamma'_{ij}(t)$ Substituting the value of $v_{ij}(t)$ for the expression given in Eq (3), we obtain a set of linear equations where the unknown quantities are $v_i(t+h/2)$ The matrix of this set of equations is

$$\begin{pmatrix}
1+\frac{h}{2}\gamma'_{12}(t) & -\frac{h}{2}\gamma'_{12}(t) & 0 & \\
-\frac{h}{2}\gamma'_{12}(t) & 1+\frac{h}{2}\gamma'_{12}(t)+\frac{h}{2}\gamma'_{23}(t) & -\frac{h}{2}\gamma'_{23}(t) & \\
0 & -\frac{h}{2}\gamma'_{23}(t) & 1+\frac{h}{2}\gamma'_{23}(t)+\frac{h}{2}\gamma'_{34}(t) & -\frac{h}{2}\gamma'_{34}(t) \\
 & & & 1-\frac{h}{2}\gamma'_{n-1,n}(t)
\end{pmatrix}$$

and the right-hand side term is

$$\begin{pmatrix} v_1\left(t-\frac{h}{2}\right)\left[1-\frac{h}{2}\gamma'_{12}(t)\right]+ha_1(t)+v_2\left(t-\frac{h}{2}\right)\left[\frac{h}{2}\gamma'_{12}(t)\right] \\ v_1\left(t-\frac{h}{2}\right)\left[\frac{h}{2}\gamma'_{12}(t)\right]+v_2\left(t-\frac{h}{2}\right)\left[1-\frac{h}{2}\gamma'_{12}(t)-\frac{h}{2}\gamma'_{23}(t)\right]+ha_2(t)+v_3\left(t-\frac{h}{2}\right)\left[\frac{h}{2}\gamma'_{23}(t)\right] \end{pmatrix}$$

[1] Y Du, H Li, and L P Kadanoff, Phys Rev Lett. **74**, 1268 (1995)

[2] G Ciccotti and A. Tenenbaum, J Stat. Phys **23**, 767 (1980)

[3] A. Tenenbaum, G Ciccotti, and R Gallico, Phys Rev A **25**, 2778 (1982)

[4] A. Tenenbaum, Phys Rev A **28**, 3132 (1983)

[5] S McNamara and W R Young, Phys Fluids A **5**, 34 (1993)

[6] M A Hopkins and M Y Louge, Phys Fluids A **3**, 47 (1991)

[7] I Goldhirsh and G Zanetti, Phys Rev Lett. **70**, 1619 (1993)

[8] P K. Haff, J Fluid Mech. **130**, 187 (1983)

[9] S McNamara and W R Young, Phys Rev E **50**, R28 (1994)

[10] In statistical mechanics the temperature is defined as the kinetic energy per degree of freedom For one-dimensional systems composed of elastic particles coupled to a thermostat the number of degrees of freedom is just the number of particles in the system (there are no constraints), this is also the case for one-dimensional systems composed of inelastic particles, whether the system is coupled to a thermostat or not.

[11] J D Weeks, D Chandler, and H C Andersen, J Chem Phys **54**, 5237 (1971)

[12] W A. M Morgado and I Oppenheim, Phys Rev E **55**, 1940 (1997)

[13] N V Brilliantov, F Spahn, J -M. Hertzsch, and T Pöschel, Phys Rev E **53**, 5382 (1996)

[14] See, for example, M P Allen and D J Tildesley, *Computer Simulation of Liquids* (Clarendon Press, Oxford 1987), p 80

[15] See, for example, W H Press, S A Teukolsky, W T Vetterling, and B P Flannery, *Numerical Recipes*, 2nd ed (Cambridge University Press, Cambridge, 1992)

[16] J L Lebowitz and Harry L. Frisch, Phys Rev **107**, 917 (1957); J L Lebowitz and H Spohn, J Stat. Phys **19**, 633 (1978)

[17] D C Rapaport, Phys Rev A **46**, 1971 (1992)

[18] See, e g , S Nosé, Prog Theor Phys Suppl **103**, 1 (1991)

[6] Phys Fluids A 3, 47 (1991)

BIBLIOGRAPHY

[1] B.J. Alder and T.E. Wainwright. Phase Transition for a Hard Sphere System. *Journal of Chemical Physics*, 27:1208–1209, 1957.

[2] M.P. Allen and D.J. Tildesley. *Computer Simulation of Liquids*. Clarendon Press, 1987.

[3] K. Andersen. Forelæsningsnoter i statistisk termodynamik, 1979. In Danish.

[4] V.I. Arnold. *Mathematical Methods of Classical Mechanics*. Springer-Verlag, 1974.

[5] P.W. Atkins. *Physical Chemistry*. Oxford University Press, 5 edition, 1994.

[6] B.P. Belousov. *Sbornik referatov po Radiatsionnoi Meditsine*, page 145, 1958. In Russian.

[7] K. Binder. Mechanisms for the dynamics of phase transitions. In S.W. Lovesey and R. Scherm, editors, *Condensed Matter Research Using Neutrons*, pages 1–38. Plenum Press, 1984.

[8] G.A. Bird. *Molecular gas dynamics and the direct simulation of gas flows*, volume 42 of *Oxford Engineering Science*. Oxford University Press, 1996.

[9] J. Boissonade. Molecular dynamics studies of long range and short range fluctuations in non-equilibrium chemical systems. *Physics Letters A*, 74(3,4):285–287, 1979.

[10] A.J. Bray. Theory of phase-ordering kinetics. *Advances in Physics*, 43(3):357–459, 1994.

[11] N.V. Brilliantov, F. Spahn, J-M. Hetzsch, and T. Pöschel. Model for collision in granular gases. *Physical Review E*, 53(5):5382–5393, 1996.

[12] D. Brown, J.H.R. Clarke, M. Okuda, and T. Yamazaki. A domain decomposition parallelization strategy for molecular dynamics simulations on distributed memory machines. *Computer Physics Communications*, 74:67–80, 1993.

[13] J.W. Cahn and J.E. Hilliard. Free Energy of a Nonuniform system. I. Interfacial Free Energy. *Journal of Chemical Physics*, 28(2):258–267, 1958.

[14] D. Carati and R. Lefever. On the chemical freezing of phase separation in immiscible binary mixtures. *Physical Review E*, 56(3):3127–3136, 1997.

[15] J.J. Christensen, K. Edler, and H.C. Fogedby. Phase segregation dynamics of a chemically reactive binary mixture. *Physical Review E*, 54(3):R2212–R2215, 1996.

[16] B.L. Clarke. Stability of complex reaction networks. *Advances in Chemical Physics*, 43:7–213, 1980.

[17] R.M. Clegg. Derivarion of Diffusion-Controlled chemical rate constants with the help of Einstein's origigal derivation of the diffusion constant. *Journal of Chemical Education*, 63(7):571–574, 1986.

[18] B.G. Cox. *Modern liquid phase kinetics*, volume 21 of *Oxford Chemistry Primers*. Oxford University Press, 1994.

[19] H.H. Diebner and O.E. Rössler. Deterministic continuous molecular-dynamics-simulation of a chemical oscillator. *Zeitschrift für Naturforschung*, 50a:1139–1140, 1995.

[20] Y. Du, H. Li, and L.P. Kadanoff. Breakdown of Hydrodynamics in a One-Dimensional System of Inelastic Particles. *Physical Review Letters*, 74(8):1268–1271, 1995.

[21] J.E. Farrell and O.T. Valls. Growth kinetics and domain morphology after off-critical quenches in a two-dimensional fluid model. *Physical Review B*, 43(1):630–640, 1991.

[22] L. Frachebourg, P.L. Krapivsky, and E. Ben-Naim. Spatial organization in cyclic Lotka-Volterra systems. *Physical Review E*, 54(6):6186–6200, 1996.

[23] D. Frenkel and B. Smit. *Understanding Molecular Simulation: From algorithms to applications*. Academic Press, 1996.

[24] K. Geisshirt. Computerens rolle i moderne kemi. *Dansk Kemi*, 77(12):9–13, 1996. In Danish.

[25] K. Geisshirt, P. Padilla, E.L. Praestgaard, and S. Toxvaerd. Controlling the temperature of one-dimensional systems composed of elastic and inelastic particles. *Physical Review E*, 57(2), 1998. (accepted).

[26] K. Geisshirt, E.L. Praestgaard, and S. Toxvaerd. Oscillating chemical reactions and phase separation simulated by Molecular Dynamics. *Journal of Chemical Physics*, 107(22):9406–9412, 1997.

[27] K. Geisshirt, S. Toxværd, and E. Præstgaard. Oscillating chemical reaction simulated by molecular dynamics. In D.P. Landau, K.K. Mon, and H.-B. Schüttler, editors, *Recent developments in computer simulation studies in condensed matter physics*, volume 9, pages 144–149. Springer-Verlag, 1996.

[28] S.C. Glotzer, E.A. Di Marzio, and M. Muthukumar. Reaction-Controlled Morphology of Phase-Separating Mixtures. *Physical Review Letters*, 74(11):2034–2037, 1995.

[29] S.C. Glotzer, D. Stauffer, and N. Jan. Monte Carlo Simulations of Phase Separation in Chemically Reactive Binary Mixtures. *Physical Review Letters*, 72(26):4109–4112, 1994.

[30] N. Goldenfeld. *Lectures on phase transitions and the renormalization group*, volume 85 of *Frontiers in physics*. Addison-Wesley, 1992.

[31] I. Goldhirsch and G. Zanetti. Clustering instability in dissipative gases. *Physical Review Letters*, 70(11):1619–1622, 1993.

[32] H. Goldstein. *Classical mechanics*. Addison-Wesley, 2. edition, 1980.

[33] G.H. Golub and J.M. Ortega. *Scientific Computing and Differential Equations*. Academic Press, 1992.

[34] J. Gorecki and K. Kitahara. Does the structure of an oscillating chemical system oscillate? *Physica A*, 245:164–180, 1997.

[35] G.H. Grant and W.G. Richards. *Computational Chemistry*, volume 29 of *Oxford Chemistry Primers*. Oxford University Press, 1995.

[36] E.A. Guggenheim. *Elements of the Kinetic Theory of Gases*, volume 6 of *The International Encyclopedia of Physical Chemistry and Chemical Physics*. Pergamon Press, 1960.

[37] P.K. Haff. Grain flow as a fluid-mechanical phenomenon. *Journal of Fluid Mechanics*, 134:401–430, 1983.

[38] J.P. Hansen and I.R. McDonald. *Theory of simple liquids*. Academic Press, 2. edition, 1986.

[39] J.P. Hansen and L. Verlet. *Physical Review*, 184:151, 1969.

[40] M. Heinrichs and F.W. Schneider. Molecular dynamics calculations of a second order kinetic phase transition in an open system (CSTR). *Ber. Bunsenges. Phys. Chem.*, 87:1195–1201, 1983.

[41] M.W. Hirsch and S. Smale. *Differential Equations, Dynamical Systems, and Linear Algebra*. Acamedic Press, 1974.

[42] W.G. Hoover. Canonical dynamics: Equilibrium phase-space distributions. *Physical Review A*, 31:1695–1697, 1985.

[43] K. Huang. *Statistical Mechanics*. John Wiley & Sons, 2. edition, 1987.

[44] H.M. Jaeger, S.R. Nagel, and R.P. Behringer. Granular solids, liquids, and gases. *Review of Modern Physics*, 68(4):1259–1273, 1996.

[45] J.T. Jenkins and S.B. Savage. A theory for the rapid flow of identical, smooth, nearly elastic, spherical particles. *Journal of Fluid Mechanics*, 130:187–202, 1983.

[46] D.A. Kofke. Direct evaluation of phase coexistence by molecular simulation via integration along the saturation line. *Journal Chemical Physics*, 98(5):4149–4162, 1993.

[47] M. Laradji, O.G. Mouritsen, and S. Toxvaerd. Spinodal decomposition in multi-component fluid mixtures: a molecular dynamics study. *Physical Review E*, 53(4B), 1996.

[48] J.L. Lebowitz and H.L. Frisch. Model of Nonequilibrium Ensemble: Knudsen Gas. *Physical Review*, 107(4):917–923, 1957.

[49] J.L. Lebowitz and H. Spohn. Transport Properties of the Lorentz Gas: Fourier's Law. *Journal of Statistical Physics*, 19(6):633–654, 1978.

[50] A.J. Lotka. Contribution to the theory of periodic reactions. *Journal of Physical Chemistry*, 14:271–274, 1910.

[51] A.J. Lotka. Undamped oscillations derived from the law of mass action. *Journal of American Chemical Society*, 42:1595–1599, 1920.

[52] M.M. Mansour and F. Baras. Microscopic simulation of chemcial systems. *Physica A*, 188:252–276, 1992.

[53] G.J. Martyna and M.E. Tuckermann. Symplectic reversible integrators: Predictor-corrector methods. *Journal of Chemical Physics*, 102(20):8071–8077, 1995.

[54] S. McNamara and W.R. Young. Kinetics of a one-dimensional granular medium in the quasielastic limit. *Physics of Fluids A*, 5(1):34–45, 1993.

[55] S. McNamara and W.R. Young. Inelastic collapse in two dimensions. *Physical Review E*, 50(1):R28–R31, 1994.

[56] N. Metropolis, A.W. Rosenbluth, M.N. Rosenbluth, A.H. Teller, and E. Teller. Equation of State Calculations by Fast Computing Machines. *Journal of Chemical Physics*, 21(6):1087–1092, 1953.

[57] R.H. Miller. A Horror Story about Integration Methods. *Journal of Computational Physics*, 93:469–476, 1991.

[58] J.J. Morales and S. Toxvaerd. The cell-neighbour table method in molecular dynamics simulations. *Computer Physics Communications*, 71:71–76, 1992.

[59] W.A.M. Morgado and I. Oppenheim. Energy dissipation for quasielastic granular particle collisions. *Rhysical Review E*, 55(2):1940–1945, 1997.

[60] O.G. Mouritsen. Computeren som værktøj i statistisk fysik. *Kvant*, pages 19–22, april 1993. In Danish.

[61] G.J. Myers. *The Art of Software Testing*. John Wiley & Sons, 1979.

[62] K.R. Naqvi. Diffusion-Controlled reactions in two-dimensional fluids: discussion of measurements of lateral diffusion of lipids in biological membranes. *Chemical Physics Letters*, 28(2):280–284, 1974.

[63] S. Nosé. A molecular dynamics method for simulations in the canonical ensemble. *Molecular Physics*, 52(2):255–268, 1984.

[64] P. Ortoleva and S. Yip. Computer molecular dynamics studies of chemical instability. *Journal of Chemical Physics*, 65(6):2045–2051, 1976.

[65] A.Z. Panagiotopoulos. Direct determination of phase coexistence properties of fluids by Monte Carlo simulation in a new ensemble. *Molecular Physics*, 61(4):813–826, 1987.

[66] L. Perko. *Differential Equations and Dynamical Systems*. Springer-Verlag, 1993.

[67] M.J. Pilling and P.W. Seakins. *Reaction Kinetics*. Oxford University Press, 1995.

[68] J. Portnow. Molecular dynamics studies of fluctuation behavior. *Physics Letters A*, 51(6):370–372, 1975.

[69] I. Prigogine and R. Lefever. Symmetry breaking instabilities in dissipative systems. *Journal of Chemical Physics*, 48(4):1695–1700, 1967.

[70] D.C. Rapaport. Unpredictable convection in a small box: Molecular-dynamics experiments. *Physical Review A*, 46(4):1971–1984, 1992.

[71] D.C. Rapaport. *The art of Molecular Dynamics Simulation*. Cambridge University Press, 1995.

[72] S.K. Scott. *Oscillations, Waves, and Chaos in Chemical Kinetics*, volume 18 of *Oxford Chemistry Primers*. Oxford University Press, 1994.

[73] A.S. Tanenbaum. *Structured Computer Organization*. Prentice Hall, 3. edition, 1990.

[74] A. Tenenbaum. Local equilibrium in stationary states by molecular dynamics. *Physical Review A*, 28(5):3132–3133, 1983.

[75] A. Tenenbaum, G. Ciccotti, and R. Gallico. Stationary nonequilibrium states by molecular dynamics. Fourier's law. *Physical Review A*, 25(2):2778–2787, 1982.

[76] S. Toxvaerd. Algorithms for canonical molecular dynamics simulations. *Molecular Physics*, 72(1):159–168, 1991.

[77] S. Toxvaerd. Hamiltonians for discrete dynamics. *Physical Review E*, 50(3):2271–2274, 1994.

[78] S. Toxvaerd. Molecular dynamics simulations of phase separation in chemically reactive binary mixtures. *Physical Review E*, 53(4):3710–3716, 1996.

[79] S. Toxvaerd and E. Velasco. Phase-stability lines, spinodals and distribution functions for binary immiscible mixtures. *Molecular Physics*, 86(4):845–855, 1995.

[80] M.A. van der Hoef and D. Frenkel. Evidence for Faster-than-t^{-1} Decay of the Velocity Autocorrelation Function in a 2D Fluid. *Physical Review Letters*, 66(12):1591–1594, 1991.

[81] E. Velasco and S. Toxvaerd. Computer Simulation of Phase Separation in a Two-Dimensional Binary Fluid Mixture. *Physical Review Letters*, 71(3):388–391, 1993.

[82] J. Verdasca, P. Borckmans, and G. Dewel. Chemically frozen phase separation in an absorbed layer. *Physical Review E*, 52(5):R4616–R4919, 1995.

[83] J.D. Weeks, D. Chandler, and H.C. Andersen. *Journal of Chemical Physics*, 54:5237, 1971.

[84] R. Westfall. *The Construction of Modern Science*. John Wiley & Sons, 1971.

[85] Y. Wu, F.J. Alexander, T. Lookman, and S. Chen. Effects of Hydrodynamics on Phase Transition Kinetics in Two-Dimensional Binary Fluids. *Physical Review Letters*, 74(19):3852–3855, 1995.

[86] A.M. Zhabotinsky. *Biofizika*, 9:306, 1964. In Russian.